ADAMA SCIENCE AND TECHNOLOGY UNIVERSITY

School of Mechanical Chemical and Materials Engineering

Hybridizing and Designing a Space-frame Chassis for Bajaj Qute

A thesis submitted in partial fulfillment of the requirements for the award of the degree of Master of Science in Automotive Engineering

By

Chala Jembere

ADVISOR: - N. RAMESH BABU(Associate Professor)

MECHANICAL SYSTEMS AND VEHICLE ENGINEERING PROGRAM

October, 2017

Adama, Ethiopia

CANDIDATE'S DECLARATION

I hereby declare that the work which is being presented in the thesis entitled “Hybridizing and Designing a Space-frame Chassis for Bajaj Qute” in partial fulfillment of the requirements for the award of the degree of Master of Science in Automotive Engineering is an authentic record of my own work carried out from February 2016 to September 2017 under the supervision of N. Ramesh Babu,Mechanical Systems and Vehicle Engineering Program, Adama Science and Technology University, Ethiopia.

The matter embodied in this thesis has not been submitted by me for the award of any other degree or diploma. All relevant resources of information used in this thesis have been duly acknowledged.

Name	Signature	Date
Chala Jembere	______________	____________

Student

This is to certify that the above statement made by the candidate is correct to the best of my knowledge and belief. This thesis has been submitted for examination with my approval.

Name	Signature	Date
N. Ramesh Babu	_______________	____________

Advisor

ADAMA SCIENCE AND TECHNOLOGY UNIVERSITY

SCHOOL OF MECHANICAL, CHEMICAL AND MATERIAL ENGINEERING

MECHANICAL SYSTEMS AND VEHICLE ENGINEERING PROGRAM

Hybridizing and Designing a Space-frame Chassis for Bajaj Qute

By

Chala Jembere

Approved by board of Examiners

______________________________ ______________

Chairman, Department graduate committee

______________________________ ______________

Advisor

______________________________ ______________

Internal Examiner

______________________________ ______________

External Examiner

ACKNOWLEDGEMENTS

First of all, I would like to thank God for he made this thesis come to completion.

Next, I am greatly thankful to my thesis advisor N.Ramesh Babu(Associate professor) at Adama Science and Technology University for providing me with definite direction, professional guidance, constant encouragement from the beginning of the work to the end.

I am thankful to Horra Trading Plc. Addis Ababa main branch for their cooperation in providing me all the necessary data on the existing Bajaj Qute.

I would also like to thank all my friends who read my thesis and gave me constructive comments throughout my work progress.

Finally, I express my very profound gratitude to my parents for providing me continuous encouragement throughout my years of study and through the process of researching and writing this thesis. This accomplishment would not have been possible without them. Thank you.

TABLE OF CONTENTS

ACKNOWLEDGEMENTS..I

ACRONYMS AND SYMBOLS..VI

LIST OF TABLES..VIII

LIST OF FIGURES..IX

Abstract..XIII

CHAPTER ONE: INTRODUCTION..1

1.1 Background..1

1.2. Statement of the Problem..2

1.3 Objectives..3

1.3.1 General Objective..3

1.3.2 Specific Objectives..3

1.4 Scope..3

1.5 Significance..4

1.6 Limitation..4

1.7 Organisation of the Thesis..4

CHAPTER TWO: LITERATURE REVIEW..6

2.1 Introduction..6

2.2 Hybrid Electric Vehicles..7

2.2.1 Series Drive-trains..7

2.2.2 Parallel Drive-trains..7

2.2.3 Series-parallel Drive-trains..7

2.3 POWERTRAIN COMPONENT SIZING FOR HYBIRDIZING..8

2.3 Acceleration Power..10

2.4 Grade-Climbing Power..12

2.5 Vehicle Mass.. 13

2.5.1 Power Unit (ICE).. 14

2.5.2 Traction Motor.. 15

2.5.3 Battery Pack.. 15

2.6 Chassis Frame...16

2.7. Load Cases of Chassis... 16

2.7.1 Lateral Bending..17

2.7.2. Horizontal Loading & Lozenging...17

2.7.3. Vertical Bending.. 17

2.7.4. Longitudinal Torsion... 17

2.8 Type of Chassis.. 18

2.8.1 Ladder Frames... 18

2.8.2 Backbone Tube Chassis... 18

2.8.3 Uni-body Frame..18

2.8.4 Space-Frame.. 19

2.9 Chassis Material... 19

CHAPTER THREE: MATERIALS AND METHODS..26

3.1 Materials... 26

3.2 Research Methods... 26

3.3 Technical Specifications of the Existing Baja Qute..28

3.4 CAD Modeling of the Existing Bajaj Qute Chassis.. 30

3.5 FINITE ELEMENT ANALYSIS (FEA) OF THE EXISTING CHASSIS.............. 31

3.5.1 Static Analysis.. 31

3.5.2 Full Frontal Impact Analysis... 34

3.5.3 Side Crash Test... 37

3.5.4 Rear Crash Test....38

3.5.5 Front Rollover Analysis....40

3.5.6 Side Rollover.... 41

3.5.7 Modal Analysis....41

3.6 DESIGN AND ANALYSIS OF THE NEW CHASSIS....43

3.6.1 The Need of Designing a New Chassis.... 43

3.7 CAD Modeling and Tube Diameter Optimization.... 44

3.8 FINITE ELEMENT ANALYSIS OF THE NEW CHASSIS....46

3.8.1 Static Analysis.... 46

3.8.2 Full Front Impact Analysis.... 48

3.8.3 Side Impact Analysis.... 49

3.8.4 Rear Impact Analysis....50

3.8.5 Front Rollover Analysis....51

3.8.6 Side Rollover Analysis.... 52

3.8.7 Modal Analysis....53

CHAPTER FOUR: RESULT AND DISCUSSION.... 54

4.1 Results and Discussion on the Existing Chassis....54

4.1.1 Static Analysis Results....54

4.1.2 Frontal Impact Analysis Results....55

4.1.3 Side Impact Analysis Results.... 57

4.1.4 Rear Impact Analysis Results....58

4.1.5 Front Rollover Analysis Results....59

4.1.6 Side Rollover Analysis Results....61

4.1.7 Modal Analysis Results.... 62

4.2 Results and Discussion on the New Chassis.... 66

4.2.1 Static Analysis Results....66
4.1.2 Frontal Impact Analysis Results....68
4.1.3 Side Impact Analysis Results....69
4.1.4 Rear Impact Analysis Results....71
4.1.5 Front Rollover Analysis Results....72
4.1.6 Side Rollover Analysis Results....73
4.1.7 Modal Analysis Results....74
4.3 COMPARISON OF THE TWO MODELS....77
CHPTER FIVE: SUMMARY, CONCLUSION, RECOMMENDATION AND FUTURE WORK....80
5.1 Summary....80
5.2 Conclusion....80
5.3 Recommendation....81
5.4 Future Work....81
References....82
Appendix A: The dimensions of the new chassis....86
Appendix B: 95th Percentile Man Ergonomic Sitting Position....87
Appendix C: Mounting Places of the Drive-line Components....89

ACRONYMS AND SYMBOLS

3D……………………………Three dimensional

AC………………..……...Alternating current

A_f……………………………Frontal area of a vehicle

AFVs………………………. Alternative fuels and vehicles

BHP…………………………Brake horse power

CAD…………….……….…Computer Aided Drafting

CATIA…….……….…..….… .Computer Aided Three-Dimensional Interactive Application

C_D……………….…………Drag coefficient

CO_2…………………………Carbon dioxide

DC………………..…..…..Direct Current

ESS………………………….Energy Storage System

EV…………………………. Electric vehicles

FEA……………….…………Finite Element Analysis

FEM………...…….…………Finite element method

FMVSS……………………....Federal Motor Vehicle Safety Standard

GHGs………………………..Greenhouse gases

HEV…………………………Hybrid electric vehicles

ICE………………………….Internal combustion engine

NHTSA……………………..National Highway Traffic Safety Administration.

Pa…………………………..Acceleraton power

Pg…………………..……….Grade climbing power

PLC……………………….. .private limited company

PST…………….………. .Power split transmission

PU………………………….Power Unit

SAE………………………..Society of Automotive Engineer

SOC………………………..State of charge

UNECE…………………….United Nation Economic Commission for Europe

θ…………………..……..Grade angle of a road

μ …………………………..Coefficient of rolling resisance

ρ ……………………………Density of air

LIST OF TABLES

Table 2.1: Specific values used for component sizing 14

Table 3.1: Material Property of High Strength Steel (ASTM A606) 26

Table 3.2: Vehicle Specification of the Existing Bajaj Qute.. 28

Table 3.3: Summary of Simulation Results of the Existing Chassis.....................................43

Table 4.1: Frequency and Maximum Deformation of the Existing Bajaj qute for the first 12 Modes.. 62

Table 4.2: Natural Frequency and Maximum Deformation of the New Chassis under the First 12 Modes...74

Table 4.3: Summary of Simulation Results of the Existing and New Chassis..................... 77

LIST OF FIGURES

Figure 2.1: Rectangular box of welded tubes 20

Figure 3.1: Flow Chart of Chassis Designing... 27

Figure 3.2: 3D CAD Model of the Existing Bajaj Qute... 31

Figure 3.3: Loading and Boundary Conditions for Static Analysis..................................... 33

Figure 3.4: Mesh used for the Analysis of the Existing Bajaj Qute..................................... 34

Figure 3.5: Load and Boundary Conditions for Front Impact Analysis.............................. 37

Figure 3.6: Loads and Boundary Condition for Side Impact Analysis................................ 38

Figure 3.7: Load and Boundary Conditions for Rear Impact Analysis............................... 39

Figure 3.8: Loads and Boundary Conditions of the Front Rollover Analysis...................... 40

Figure 3.9: Loads and Boundary Conditions of Side Rollover Analysis............................. 41

Figure 3.10: 3D CAD Model of the New Chassis... 45

Figure 3.11: Loading and Initial Boundary Conditions for Static Analysis......................... 47

Figure 3.12: Mesh Used for the New Chassis Analysis... 48

Figure 3.13: Loading and Initial Boundary Conditions for Frontal Impact Analysis........... 49

Figure 3.14: Loading and Boundary Conditions for Side Impact Analysis.......................... 50

Figure 3.15: Loading and Boundary Conditions for Rear Impact Analysis......................... 51

Figure 3.16: Loading and Boundary conditions for Front Rollover Analysis...................... 52

Figure 3.17: Loading and Boundary Condition for Side Rollover Analysis........................ 53

Figure 4.1: Simulation Results of the Static Analysis... 54

Figure 4.2: Equivalent stress under Frontal Impact Analysis.. 55

Figure 4.3: Simulation Results of the Frontal Impact Analysis... 56

Figure 4.4: Simulation Results of Side Impact Analysis... 57

Figure 4.5: Simulation Results of the Rear Impact Analysis... 59

Figure 4.6: Simulation Results of the Front Rollover Analysis... 60

Figure 4.7: Simulation Results of Side Rollover Analysis.. 61

Figure 4.8: Natural Frequency vs Modes of Vibration.. 63

Figure 4.9: Maximum Deformation vs Modes of vibration...64

Figure 4.10: Mode shapes at the 2nd, 5th,7th and 10th Natural Frequencies respectively....... 65

Figure 4.11: simulation Results of Static Analysis...66

Figure 4.12: simulation Results of Front Impact Analysis.. 68

Figure 4.13: Equivalent Stress Results Under the Frontal Impact Analysis.........................69

Figure 4.14: Simulation Results of Side Impact Analysis... 70

Figure 4.15: Simulation Results of Rear Impact Analysis...71

Figure 4.16: Simulation Results of Front Rollover Analysis...72

Figure 4.17: Simulation Results of Side Rollover Analysis... 73

Figure 4.18: Natural Frequency vs Modes of Vibration.. 75

Figure 4.19: Maximum Deformation vs. Modes of Vibration...75

Figure 4.20: Mode Shapes of the 3rd, 6th, 8th and 11th modes of vibration respectively........76

Figure 4.21: Maximum Deformation vs Modes of Vibration...79

Figure 2.1: Rectangular box of welded tubes [41].. 20

Figure 3.1: Flow Chart of Chassis Designing...27

Figure 3.2: 3D CAD Model of the Existing Bajaj Qute... 31

Figure 3.3: Loading and Boundary Conditions for Static Analysis... 33

Figure 3.4: Mesh used for the Analysis of the Existing Bajaj Qute.. 34

Figure 3.5: Load and Boundary Conditions for Front Impact Analysis..37

Figure 3.6: Loads and Boundary Condition for Side Impact Analysis.. 38

Figure 3.7: Load and Boundary Conditions for Rear Impact Analysis..39

Figure 3.8: Loads and Boundary Conditions of the Front Rollover Analysis...40

Figure 3.9: Loads and Boundary Conditions of Side Rollover Analysis.. 41

Figure 3.10: 3D CAD Model of the New Chassis..45

Figure 3.11: Loading and Initial Boundary Conditions for Static Analysis....................................47

Figure 3.12: Mesh Used for the New Chassis Analysis.. 48

Figure 3.13: Loading and Initial Boundary Conditions for Frontal Impact Analysis...................................... 49

Figure 3.14: Loading and Boundary Conditions for Side Impact Analysis.. 50

Figure 3.15: Loading and Boundary Conditions for Rear Impact Analysis...51

Figure 3.16: Loading and Boundary conditions for Front Rollover Analysis..52

Figure 3.17: Loading and Boundary Condition for Side Rollover Analysis..53

Figure 4.1: Simulation Results of the Static Analysis..54

Figure 4.2: Equivalent stress under Frontal Impact Analysis..55

Figure 4.3: Simulation Results of the Frontal Impact Analysis.. 56

Figure 4.4: Simulation Results of Side Impact Analysis..57

Figure 4.5: Simulation Results of the Rear Impact Analysis.. 59

Figure 4.6: Simulation Results of the Front Rollover Analysis.. 60

Figure 4.7: Simulation Results of Side Rollover Analysis..61

Figure 4.8: Natural Frequency vs Modes of Vibration...63

Figure 4.9: Maximum Deformation vs Modes of vibration.. 64

Figure 4.10: Mode shapes at the 2^{nd}, 5^{th},7^{th} and 10^{th} Natural Frequencies respectively....................................65

Figure 4.11: simulation Results of Static Analysis...66

Figure 4.12: simulation Results of Front Impact Analysis..68

Figure 4.13: Equivalent Stress Results Under the Frontal Impact Analysis.. 69

Figure 4.14: Simulation Results of Side Impact Analysis..70

Figure 4.15: Simulation Results of Rear Impact Analysis.. 71

Figure 4.16: Simulation Results of Front Rollover Analysis... 72

Figure 4.18: Natural Frequency vs Modes of Vibration..75

Figure 4.19: Maximum Deformation vs. Modes of Vibration.. 75

Figure 4.20: Mode Shapes of the 3rd, 6th, 8th and 11th modes of vibration respectively.................................... 76

Figure 4.21: Maximum Deformation vs Modes of Vibration... 79

Abstract

Fossil fuels supply the majority of world energy demand and the majority of fossil fuels is consumed by vehicles. As a result of this, the world's oil reservoirs are heavily exploited. Besides, emission from combustion of fossil fuels is highly polluting the environment. Hybrid Electric vehicles are a breakthrough to minimize these problems. Four wheeled Bajaj Qute is becoming a popular and common means of short distance transport in Ethiopia. Qute uses a conventional petrol engine for propulsion. As a result, it is polluting the environment. Therefore, it is good to change this vehicle to its equivalent Hybrid Electric one. In this thesis, the strength of the existing Bajaj Qute chassis was analyzed and a new space-frame chassis was designed for a Hybrid Electric Bajaj Qute which is equivalent to the existing vehicle in performance. This was done by using CATIA V5 for 3D modeling and ANSYS 16.0 for Finite Element Analysis. With the new model, better performance under the static loading, side impact, rear impact, front rollover and side rollover has been achieved.

Keywords: *Space-frame Chassis, Quadri-cycle, Finite Element Analysis. Front Impact, Side Impact, Rear Impact, Front Roll-over, Side Roll-over.*

CHAPTER ONE

INTRODUCTION

1.1 Background

The past decades have made the internal combustion engine (ICE) the standard power source for vehicles due to their low cost, high power output, readily availability of fuel and ability to operate long distances in a wide range of temperatures and environmental conditions. However, conventional IC engines bear the drawbacks of poor fuel economy and environmental pollution making it difficult to satisfy stringent environmental regulations. Fossil fuels supply nearly 85% of world energy demand [1]. Because of this, the world's oil reservoirs are heavily exploited and the recent prediction assumes that petroleum oil will probably be exhausted by 2050 [2] if it continues to be consumed as today. In addition to these, more recently, concerns have been growing over emissions of carbon dioxide (CO_2), the most important of the greenhouse gases (GHGs) that cause serious problems associated with global climate change and recent researches show that about 25% of total industrial CO_2 emissions are produced by vehicles [2]. For these reasons, nowadays, the development and adoption of alternative fuels and vehicles (AFVs) and electric and hybrid vehicles are very important both for environmental protection and preserving fossil fuel for the future.

Battery-powered electric vehicles (EV) possess some advantages over conventional vehicles, such as high energy efficiency and zero toxic emission during operation. However, the performance, especially the operation range per battery charge, is far less competitive than conventional vehicles. Long charging time, limited drive range due to limited on board battery pack are concerns that need to be considered in EVs. Hybrid electric vehicles (HEV), which use more than one power sources have the advantages of both ICE vehicles and EV [3].

Hybrid Electric Vehicles (HEV) are vehicles whose power source is provided from more than one sources such as the combination of an internal-combustion engine with one or two electric motors. Compared to conventional vehicles, hybrid electric vehicles are more fuel efficient. In HEVs, the ICE operation can be optimized to operate within its most efficient range and regenerative braking energy can be recovered, there by significantly increasing the overall vehicle efficiency. Among the possible drive trains of HEV, in the parallel HEV, the battery alone provides power for low-speed driving conditions where internal combustion engines are less efficient and in accelerating, long highways, or hill climbing the electric motor provides additional power to assist the engine. This allows a smaller, more efficient engine to be used. [2].

In this thesis, a space-frame chassis was designed for a low cost intra-city public transport hybrid electric small quadricycle. 'Quadricycle' means a four-wheel vehicle meeting the classification criteria for L6e or L7e category vehicles. Bajaj Qute is selected for this reason.

Bajaj Qute is a quadricycle launched by the Indian automotive company, Bajaj-Auto, as a replacement for the currently used three wheeler vehicles and it is being used as an intra-city short distance transport in the developing countries including Ethiopia. Qute uses a monocoque frame and a 216 cc rear engine, rear wheel drive petrol engine producing 13 bhp power and 19.6 Nm of peak torque along with a five speed manual transmission having a top speed of 70 km/h and travels 35 km/l. Qute is designed to be compact, with a small turning circle radius of 3.5 m. and it has a Length of 2752 mm, Width of 1312 mm, height of 1653 mm and Wheelbase of 1925 mm [20].

1.2. Statement of the Problem.

Fossil fuels supply the majority of world energy demand. Because of this, the world's oil reservoirs are heavily exploited. In addition to this, more recently, concerns have been rising over emissions of carbon dioxide (CO_2), the most important of the greenhouse gases (GHGs) that causes serious problems associated with global climate change. Recent researches show that about 25% of total industrial CO_2 emissions are produced by vehicles. This shows that the conventional vehicles are highly polluting the environment. Bajaj Qute Uses conventional type petrol engine. In this thesis, the convensional Bajaj Qutes was hybridized and transformed into its equivalent hybrid electric vehicle and a space-frame chassis was designe for the Hybrid Electric Bajaj Qute.

1.3 Objectives.

1.3.1 General Objective.

The general objective of this thesis is to analyze the performance of the existing Bajaj Qute Chassis and design a space-frame chassis for Hybrid Electric Bajaj Qute.

1.3.2 Specific Objectives

The specific objectives of this thesis are:

- To collect data on the existing conventional Bajaj Qute,
- To develop 3D model of the existing Bajaj Qute chassis.
- To evaluate its strength under Finite Element Analysis.
- To estimate the weights of driveline components for hybridizing Bajaj Qute.
- To design a space-frame chassis for Four Wheeler Hybrid Electric Bajaj Qute, analyze its performance and compare the results with the existing chassis results.

1.4 Scope

This project requires extensive knowledge about automobile chassis types, and understanding the nature of the loads and load transfer in chassis structures, construction of chassis, materials used for chassis and knowledge of Finite Element Analysis. Also knowledge of the current research status on the different types of automobile chassis needs to be acquired. The scope of this thesis is upto modeling the chassis of the exisyting Bajaj Qute, Making FEA of the chassis under static condition, Determining the weght of the driveline components for hybridizing, modeling a spaceframe chassis for the hybridized Bajaj Qute and making FEA of the new model under static condition.

1.5 Significance

The results of this thesis work are very important for the Horra Trading plc. in case the company wants to upgrade the conventional type Bajaj Qute to the modern Hybrid Electric one. By upgrading to the Hybrid Electric vehicle with the new chassis, better fuel economy, better environmental protection and better driver and passengers safety in case of accident can be obtained.

1.6 Limitation

The geometry of the existing chassis, monocoque type, was very complex and the computer used for analysis could not run explicit dynamic simulation of the existing chassis. Therefore, the impact analysis was made under static analysis by determining the magnitude of energy that transfers from one vehicle to the other vehicle taking that the two colliding vehicles are of the same type. Then energy that will be transferred during the impact was applied as a uniformly distributed load on the model under static condition. This neglects the effect of inertia and may have significant influence on the results.

The other point is that the design of tubular space frame was made by using Finite Element Analysis (FEA) model and no analytical modeling is made. It should be noted that the strength analysis performed here pertains to static load case scenarios and no vehicle handling tests are performed on the chassis.

1.7 Organisation of the Thesis

This report consists of eight chapters. The first chapter is the introduction part. It includes the background of the study, problem statement, objectives, scopes, limitations, significance of the study and organisation of the report. Chapter two focuses on the literature review based on the previous chassis designing experiments. The types of hybrid electric vehicle power trains together with their merits and demerits, the components of the hybrid electric power trains, about the types Automobile chassis, chassis material and different researches done on the designing of Automobile chassis have been briefly discussed, summarized and presented under this chapter. Chapter three discusses about the materials used and methodology followed during the study. Generally, it gives the procedures followed throughout the study. Chapter four discusses about the estimation of the weight of the components added to the power train. Chapter five discusses about the modeling and analysis of the existing Bajaj Qute Chassis. The procedures used to make the static analysis, front impact analysis, side impact analysis, rear impact analysis, rollover analysis and modal analysis of the existing chassis has been clearly given. So, this chapter has great influences to increase understanding on the parameters that influence the performance of a chassis and is very helpful in designing a new chassis. Besides, the details of used simulation settings and boundary conditions are briefly described. The data from the analysis results are also explained at the end of each analysis types. The generated data equivalent stress, total deformation and safety factor are presented in the form of tables and graphics for quantitative and qualitative discussion respectively. Chapter six presents about the designing of the new chassis. The importance of designing the chassis, definition of the vehicle type under consideration, about the designing criterion, about the ergonomics, Rule and regulations to be considered, type of the chassis selected together with its merits and demerits have briefly been discussed. The simulation of the new chassis has also been made and the results are recorded in the form of tables and figures. Chapter seven discusses about the comparison of the performance of the two chassis types. The last chapter, chapter eight, consists of conclusion, recommendation and future work.

CHAPTER TWO

LITERATURE REVIEW

2.1 Introduction

Since the inception of the motor-vehicle industry, fuel vehicles have maintained the top spot as the affordable and convenient source of energy. The first electric vehicles were small electric rail cars, which were demonstrated in the 1830s [22]. Unfortunately, they required better batteries than the galvanic cells that existed at the time. Batteries that could be recharged numerous times were invented in 1860s [23]. This seemed a great success for electric vehicles to be commercially practical. However, even with the new batteries, small electric rail cars could not compete with the giant steam-powered locomotives of the day [2].

Since the 1970s, it has been tried a lot to improve batteries, but even the best electric cars are still only able to travel a fraction of the distance of the average gasoline automobile[23]. Since batteries stubbornly refused to improve, the researchers started to find another option. One solution was the hybrid vehicles, which use both an electric motor and a gasoline motor. In the spectrum of the transportation history, hybrid vehicles only recently broke into the industry with the widespread popularity of the Toyota Prius [24]. In the mid-1990s Toyota introduced the first commercial hybrid electric vehicle (HEV), the Prius [24]. This vehicle uses a small gasoline motor supplemented by an electric motor. The combination gives good acceleration and gas mileage of up to about 50 miles per gallon [24].

Today, different models of hybrid electric vehicles such as: Honda Accord Hybrid, Ford C-Max Hybrid, Honda Civic Hybrid, Lexus CT200h, Volkswagen Jetta Hybrid, Ford Fusion Hybrid, Hyundai Sonata Hybrid and different others appear on the market [25].

The purpose of this thesis work is to design a space-frame chassis for a small Hybrid Electric intra-city public transport quadricycle. For this reason, an overview of hybrid electric vehicles structure was made as follows.

2.2 Hybrid Electric Vehicles

Hybrid Electric Vehicle (HEV) means a vehicle that, for the purpose of mechanical propulsion, draws energy from consumable fuel and battery, capacitor, flywheel/generator or other electrical energy or power storage device. Together, these features result in better fuel economy without sacrificing performance. In addition to these, a hybrid electric vehicle captures energy normally lost during braking by using the electric motor as a generator and stores the captured energy in the battery. Hybrid vehicle propulsion system is mainly comprised of prime mover (ICE), Electric motor with DC/DC converter, DC/AC inverter, and controller, Energy storage system and Transmission. There are three most common drivetrain layouts for HEVs [4].

2.2.1 Series Drive-trains

In series hybrids, the wheels are solely driven by the electric motor. Thus the engine is not directly coupled to the wheels of the car, but to a generator, which converts the mechanical energy of the engine to electric energy. This electric energy is then split to charge the battery or drive the motor which is connected to the transmission. When more power is required to drive the vehicle, the motor draws power from both the battery and the engine[39].

2.2.2 Parallel Drive-trains

In a Parallel Hybrid, there are two parallel paths to power the wheels of the vehicle: an engine path and an electrical path. The transmission couples the motor/generator and the engine, allowing either, or both, to power the wheels [4].

2.2.3 Series-parallel Drive-trains

Series-parallel drive-trains merge the advantages and complications of the parallel and series drive-trains. By combining the two designs, the engine can drive the wheels directly, as in the case of the parallel drive-train or it can be effectively disconnected with only the electric motor providing power, as in the case of series drive-train. The Toyota Prius made series-parallel drive-trains a popular design. [29].

This system incurs higher costs than a pure parallel hybrid since it requires a generator, a larger battery pack, and more computing power to control the dual system [29].

2.3 POWERTRAIN COMPONENT SIZING FOR HYBIRDIZING

Argonne National Laboratory conducted a research on parameters that influence the performance of HEVs and developed empirical formulas for drive train component sizing which are used in this chapter. The constraints that should be given a special attention while sizing the drivetrain components are [13]:

0-60 miles per hour acceleration time in less than 12 seconds. The vehicle starts from rest with a state of charge of 0.7 and accelerates to 60 miles per hour.

50-70 miles per hour acceleration time in less than 8 seconds.

0-30 miles per hour acceleration time less than 5 seconds in all electric operation. This is assumed to be the lower performance limit of a vehicle that is drivable in a city environment in all electric operation. The vehicle starts at rest with a state of charge of 0.7 and the engine is not allowed to start at any time in the performance test.

6.5% grade at 55 miles per hour for 1200 seconds. The vehicle is allowed to use both engine and electric power. The initial state of charge of the vehicle is 0.7 and the final state of charge at the end of the test must be higher than 0.2.

Top speed at least 90 miles per hour. The vehicle at 0.7 state of charge must be able to go faster than 90 miles per hour with both engine and electric power.

There are many other performance qualities that can be considered. However, the optimization gets significantly more complicated as more constraints are added.

It is important to know the power requirement of a vehicle to determine the size of the power train components. The required power is used to overcome the rolling resistance, aerodynamic resistance and to determine the grade-ability of the vehicle.

The force required to move a vehicle against the rolling resistance is given by [32]:

$$F_r = \mu * m * g \text{..}(2.1)$$

Where, 'F_r' is the force needed to overcome the rolling resistance, 'μ' is the coefficient of the rolling resistance, m is the mass of the vehicle in 'Kg' and "g" is the gravitational acceleration in m/s^2.

Then the power needed to overcome the rolling resistance is determined as [32]:

$$P_r = F_r * V \text{..} (2.2)$$

Where, P_r is the power required to overcome the rolling resistance and V is the velocity of the vehicle in m/s.

On the other hand, the force required to overcome the aerodynamic drag force is determined as [32]:

$$F_d = \frac{\rho * C_D A_F}{2} * V^2 \text{...}(2.3)$$

Where, ρ is the density of air, 1.225 kg/m^3, C_D is the coefficient of drag, 0.33, A_F is the frontal area, 2.01 m^2, and V is the velocity of the vehicle, 24.58 m/s (55 mph).

Then the power required to overcome the aerodynamic resistance is determined as [32]:

$$P_d = F_d * V \text{...}(2.4)$$

Where, P_d is the power required to overcome the aerodynamic drag and V is the vehicle velocity in m/s.

The other parameter that must be determined is the grade-ability of the vehicle. The force required to overcome the maximum grade is determined as [32]:

$$F_g = mg * sin\phi \text{...}(2.5)$$

Where, F_g is the force required to overcome the maximum grade and, ϕ is the angle of inclination or slope.

Then the minimum power required to overcome the maximum grade is [32]:

$$P_g = F_g * V \text{..} (2.6)$$

Where, P_g is the power required to overcome the maximum slope and V is the vehicle velocity in m/s.

Then the minimum power required to move the vehicle up a grade is given by[32]:

$$P_{veh} = P_g + P_r + P_d \text{..} (2.7)$$

Hybrid electric vehicles (HEVs) are expected to meet two performance criteria in order to compete successfully with conventional vehicles. The first criterion is the time required to accelerate from zero to 60 miles per hour and the second is the ability to negotiate a minimum grade of 6.5^0 at a constant speed of 55 miles per hour (24.59m/s) for 20 minutes. In order to fulfill these requirements, the power required is estimated for parallel HEV topology considering the power required to accelerate on a leveled road and the power required to negotiate the 6.5% grade at 55 miles per hour (24.59m/s). Then the following empirical formula is used to determine the size of the components.

2.3 Acceleration Power

A hybrid vehicle that has an inertia mass of M_v and is accelerating on a flat road (i.e., 0° grade) requires a power P_a specified by the following equation at the wheels [13].

$$P_a = M_v V \frac{dv}{dt} + \frac{1}{2}\rho A C_d V^3 + M_v g V C_r \text{...} (2.8)$$

Where, v is vehicle speed, ρ is air density, A is vehicle frontal area, C_d is Coefficient of aerodynamic drag, g is gravity, and C_r is coefficient of rolling resistance.

Since the vehicle is accelerating from a stop to a maximum speed v_m , the acceleration power requirements can be restated by integrating the first term from zero to v_m.

$$P_a = \frac{M_v}{t_m}\left\{\frac{1}{2}V_m^3 + C_r g \int_0^{t_m} v\, dt\right\} + \frac{\rho A C_d}{2t_m}\int_0^{t_m} V^3\, dt \text{...} (2.9)$$

Where, t_m is the time taken to reach the maximum speed. The speed v in equation 4.9 is a function of time t. Assuming that the vehicle speed and time relationship is approximated by a hyperbolic function, speed v in equation 2 can be expressed as x [13]:

$$V = V_m\left(\frac{t}{t_m}\right)^x \text{...}(2.10)$$

The simplified equation for acceleration power P_a can be written as shown below[32]:.

$$P_a = a_1 M_v + b_1 \text{...}(2.11)$$

Where, $\boldsymbol{a_1 = \frac{v_m^2}{2t_m} + \frac{1}{1+x} C_r g v_m}$

and

$$b_1 = \frac{\rho A C_d}{2t_m}\int_0^{t_m} v^3\, dt = \frac{1}{2(1+2x)}\rho A C_d v_m^3 \text{...}(2.12)$$

The acceleration power estimates from the above described procedure represent power delivered at the wheels. Each component has its own power conversion efficiency and some losses are involved in mechanical components such as bearings. A design factor, k, is used to account for other losses and contingencies and the acceleration power becomes[13]:

$$P_a = k(a_1 Mv + b_1) \text{...}(2.13)$$

In the case of Bajaj Qute, the gross mass of the vehicle, $M_v = 760Kg$, $A_F = 2.07m^2$, $C_r = 0.008$, $V_m = 19.44 m/s$, $C_D = 0.33$, $t_m = 12 s$, $\rho = 1.225 kg/m.^3$ The value of X can be taken as 0.56[13]:

$$a_1 = \frac{V_m^2}{2t_m} + \frac{1}{1+x} C_r g V_m \text{...}(2.14)$$

$$= 19.442/(2*12) + 1/1.56*0.008*9.81*19.44$$

$$= 16.72438154$$

$$b_1 = \frac{1}{2(1+2x)} \rho A C_d v_m^3$$

$$= 1/(2(1 + 2 * 0.56)) * 1.225 * 2.07 * 0.33 * 19.443$$

$$= 2899.83505$$

Then ,

$$pa = k(a1Mv + b1)$$

$$pa = 1.1 * (16.72 * 760 + 2899.83)W$$

$$pa = 17167.733W$$

$$= 17.17KW$$

2.4 Grade-Climbing Power

Power (P_g) required to negotiate a grade that is represented by angle θ at a constant speed v_g could be written as follows [13]:

$$P_g = \frac{1}{2} \rho A C_d v_g^3 + M_v g v_g sin\theta + M_v g C_r cos\theta \quad \text{...(2.15)}$$

This equation can be simplified as[13]:

$$P_g = cM_v + d \quad \text{..(2.16)}$$

Where, $c = g v_g (sin\theta + C_r cos\theta)$ and

$$d = \frac{1}{2} \rho A C_d v_g^3$$

Taking a design factor, k=1.1, to account for mechanical losses and contingencies, the grade climbing power becomes [13]:

$$Pg = k(cMv + d)$$

$$C = 9.81 * 24.8 * (sin6o + 0.008 * cos6o)$$

$$= 27.36431365$$

$$d = 0.5 * 9.81 * 2.07 * 0.33 * 26.83$$

$= 5847.842696$

Then,

$P_g = k(cMv + d)$

$= 1.1(27.36\, X\, 760 + 5847.84)$

$P_g = 29305.584W$

$= 29.3KW$

2.5 Vehicle Mass

In the case of a hybrid vehicle, a smaller power unit (PU), a motor and an inverter, a generator, a battery pack, and a gear-drive or transmission (depending upon the hybrid design) will replace the conventional engine and transmission.

The drive train has several components, each with its own efficiency and specific power. The efficiency helps determine the power rating for the component, and the specific power determines it's mass. The drive train mass is specified as [13]:

$$M_{dt} = M_{pu} + M_{bat} + M_{mot} + M_{gen} + M_{tran} \quad (2.17)$$

Where,

M_{pu} = PU Mass, M_{bat} = Battery mass, M_{mot} = Motor and inverter mass, M_{gen} = Generator mass, and M_{tran} = Transmission mass.

Let $S_{pu}, S_{bat}, S_{mot}, S_{gen},$ and S_{tran} be the specific power for each of the five components and $P_{pu}, P_{bat}, P_{mot}, P_{gen},$ and P_{tran} is the power ratings. Then mass of each component can be computed as power divided by specific power[13]:

$$M_{pu} = \frac{P_{pu}}{S_{pu}} \quad (2.18)$$

$$M_{bat} = P_{bat}/S_{bat} \quad (2.19)$$

$$M_{mot} = P_{mot}/S_{mot} \quad (2.20)$$

$$M_{mot} = P_{mot}/S_{mot} \quad (2.21)$$

$$M_{gen} = \frac{P_{gen}}{S_{gen}} \quad (2.22)$$

$$M_{tran} = P_{tran}/S_{tran} \quad (2.23)$$

These mass and specific power values are for the complete component assembly including auxiliary and/or supporting units. For example, the motor assembly includes the inverter.

The values given in the following table are taken from the Toyota prius data and it has been used for component size estimation in this thesis [13].

Table 2.1: Specific values used for component sizing [13]

Battery	
Specific power at 20% SOC (W/Kg)	335
Specific energy (Wh/Kg)	49
Motor & generator(Permanent Magnet)	
Specific Power (W/kg)	360
Power unit (Gasoline)	
Specific Power (W/kg)	325
Motor with inverter	
Specific Power (W/kg)	360
Efficiency (%)	
Motor & inverter	90
Generator	95
Transmission	90

2.5.1 Power Unit (ICE)

The ICE is assumed to supply all the power needed to climb up an incline [13]:.

$$P_{pu} = P_g/\eta_{trans}$$

$$= 29.3\ KW/0.9$$

$$= 32.6\ KW$$

2.5.2 Traction Motor

The traction motor is assumed to supply the difference between the power needed to negotiate an incline and the power needed to accelerate the vehicle to 60 miles per hour in 12 s on a leveled road . Then the required power of the motor is [13]:

$$P_{mot} = (P_g - P_a)/\eta_{tran}$$

$$= \ ((29.3 - 17.17))/0.9\ KW$$

$$= 13.5\ KW$$

Mass of the traction motor can be estimated as [13]:

$$M_{mot} = P_{mot}/S_{mot}$$

$$= (13500)/360\ Kg$$

$$= 37.5\ Kg$$

2.5.3 Battery Pack

The battery supplies the difference between the power required to accelerate from zero to 60 miles per hour and that for grade climbing [13]:

$$P_{bat} = (P_g - P_a)/\eta_{trans}\eta_{mot}$$

$$= ((29.3 - 17.17))/((0.9 * 0.9))\ KW$$

$$= 14.2\ KW$$

Mass of the battery pack can be estimated as [13]:

$$M_{bat} = P_{bat}/S_{bat}$$

$$= 14200/335 kg$$

$$= 42.4kg$$

2.6 Chassis Frame.

The concept of chassis carries different connotations, depending on its area of application. In this thesis, the chassis is interpreted as the primary structure of a car, which carries and connects all systems and components of a vehicle. It is essentially the foundation of the car. Being the primary structure, the chassis has the fundamental duties of supporting the weight of all components of the car and taking the role of absorbing all loads resulted from longitudinal, lateral and vertical accelerations of the car during its operation without structural failure [33].

The chassis has certain attributes to possess to perform its roles for a car. These attributes guide the design and analysis of the chassis and its subsequent physical test when the chassis is manufactured

A chassis should have the following properties[6]:

The lightest possible weight in order to assist the car to achieve the highest possible performance.

High structural stiffness in order to have minimum deformations upon loading.

It must be able to withstand the impact loads and absorb the kinetic energy during impact.

A chassis must have both durability and reliability for the car to perform well. Low durability and reliability in the chassis induces inconsistency to the performance of the car.

A chassis has to be easily manufacturable.

2.7. Load Cases of Chassis

It is important to know about loads that the chassis has to withstand during the operation of the car so that the analysis can be conducted. In the design and analysis of the chassis, there are generally four types of static load cases [28]. These load cases are:

2.7.1 Lateral Bending

This load arises when the car moves about a corner at high speeds. The magnitudes of these forces depend on the speed of the car, the radius of the corner and the degree of the road banking. This load case is essential for areas of the chassis which are directly connected to the suspension. Chassis members in this area support the suspension directly and hence stresses in these members can be several times higher than those in members of other areas of the chassis [28].

2.7.2. Horizontal Loading & Lozenging

Horizontal loading load case arises when the car brakes or accelerates. When there is non-uniformity in traction, horizontal lozenging load case results. Same as the load case of lateral bending, this load case is essential for areas of the chassis which are directly connected to the suspension [28].

2.7.3. Vertical Bending

Vertical Bending arises from supporting the weight of all components of the car. Among them, those that are more dominant are driver, engine and differential system. Under dynamic condition, the magnitudes of these weights can be several times higher than those when they are in static condition [28].

2.7.4. Longitudinal Torsion

This load case is of the most importance for the chassis because of its influence on the structural torsional stiffness of the chassis, which contributes significantly towards the track performance of the car, particularly in the aspect of handling. This load case arises when the car strikes a bump or navigates corners at high speed. The chassis is twisted because of loads acting on one corner or two oppositely opposed corners of the car. The structural torsional stiffness of the chassis is highly significant because the ability of the suspension to tune the car's handling characteristic for high performance depends on it. Flimsy chassis renders the suspension to be useless and ultimately adversely influences the performance of the car [28].

2.8 Type of Chassis.

Ever since the invention of wheels, human beings have been attempting to create better modes of transport to mobilize people and cargoes from places to places. It was intuitive that a sort of structure has to be engineered for such purpose and this structure holds the key to the realization of that purpose because of its essentiality in connecting wheels and other important systems together. For these reason, different chassis types have been developed [28].

2.8.1 Ladder Frames.

Ladder chassis was used primarily as the structure for body-on-chassis construction, in which a separately manufactured body was mounted onto the chassis. In such construction, two parallel longitudinal beams with channel cross section laid on each side of the chassis and were reinforced with lateral cross members of the same cross section in a manner that is similar to the ladder configuration. The main consideration for this chassis was its structural bending stiffness and little attention was paid to structural torsional stiffness. Ladder chassis was popular mainly due to its ease of manufacturing and good bending stiffness. Today, ladder chassis is still widely used for heavy duty vehicles because of its extreme simplicity [30].

2.8.2 Backbone Tube Chassis

The back-bone tube design is very commonly found in sports cars. It consists of a strong tubular back bone which is usually rectangular in cross section that connects the front and rear suspension attachments of the vehicle [30].

2.8.3 Uni-body Frame

It is also known as the monocoque structure. In this design the vehicle frame and body are integrated into one single strong structure. It is a fully integrated body structure where the entire car is a load carrying unit that handles all the loads experienced by the vehicle i.e. the forces acting on the vehicle during motion, as well as the cargo loads. This frame is used now a day in most of the cars. Due to elimination of long frame it is cheaper and due to less weight most economical and its disadvantage is that repairing is difficult [30].

2.8.4 Space-Frame

Tubular space-frame construction was firstly initiated in the aerospace industry back in the era of World War II. As there were little breakthrough in the development of the chassis for racing application, researchers began to look for inspiration beyond the automobile industry and came to realize the possible application of the tubular space-frame construction to the chassis construction. In this chassis construction, multiple extrusions are spatially arranged in a truss-liked manner. These extrusions are usually small in cross section and are orientated such that each chassis member is only loaded in either tension or compression. During that time, race engineers were astonished with this chassis construction because of its effectiveness in improving the chassis structural torsional stiffness. With the advent of the tubular space-frame chassis, the development of the race car took a huge leap. As time progressed, race cars became lighter, faster and more predictable because of the excellent characteristics of tubular space-frame chassis. Still, there are drawbacks with this type of chassis construction. The manufacturing of tubular space-frame chassis is usually labor-intensive and time-consuming. Elaborate fixtures and jigs are required in order to precisely weld the chassis. Nevertheless, the tubular space-frame chassis was a major improvement in the development of the chassis despite these issues [30].

2.9 Chassis Material

When designing a chassis for optimal performance, a high stiffness to weight ratio is often wanted. The choice of material alone reveals nothing about how well the chassis will perform, its geometry and shape must also be considered. Generally, different grade steels, aluminum alloy etc. can be used depending on the type of the chassis [6].

Different researchers have made a study on optimizing and modification of chassis design. Some of them are summarized as follows:

Vikram Nair. (2012), Conducted a research on determining factors which affect the performance of space-frame chassis to improve its effectiveness of triangulation members for a Formula SAE Race car Frame. The aim of his work was to suggest factors which have significant effect on the torsional stiffness of a space frame without contributing excessively to its weight. The main focus was to maximize stiffness to weight ratio for a simple rectangular space frame while keeping various stresses acting along the section under the yield strength of the material. The node - element models were created in ANSYS classic and were analyzed for various load cases that are representative of the loads on a formula SAE chassis during operation. The procedures followed during the analysis were:

First, the node-element of a rectangular section of the frame model was created in ANSYS APDL and the required forces and boundary conditions were defined.

Then one parameter of the model was varied, such as the base length. Then, the deflection and peak stresses were recorded on a spreadsheet.

Next, the thickness and the outer diameter of the tube were varied.

Again, by adding triangulation of varying outer diameters and thicknesses, the frame was analyzed.

At the end, comparison and contrast of the results obtained in the spreadsheet were made to see the variance in stiffness to weight to the varying design parameters.

Here one a part of the model under investigation.

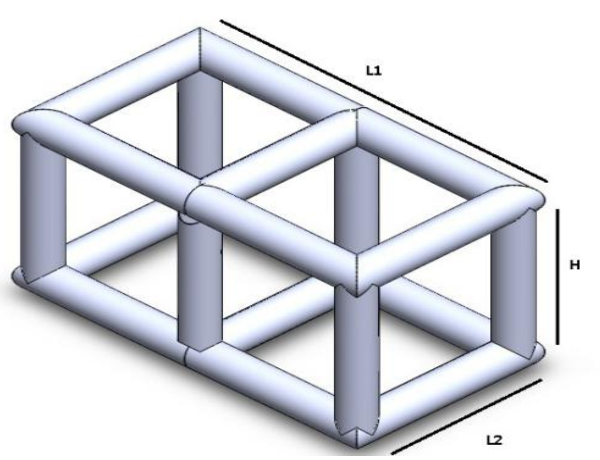

Figure 2.1: Rectangular box of welded tubes [41].

From the results, he concluded that:

1. The thickness of a tube for a fixed outer diameter has negligible effect on the stiffness to weight ratio. The stiffness is a function of the moment of inertia of the chassis about the neutral axis and the stress is a function of the section modulus of the chassis.

2. For a torsional case, the stiffness to weight ratio of a rectangular frame decreases with an increase in the ratio of the length of its sides L_1 and L_2, where L_1 is the moment arm, and the change in stiffness to weight is negligible for L_1/L_2 ratio greater than approximately 3. Hence for a rectangular section with L_1/L_2 ratio greater than 3, triangulation will be required and the increase in the stresses for a given size of tube with respect to the length ratio is small.

3. For a bending case, the stiffness to weight ratio of a rectangular frame also decreases with an increase in the ratio of the length of its sides L_1 and L_2 and the change in stiffness to weight is negligible for L_1/L_2 ratio greater than approximately 2. Similarly for a rectangular section with L_1/L_2 ratio greater than 2, triangulation will be required.

4. The angle variation of 30° to 60° considerably affects the stiffness to weight ratio of the structure. This indicates that the maximum number of triangles that can be created by keeping the angular variation between these limits would contribute positively to the stiffness to weight ratio of the structure.

5. The maximum number of triangles to achieve the highest stiffness to weight ratio for bracing a rectangular section is 2.

6. The stiffness to weight ratio increases for a uniform increase in outer diameter and thickness of the tube i.e., the thickness to outer diameter ratio remains constant.

7. The length or the length ratio has the highest effect on the stiffness to weight ratio as compared to outer diameter and thickness for a torsional case.

Madhu Ps. and Venugopal T R. (2014), Made Static Analysis, Design Modification and Modal Analysis of Structural Truck Chassis Frame. PRO-E software was used for developing 3D modeling and ANSYS was used for Finite Element Analysis. The chassis under investigation was constructed of Carbon steel, AISI 1080, which has Young's modulus (E) of 215 GPa, Yield strength of 800 MPa, Poisons ratio of 0.285 and Density of 7800kg/m^3. The chassis was constructed of two long rails and four cross members. Under the static analysis, they observed that the maximum Von mises stress was 181.69 MPa and the maximum deflection was 5.65 mm. the allowable stress was less than the yield strength, so stresses was not a critical issue, but deflection of chassis frame was about 5.64 mm which needed improvement. In order to minimize the deflection, they used different techniques. First they re-positioned the position of the third cross members and analyzed the result. Then they added additional fifth cross members to reduce the deflection without significant increase in the stress. Again in the third iteration they again added additional 6th cross member to further reduce the deflection and reduced the deflection to 3.706 mm [7].

Suraj Aru.et al. (2014), Designed multi-tubular space frame for terrain vehicles powered by a 300 cc engine. Pro-E software was used for developing the 3D modeling and ANSYS workbench 14.0 was used for finite element analysis. Front Impact, Side Impact, Roll-over and torsional stiffness analysis were made. They optimized the pipe diameter at different positions and they concluded that:

In the case of front impact and side impact analysis, the deformation of the front most member of the roll cage must be less than 10% of the clearance between driver roll cage members ensuring the safety of the driver. Though the factor of safety in front impact is 1.116 and in side impact is 1.446, deformation is within limit, ensuring that the driver is safe.

For front roll over, the deformation is important than the maximum stress. The deformation was 4.6033 mm and it is safe for the driver [8].

Nagarjuna Reddy.Y and Vijaya Kumar.S.(2011), Made a Study of different Parameters on the Chassis space frame for the sports car by using FEA. The model of the chassis space frame was developed using CATIA V5 and then imported to ANSYS 11.0 for FEA. Static analysis and modal analysis were made on the chassis. The overall length of the chassis was 2650 mm, the wheelbase was 2000 mm and its weight was 35 kilograms. During the analysis, the following assumptions were made:

The tyres were considered as linear springs.

The mass of the engine, gearbox and the other components were lumped and placed at center of gravity location of nodes.

The material used for the chassis had: young's modulus= 206900 MPa and density of 7850 Kg/m^3 and poisons ratio= 0.27. The outer diameter of the tube used was 13.1mm and the inner diameter was 11.75 mm. From the analysis results, they concluded that the chassis was stiff enough to carry all the loads applied on it under the static conditions [31].

Damtie Enawgew.(2013), Made a strength analysis of three wheeled vehicles. The software used for 3D modeling was CATIAV5 and ANSYS workbench 14 for FEA. The baseline vehicle used a semi monocouque chassis. The existing chassis was analyzed under static loading, front bump case, rear bump case, front impact, side impact and rear impact. Finally he designed a space-frame chassis. The main thing done in this research was changing semi-monocoque type of the existing structure to a space frame. He concluded that the results that he obtained was better in strength and stiffness, easy to manufacture and cost effective than the baseline model [10].

Eswar Vijayakumar. (2013), Made a Chassis Strength Evaluation and Rollover Analysis of a Single Seat Electric Car. The aim of the thesis was to build a single seat electric car. In this thesis, mass of the vehicle and the center of gravity position of the static vehicle were estimated and it was used to perform the chassis strength analysis and rollover analysis. For chassis strength analysis, three frame variants were analyzed with various beam cross sections and frame features such as fillets and gussets to optimize for torsional stiffness, bending stiffness, stress generated and weight. For steady state rollover analysis, the vehicle was tested for rollover tendency on various maneuvering conditions, road friction conditions, bank angles and vehicle property such as center of gravity location of the vehicle. Both analytical model and finite element analysis models were presented. The height of center of gravity for the baseline vehicle setup was 0.45 m and the load distribution was 63% in the rear axle and 37% in the front axle. From the results, he concluded that: the stress generated was higher in torsional test when compared to bending test and the torsional stiffness and the bending stiffness of the frame increases, with an increase in the number of structural members.

Ahmad Zainal Taufik et al. (2014), Designed and analyzed electric car chassis. CATIA V5 was used for the modeling. The chassis was modeled as beam elements with circular hollow sections from mild steel AISI 1018 having outer diameter of 32mm and 1.5mm thickness. A static analysis was performed on the chassis frame. The chassis was simulated with nine different loading conditions starting from 700 N to 1500 N. with a safety factor of 1.5. Simply supported constraints were used on the front and rear wheelbase points and the model was meshed as the tetrahedron meshes each element having a size of 3 mm. In most loading conditions, maximum stresses were below the yield stress and they concluded that the chassis was capable of dealing with the applied loads [9].

Rohit Walia. (2017), Performed structural strength analysis of car chassis under static and dynamic conditions. Solid work software was used for 3D modeling and ANSYS was used to make finite element analysis. The purpose of the research work was to determine the natural frequencies and mode shapes of the chassis under dynamic loading. In finite element analysis, the model of the chassis was created using 10 nodes tetrahedron elements and normal mode analysis was made. The results showed that, the first seven natural frequencies of the car chassis were below 100Hz and vary from 47.423 to 79.531Hz. He concluded that the overall modification performed on the chassis resulted in an improvement of the natural frequency by 30%, increased the torsional stiffness by 54% and reduced the total deflection by 34% but the overall weight of the new chassis was increased by 12% than the baseline model[11].

Harinath and Sartaj Patel. (2016), Designed, analyzed and optimized a race car chassis with the intension of stress on minimization and increasing the structural performance of the car. The whole car was modeled according to the 95th percentile male that can fit inside the cock-pit of the chassis. The protection was designed to the race car for driver safety using structural members. The structural members or triangulations were designed in such a way that the stresses were reduced in the front impact, rear impact, side impact and roll over collision of the chassis. Later the dimensions were taken for optimization. For this reason, the system was analyzed 65 times to arrive at the final dimension of the chassis.

Meanwhile, torsional rigidity was checked for the final dimensions and they concluded that all the stresses were below the material limit and the chassis was acceptable for manufacturing [12].

CHAPTER THREE

MATERIALS AND METHODS

3.1 Materials

The existing chassis is monocoque type which is made of high strength structural steel (ASTM A606) having the following properties.

Table 3.1: Material Property of High Strength Steel (ASTM A606) [20]

Material	**Density [g/cm^3]**	**Yield strength [Mpa]**	**Tensile Strength[Mpa]**	**Elastic Modulus [Mpa]**
A606	7.87	345	483	200

3.2 Research Methods

To conduct the proposed work, systematic procedures were followed as follows. First of all related literature on designing automobile chassis were reviewed. Following the literature review, collection of relevant data on the conventional Bajaj Qute took place by going to the companies which import the vehicle to Ethiopia and by direct field measurement. Having collected all the necessary data, 3D model of the existing four wheeler Bajaj Qute chassis was developed by using CATIA V5 software. Then the modeled chassis was imported to ANSYS 16.0 and analyzed for its performance under the application of different loads. Then having identified for the limitations of the existing chassis, the new proposed chassis was designed for four wheeler hybrid electric Bajaj Qute. After that, analysis of the new chassis was made to see its performance under different load conditions. Then repeated remodeling and analysis of the new design was made until the desired simulation result was obtained. Finally, comparison of the performance of the new chassis and the existing chassis was made and conclusion was given. Generally, the work flow chart is given in figure 3.1 below.

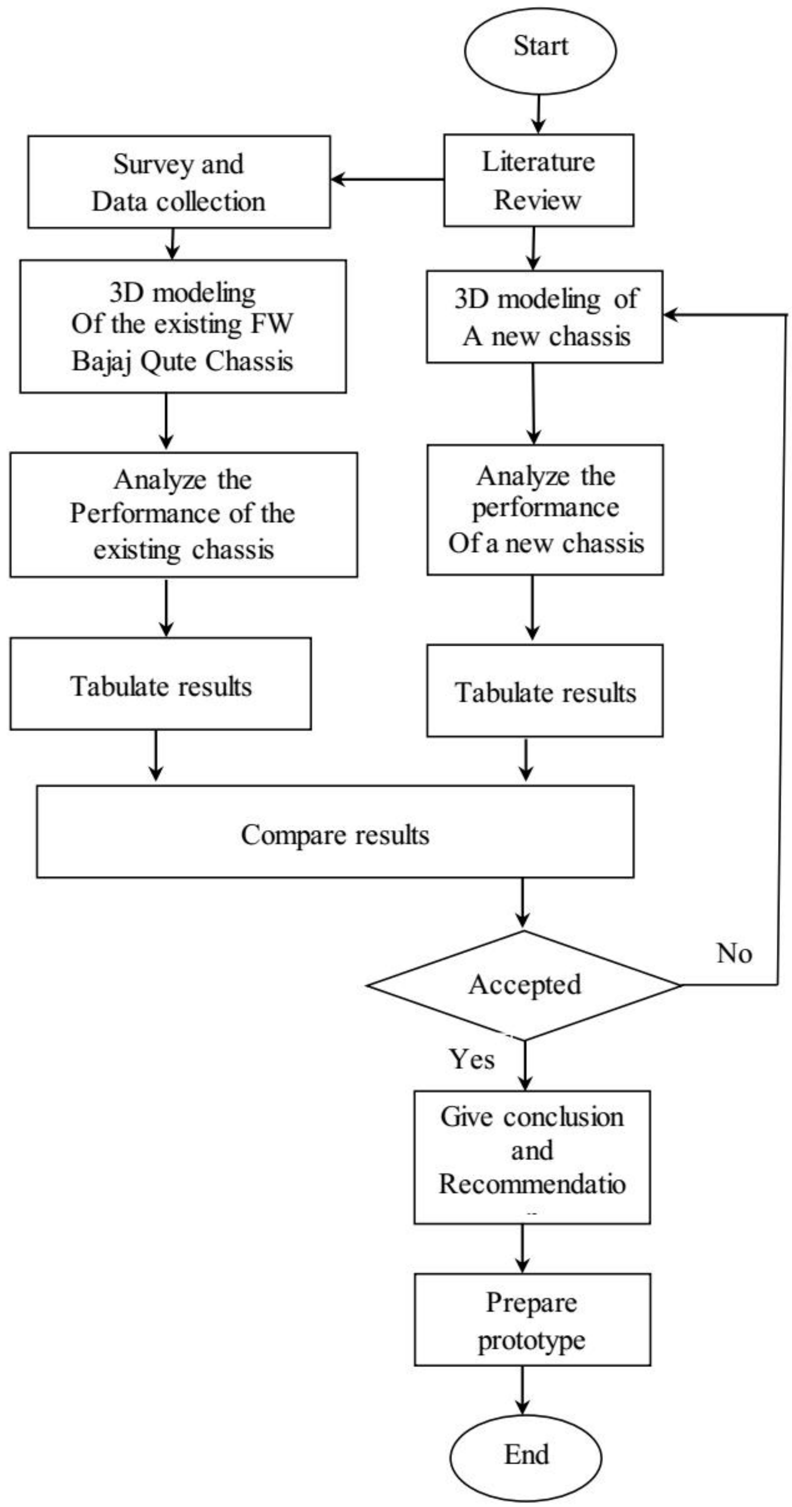

Figure 3.1: Flow Chart of Chassis Designing

3.3 Technical Specifications of the Existing Baja Qute

The technical specification of the existing Bajaj Qute was obtained from training manual of Bajaj qute and from field measurement. The training manual was provided by Horra Trading PLC. Main office, Addis Ababa[20]. Horra Trading is the only importer of Bajaj Qutes to Ethiopia.

Table 3.2: Vehicle Specification of the Existing Bajaj Qute.

ENGINE &TRANSMISSION	
Engine Type	Four stroke, spark ignition single cylinder oil cooled
Bore X Stroke(mm)	63.5*68.4
Engine Displacement(cc)	216.6
Compression ratio	11;1
Power	9.9KW @ 5500+ 250rpm as per IS14599:1999
Torque	19.6Nm @ 4000+ 150rpm as per IS; 14599:1999
Starting	Electric start
Spark plug	3 spark plugs
Spark plug gap(mm)	Central(0.8-0.9),side left hand and right hand(0.6-0.7)
Idling speed	1250±150 rpm as per IS; 14599:1999
Clutch	Wet multi disc clutch
Transmission	Constant mesh manual 5 forward and 1 revers speed
CHASSIS AND BODY	
Chassis Type	Monocoque chassis
SUSPENSION	
Front	Independent suspension, Twin leading arm

Rear	Independent suspension, coil spring semi trailing arm
Brakes	Hydraulic with H-split. All drum with diameter 180mm
Parking	Mechanical (cable operated) hand operated rear wheel braking
WHEEL RIM	
Front	135/70R12 (Radial Tubeless)
Rear	135/70R12 (Radial Tubeless)
Spare	135/70R12 (Radial Tubeless)
TYRE PRESSURE	
Front and Spare	2.1Kg/cm^2(30PSI)
Rear	2.4Kg/cm^2(34PSI)
Fuel Tank Capacity	8 liters(Nominal petrol)
ELECTRICAL SYSTEM	
Battery	12V,26AH
Head Lamp	35 X 35 W HS1
Tail Stop Lamp	5 X 21W
Side indicator Lamp	5W
Horn	12V DC-DIA 82
Reverse Lamp	10W
Wiper Motor	10volts single speed
Engine Management	ECU, Fuel injected
F/R Indicator Lamp	10W
Front position Lamp	3W
Cabin light	10W

DIMENSION	
Length	2752mm
Width	1312mm
Height	1652mm
Wheel Base	1925mm
Ground Clearance	180mm, Unladen
RECOMMENDED OIL GRADE AND QUANTITY	
Engine Oil	SAE10W30 API'SL'JASO'MA2' Grade upto ambient temperature of 5^{o}C. For ambient temperatures less than 5deg cel,5W30 or lower grades are recommended
Coolant	Ethylene glycol, distilled water 50:50 ratio pre mixed
Brake Fuid	DOT3
Windshield Washer	distilled water
Grease	NLGI 3

3.4 CAD Modeling of the Existing Bajaj Qute Chassis.

CATIA V5 was used to develop 3D modeling of the chassis. The parts which have different thickness were modeled differently in part design and then assembled in assembly design. The assembly was then saved in 'igs' format which was later imported to ANSYS for FEA. The assembly of the 3D model of the existing chassis is shown in figure 3.2

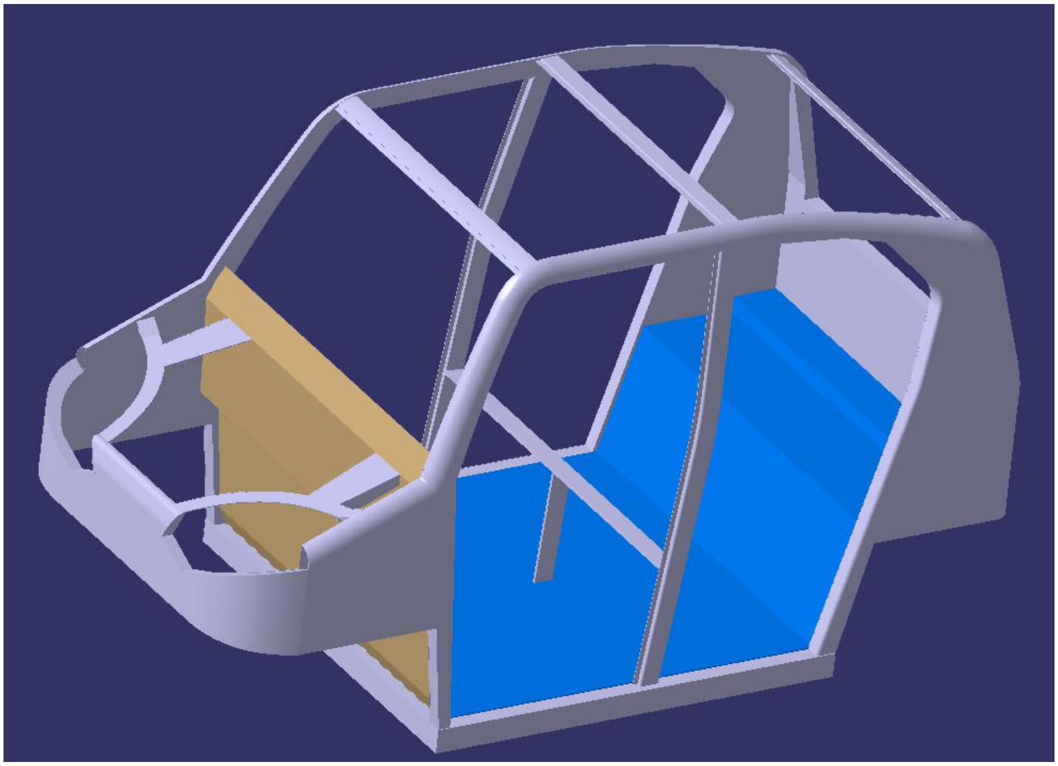

Figure 3.2: 3D CAD Model of the Existing Bajaj Qute

3.5 FINITE ELEMENT ANALYSIS (FEA) OF THE EXISTING CHASSIS

Finite Element Analysis (FEA) is a numerical method for solving problems of engineering and mathematical physics. It is useful tool for problems with complicated geometries, loadings, and material properties where analytical solutions cannot easily be obtained [38].

3.5.1 Static Analysis.

A static strength analysis calculates the effects of steady loading conditions on a structure, while ignoring inertia and damping effects, such as those caused by time-varying loads. This analysis determines the displacements, stresses, strains, and forces in structures or components caused by loads that do not induce significant inertia and damping effects [10].

The loads were due to the weight of components and capacity of the vehicle (passengers + driver + payload). The support loads from the axles were distributed through spring hangers. The loads were applied as a uniformly distributed load on the seat area and as point load at the suspension mounting points. The unladen weight of the vehicle was divided between the front and the rear axle taking 48% load distribution on the front axle and these loads were applied as a point load at the midpoint of the axle. These point loads are statically equivalent to the actual distributed load.

The applied loads are:

The load due to the unladen weight of the vehicle and payload. The unladen weight of the vehicle and payload is $440\ \mathrm{kg}$ and hence, $440 * 9.81\mathrm{N} = 4316.4\mathrm{N}$ force was applied on the two axles taking 48% load distribution on the front axle. The front axle receives a load of $0.48 * 4316.4\mathrm{N} = 2071.872\mathrm{N}$ and the rear axle receives a load of $4316.4\mathrm{N} - 2071.872\mathrm{N} = 2244.528\ \mathrm{N}$.

The load due to the capacity of the vehicle. The vehicle is 4 seat vehicle including the driver. Hence, 80*9.81N = 784.8N force is applied on each seat area of $250\mathrm{mm} * 350\mathrm{mm}$ as a uniformly distributed load. The magnitude of the uniformly distributed load(P) becomes:

$$P = \frac{784.8\mathrm{N}}{0.25 * .035\mathrm{m}^2}$$

$$= 8969.142857\ \mathrm{Pa}.$$

In order to get the axle supporting reaction loads, the total vehicle mass is 760kg and therefore, the weight(W) of the vehicle will be:

$$W = 760 * 9.81\mathrm{N} = 7455.6\mathrm{N}$$

Therefore, totally 7455.6N static load was applied on the vehicle.

Taking 48% load distribution on the front axle, the front axle receives (R_f):

$R_f = 0.48 * 7455.6\mathrm{N} = 3578.7\mathrm{N}$;Where, R_f is the total load on the front axle. Then, each right and left suspension develops:

R_{fr}=Rf_l=3578.7/2N = 1789.4N; where, R_{fr} is the reaction force at the front, right suspension mounting point and Rf_l is the reaction force at the front, left suspension mounting point.

The rear axle receives (R_r) of 3876.9N force; where, R_r is the total axle load at the rear axle.

Hence, each suspension mounting point develops

R_{rr}=R_{rl}=$\frac{3876.9}{2}$N =1938.45 N reaction force which was directed vertically upward; where, R_{rr} is the rear, right suspension reaction force and R_{rl} is the rear, left suspension reaction force.

Finally, the lower edges of the chassis were constrained in the Z direction.

Generally, the load and boundary condition used to make the static analysis is shown in the figure 3.3.below.

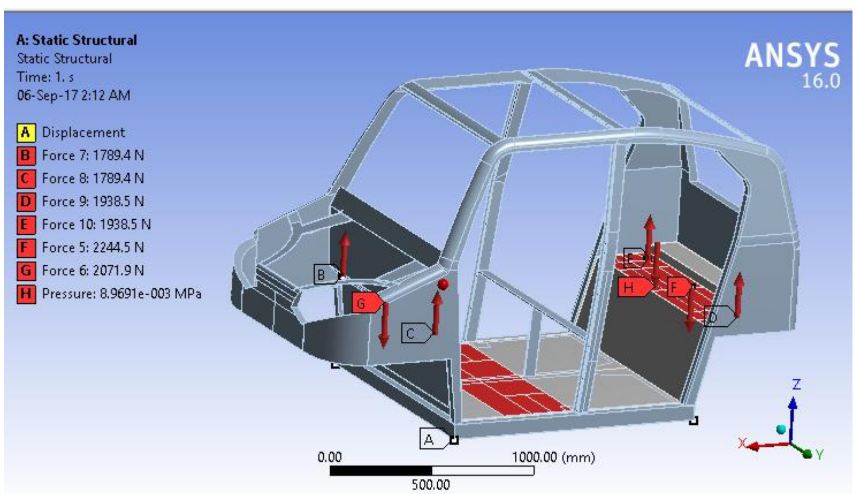

Figure 3.3: Loading and Boundary Conditions for Static Analysis

Totally, fine tetrahedral mesh was applied on the whole components of the model. In order to get good results, highly refined mesh was used on windshield pillars, roof side rail, roof cross beams, on instrument panel, floor, on the front bumper, on joint points of the instrument panel with the side fenders and around the joints where more stress concentration is suspected. Before deciding the quality of mesh to be used, mesh convergence analysis was made repeatedly and finally the mesh which showed the same results was selected.

Generally, 307405 nodes and 152258 elements were used. The mesh is shown in figure 3.4 below.

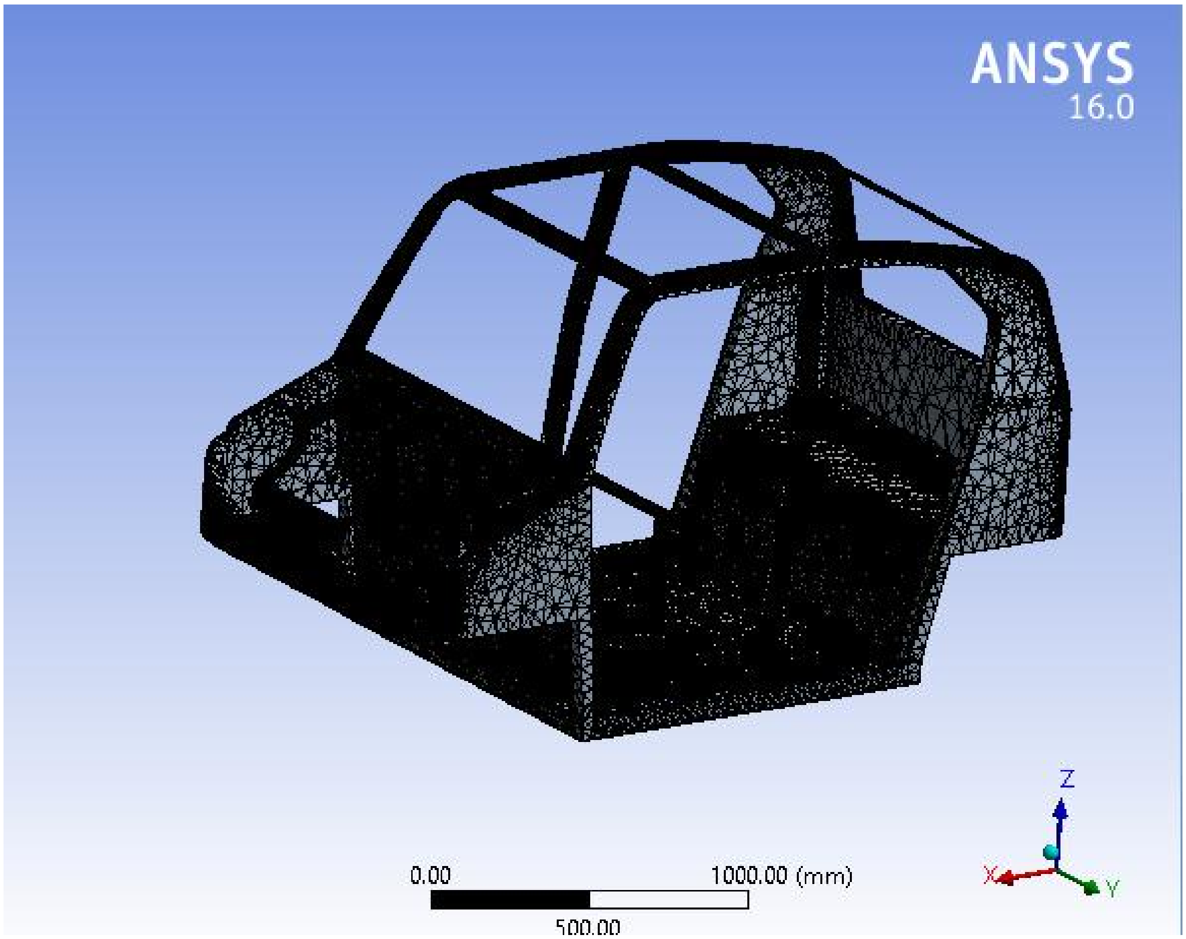

Figure 3.4: Mesh used for the Analysis of the Existing Bajaj Qute

3.5.2 Full Frontal Impact Analysis

The front impact analysis was made to see the safety level of the driver and passengers in case of a head on collision.

There are three frontal crashworthiness tests specified in National Highway traffic safety Administration (NHTSA). The agency established a frontal impact test program whose protocol is based on the Federal Motor Vehicle Safety Standards (FMVSS), the U.S.A standards. These are the full-frontal, right and left-oblique frontal (± 30 degrees from perpendicular), and 40 percent offset-frontal. From these three, high injury rate was recorded in full frontal impact and for this reason, only the full frontal impact analysis has been selected for analysis in this thesis [34].

Under the frontal collision, the frontal components should not be jostled rearward and impact into the front-door hinges and door latch system. There must not be any intrusion of frontal structures rearward through the windshield into the passengers' compartment. The front passengers and the driver should have the protection of a seatbelt-restraint system, preferably integrated within tough seats, with strong anchorages [16].

In this thesis, the front impact analysis was made according to the U.S.A standard requirements as it is mentioned in the Federal Motor Vehicle Safety Standards (FMVSS) [16]. It declares that, "When a vehicle traveling longitudinally forward at any speed up to and including 48.3 Km/h impacts a fixed collision barrier that is perpendicular to the line of travel of the vehicle, no part of the vehicle outside the occupant compartment, except windshield molding and other components designed to be normally in contact with the windshield, shall penetrate the protected zone template to a depth of more than 6.4 mm." The velocity 48.3Km/h was specifically selected for analysis because, vehicles of this category are used in city driving and this velocity was the most commonly encountered velocity in city driving.

Taking the maximum speed mentioned, 48.3Km/h (13.33m/s), the Energy transferred, when two objects of masses m_1 and m_2 having velocity of u_1 and u_2 respectively collide (For a perfectly inelastic collision) will be [10]:

$$E_t = \frac{m_1 * m_2 * (u_1 - u_2)^2}{2(m_1 + m_2)} \quad \text{..........(3.1)}$$

In the case of Bajaj qute, both m_1 & m_2 are two Baja qutes with similar masses & the vehicle m_2 is at rest. Hence, $m_1 = m_2$ & $u_2 = 0$ then,

$$E_t = \frac{2m_1(u_1 - 0)^2}{2(2m_1)}$$

$$E_t = 0.25 * m_1 * u_1^2$$

Then the impact force becomes, $F = \frac{E_t}{t}$

The gross weight of Bajaj qute, is $760\ kg$ and the maximum velocity specified in Federal Motor Vehicle Safety Standards (FMVSS) for front impact analysis is 48.3Km/h (13.33m/s)[16]. Hence the impact force becomes,

$$F = 0.25 * 760 * 13.33^2 N$$

$$= 33777.78\ N$$

This force was applied as a uniformly distributed load on the frontal area of 0.105 m^2 which was determined from the geometry of the vehicle. Then, the uniformly distributed load (P) equals:

$$P = \frac{33777.78N}{0.105m^2} = 321693.1429Pa.$$

Therefore, $321693.1429Pa$ load was applied in addition to the static loads. The lower edges of the chassis were constrained in the X, Y and Z direction.

Generally, the loading and boundary condition is shown in figure3.5.

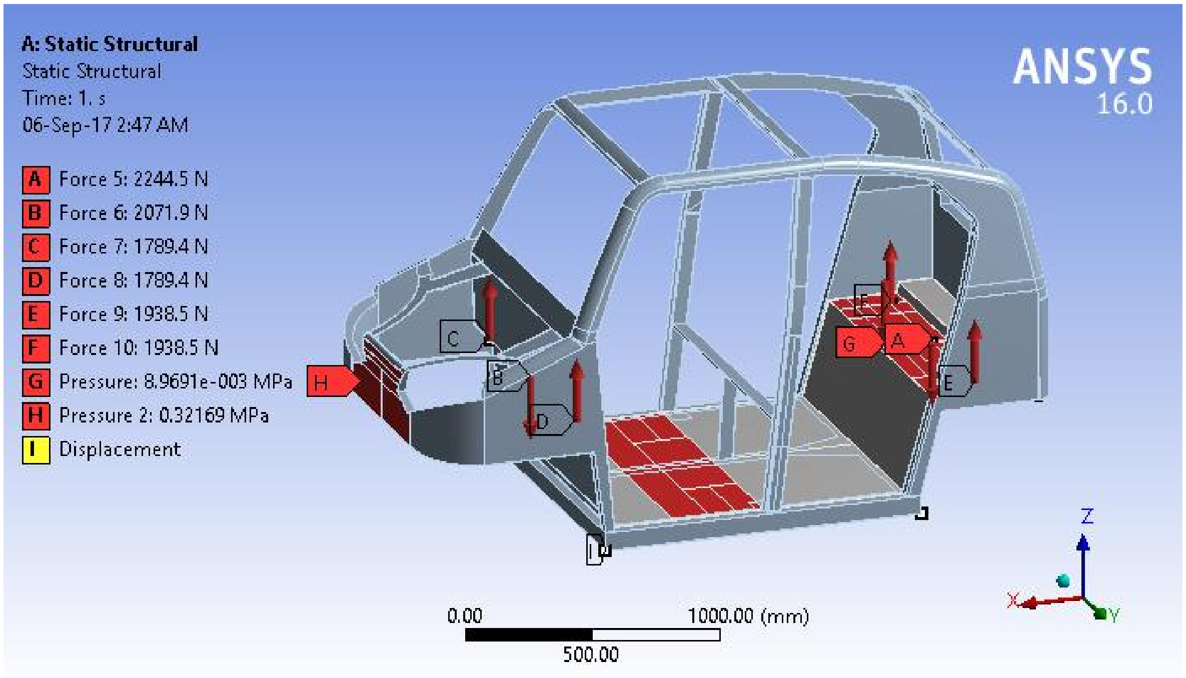

Figure 3.5: Load and Boundary Conditions for Front Impact Analysis

3.5.3 Side Crash Test

Side impact analysis of the vehicle was made to see the strength of the chassis in the case of accident involving the vehicle hit by another vehicle from side.

In order to have good passengers' safety under side impacts, the vehicle should have strong frame members and the sections that are at the outermost periphery of the vehicle body. These members should be internally reinforced with a baffle plate, or with rigid-foam filling, or both. Such reinforcement measures will typically increase the compressive and bending strength of the hollow member that it is filling. The doors should have internal reinforcement beams, with strong hinges and door-latch system. The cab should have side curtain airbags that inflate in side impacts, and in rollovers. The side windows must be of enhanced protective-glass design [42].

The impact force which was determined in section 5.4.2 was applied as a uniformly distributed load on the area of $0.175 m^2$ which was determined from the geometry of the vehicle. Then the magnitude of the uniformly distributed load (P) will be:

$$P = \frac{33777.78N}{0.175m^2} = 193015.8857Pa.$$

The lower edges of the chassis which is on the opposite side to the side on which the impact force was applied was constrained in X, Y, and Z direction. The other static loading forces and the mesh remained the same.

Generally, the initial boundary conditions and load definition is shown in figure 3.6.

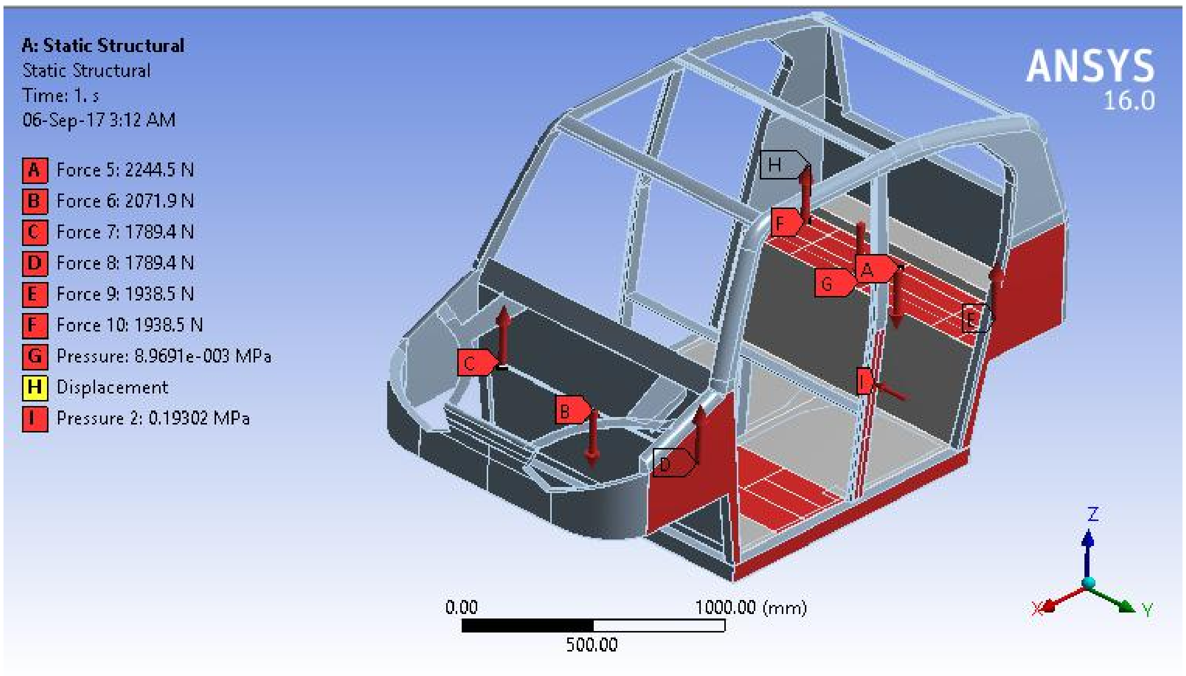

Figure 3.6: Loads and Boundary Condition for Side Impact Analysis

3.5.4 Rear Crash Test

Rear impact analysis of a vehicle was made to see the strength of the chassis in the case of accident involving the vehicle hit by another vehicle from the rear.

To have a good safety in the case of rear impact, the seats should be designed with high backrests and integrated head restraints to help keep the head, neck, and upper torso in safe alignment during the dynamics of a crash. Roof pillars, windshield header, side rails, and cross-members, all internally reinforced with baffle plates and lightweight-rigid foam, thereby increasing each member's compressive and bending strength [42].

In the case of rear crash test, the impact force which was determined in section 5.4.2 was applied as a uniformly distributed load on the area of $0.12m^2$ which was determine from the geometry of the vehicle. The magnitude of the uniformly distributed load (P) will be:

$$P = \frac{33777.78N}{0.12m^2} = 281481.5Pa.$$

The lower four edges of the chassis were constrained in all directions.

The mesh and the other static loading forces remained the same.

Generally, the initial boundary conditions and load definition is shown in figure 3.7.

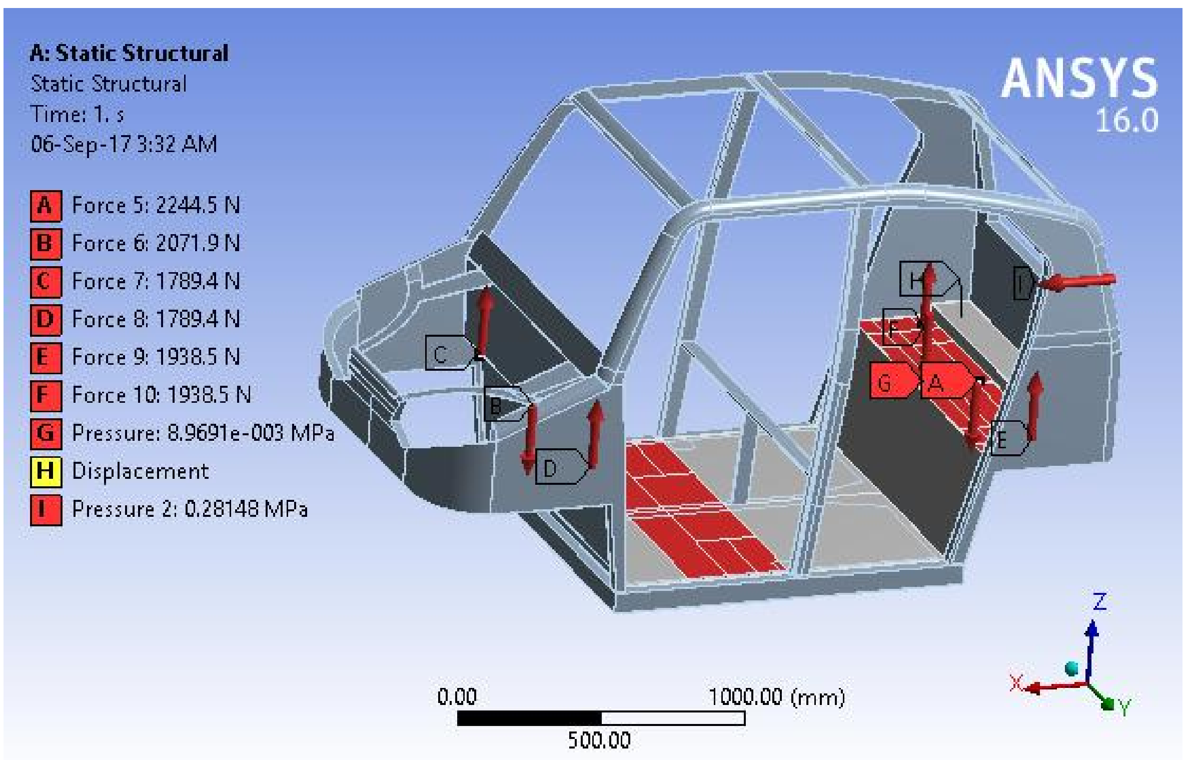

Figure 3.7: Load and Boundary Conditions for Rear Impact Analysis

3.5.5 Front Rollover Analysis

Rollover analysis of the vehicle was made to see the strength of the roof in the case of a rollover accident. The windshield pillars and front roof cross beam should be strong enough to carry the load in the case of front rollover accident [42].

The Federal Motor vehicle Safety Standard (FMVSS) declares the rollover analysis shall be made by applying a force equal to 3.0 times the unloaded weight of the vehicle in kilograms and multiplied by 9.8, for vehicles weighing less than 2,722 kg on the roof structures [19].

The total unloaded vehicle mass is 440 kg and therefore $3 * 440 * 9.8\ \mathrm{N} = 12936\mathrm{N}$ was applied as a uniformly distribute load on the area of 0.09 m^2 which was determined from the geometry of the vehicle. Therefore, the magnitude of the uniformly distribute load (P) becomes:

$$P = \frac{12936\mathrm{N}}{0.09\mathrm{m}^2}$$

$$= 143733.33\ \mathrm{Pa.}$$

Generally, the loading and boundary condition is shown in figure 3.8.

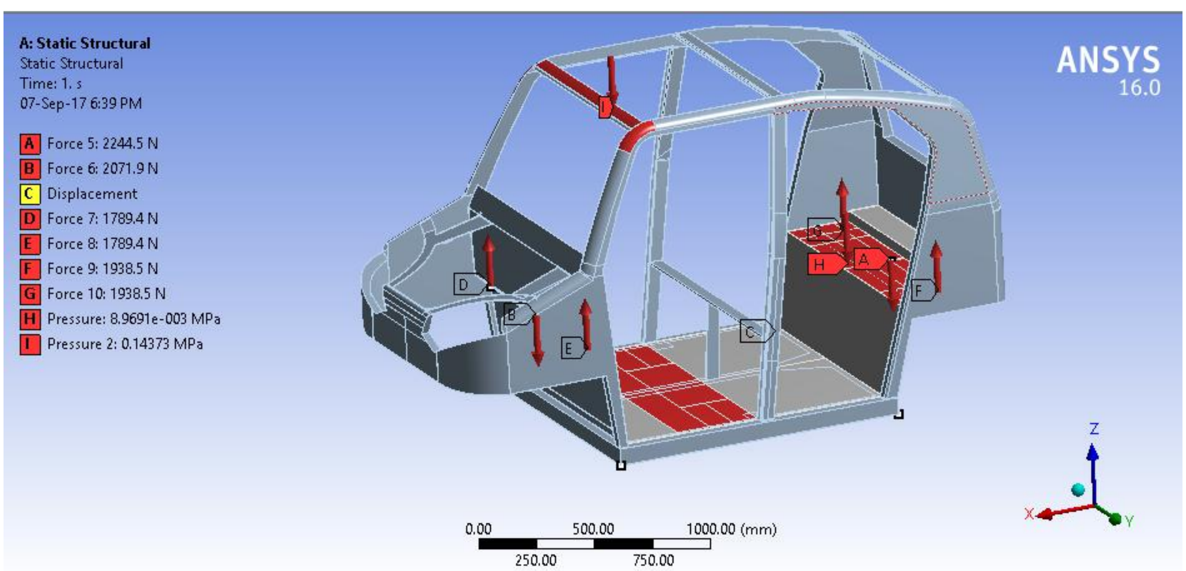

Figure 3.8: Loads and Boundary Conditions of the Front Rollover Analysis

3.5.6 Side Rollover

The roof structural integrity should be capable of being maintained in a dynamic lateral rollover analysis. Side-curtain airbags should inflate when the sensors determine that a lateral rollover sequence is beginning [42].

To make the side rollover analysis, the boundary conditions remain the same as that of front rollover analysis except the load that was applied on the front cross beam of the roof. The area on which the uniformly distributed load was applied in case of side rollover accident is $0.13m^2$ and it was determined from the geometry of the vehicle. Then the uniformly distributed load (P) was:

$$P = 99507.69231Pa.$$

This load was applied to the roof side rail.

The loading and boundary condition is shown in the figure 3.9.

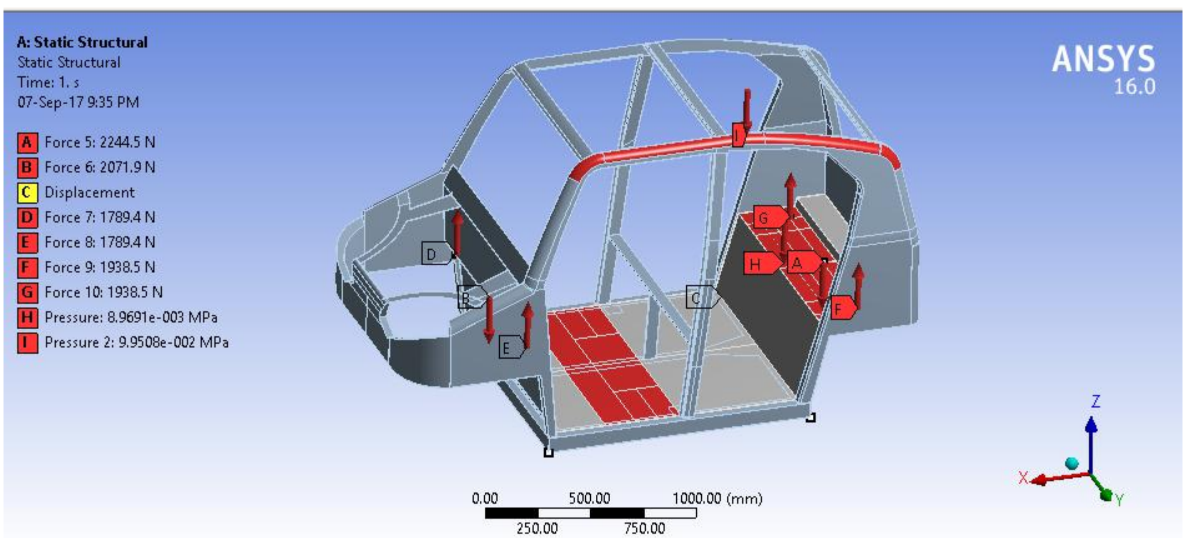

Figure 3.9: Loads and Boundary Conditions of Side Rollover Analysis

3.5.7 Modal Analysis

When a vehicle travels on a road, the chassis is excited by dynamic forces induced by the road roughness, engine, transmission and other vibration sources. Under such various dynamic excitations, the chassis tends to vibrate. Static analysis does not consider the variation of load with respect to time. Variation in variables with respect to time couple is predicted through dynamic analysis. Dynamic analysis predicts these variables with respect to time/frequency. The modal analysis is used to find the natural frequency and mode shapes of structures [42]. A mode is a shape of deformation with a corresponding natural frequency at which the structure absorbs all the available energy supplied by an excitation. If any one of the natural frequencies matches with excitation frequency, the frame doesn't satisfy the dynamic characteristics and resonance occurs. Resonance is the condition of the chassis where failure occurs [43].

3.6 DESIGN AND ANALYSIS OF THE NEW CHASSIS

3.6.1 The Need of Designing a New Chassis

It was observed from the simulation results that, the performance of the existing chassis was not good under side impact, rear impact and front rollover. The simulation results of the existing chassis are summarized in table 3.3.

Table 3.3: Summary of Simulation Results of the Existing Chassis.

Analysis type	**Maximum equivalent stress [Mpa]**	**Maximum deformation[mm]**	**Safety factor**	**Remark**
Static Analysis	150.72	1.34	1.6	Good
Full frontal impact	2228.6	21.69	0.11	Poor
Side impact	857.46	10.47	0.29	Poor
Rear impact	2645.2	17.65	0.09	Poor
Front roll-over	2623.4	37.03	0.09	Poor
Side roll-over	701.14	3.45	0.35	Good

As it can be seen from table 3.3, the existing vehicle is not safe under the side impact, rear impact and front rollover. Therefore, a vehicle which has better safety level under these accidents is needed.

On the other hand, as it can be seen from the modal analysis (figure 5.16), the deformation of the existing chassis is highly fluctuating under the first 12 modes which indicate that, there are some weak components in the structure. From figure 5.16, the peak deformation existed at the 10^{th} mode and emphasis has to be given to the deflection of the chassis in this mode of vibration.

To minimize these shortcomings of the existing chassis, a new space-frame chassis has been designed.

3.7 CAD Modeling and Tube Diameter Optimization

The CAD modeling of the new chassis has been through repeated modifications. As much as possible, it is required that, the total weight of the vehicle should be small to have better acceleration and good fuel economy. To fulfill this requirement, small diameter pipe with small thickness is preferable. On the other hand, the safety of the chassis has to be higher and higher as much as possible (high rigidity). To fulfill this criterion, a large diameter pipe with a large thickness is preferable. These two points contradict with each other and optimization has to be made between the two. For this reason, pipes with different diameters have been selected and optimization has been made on its thickness. First, the chassis with a minimum allowed outer diameter of 25.4 mm was selected and its internal thickness was varied from the minimum allowed thickness value (2.41 mm) up to 5 mm and its performance was observed by simulating the chassis under static loading condition in ANSYS. Pipes with this outer diameter showed high equivalent stress under static loading. Then a pipe with outer diameter of 35 mm was modeled and its inner thickness value was varied from 2.41mm (minimum thickness allowed) up-to 5mm and its performance was evaluated under static loading condition in ANSYS. Again all the derivatives of this outer diameter pipes showed high equivalent stress under static loading. Then, the inner diameter of the pipe was taken to be 35mm and the outer thickness of the pipe was varied from 2.41mm up-to 5mm and its performance was observed. Then a pipe with outer diameter of 39 mm and inner diameter of 35mm (4 mm thickness) showed good result under static loading and it was selected for further analysis.

The 3D model of the selected chassis was made in CATIAV5 and it is shown in figure 3.10 below.

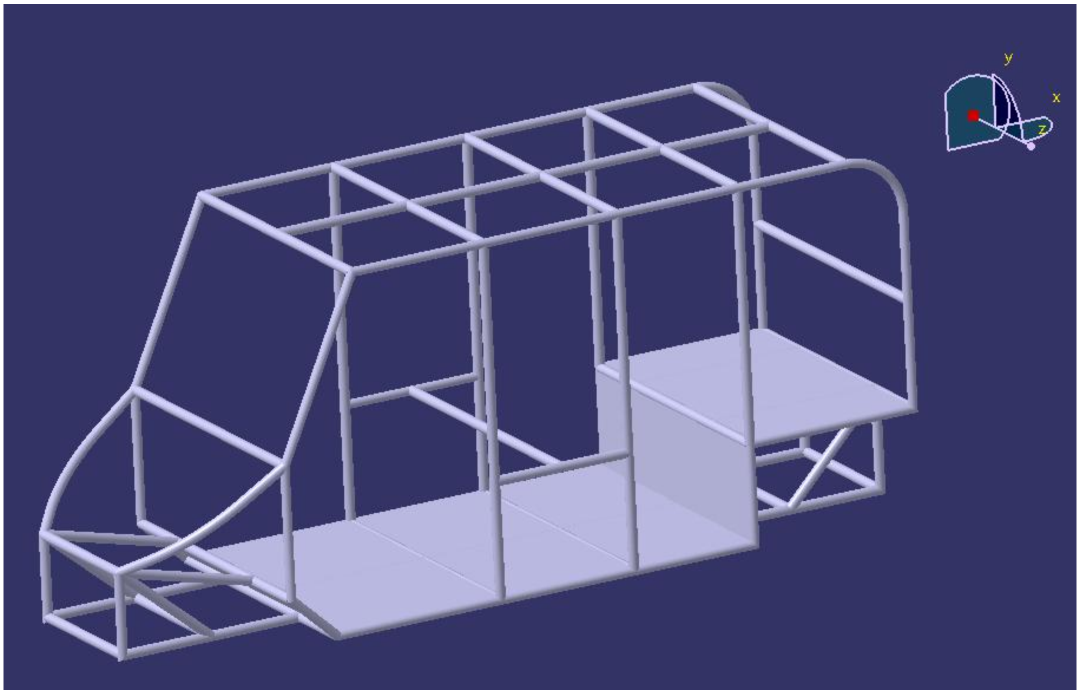

Figure 3.10: 3D CAD Model of the New Chassis.

The dimensions of the new chassis are given in Appendix A.

Emphasis has been given to ergonomic consideration to ensure the comfort of driver and passengers. In this thesis, to have sufficient space for seats, the seat spacing requirement for passenger vehicles have been taken to fulfill the requirements for the 95th percentile male. The 95th percentile itting poition is shown under qppendix B.

Sufficient space has been left for placing the battery pack and mounting the drive train components. The vehicle is four seat vehicle. The battery pack is placed at the rear of the first seat row and in-front of the rear seat row on the floor at a safe place. The battery pack is free of the front impact and rear impact. In the case of the side impact, good protection zone has been created on the geometry of the vehicle to protect the passengers and the battery pack from the impact. Furthermore, by placing the battery pack at this place, the weight distribution of the vehicle will not be altered and as a result of this good vehicle handling can be achieved. The placement of the driveline components is shown under Appendix C.

3.8 FINITE ELEMENT ANALYSIS OF THE NEW CHASSIS.

3.8.1 Static Analysis

The mass of the parallel hybrid electric vehicle can be estimated as 5% greater than the mass of its equivalent conventional vehicle [13]. In this thesis, only traction motor and traction battery pack were added to the conventional vehicle powertrain and for this reason, the estimated weights of this components are added to the weight of the existing vehicle to estimate the over whole weight of the new vehicle.

The Procedures followed in the analysis of the existing chassis were repeated in this analysis. The applied loads are given below.

The mass of the estimated battery pack is 42.4Kg and the mass of the traction motor is 37.5Kg. The sum of the two will be 37.5Kg + 42.4Kg =79.9Kg. the total mass of the existing vehicle without passengers and driver is 440Kg. hence adding the weight of the battery pack and traction motor to the existing vehicle weight, the weight of the new vehicle without passengers and driver will be $440\text{Kg} + 79.9\text{Kg} = 519.9\text{Kg}$ which is still lower than the limited mass of the vehicles under L7e category. Therefore, the total load due to this mass will be 519.9Kg*9.81 =5100.22N. Taking 48% load distribution on the front axle, the front axle will be loaded by $0.48 * 5100.2\text{N} = 2448.1\text{N}$ and the rear axle will be loaded by $0.52 * 5100.2\text{N} = 2652.1\text{N}$.

The vehicle is 4 seat vehicle. Therefore the $80\text{Kg} * 9.81\text{m/s2} = 784.8\text{N}$ force was applied as a uniformly distribute load at each seat position.

The uniformly distributed load will be:

In order to determine the reaction forces at each suspension mounting point, the total mass of the vehicle is 839.9Kg. Taking 0.48% load distribution on the front axle, the front axle receives a load of 0.48*839.9*9.81N=3954.92112N. Hence, each left and right front suspension develops a reaction force of $3954.92N/2 = 1977.46056\text{N}$. On the other hand the rear axle receives a load of $0.52 * 839.9 * 9.81\text{N} = 4284.49788\text{N}$. Then each left and right rear suspension develops reaction force of $4284.5\text{N}/2 = 2142.25\text{N}$.

The lower edges of the chassis were constrained in X, Y and Z direction.

Generally, the load and boundary conditions are shown in figure 3.11 below.

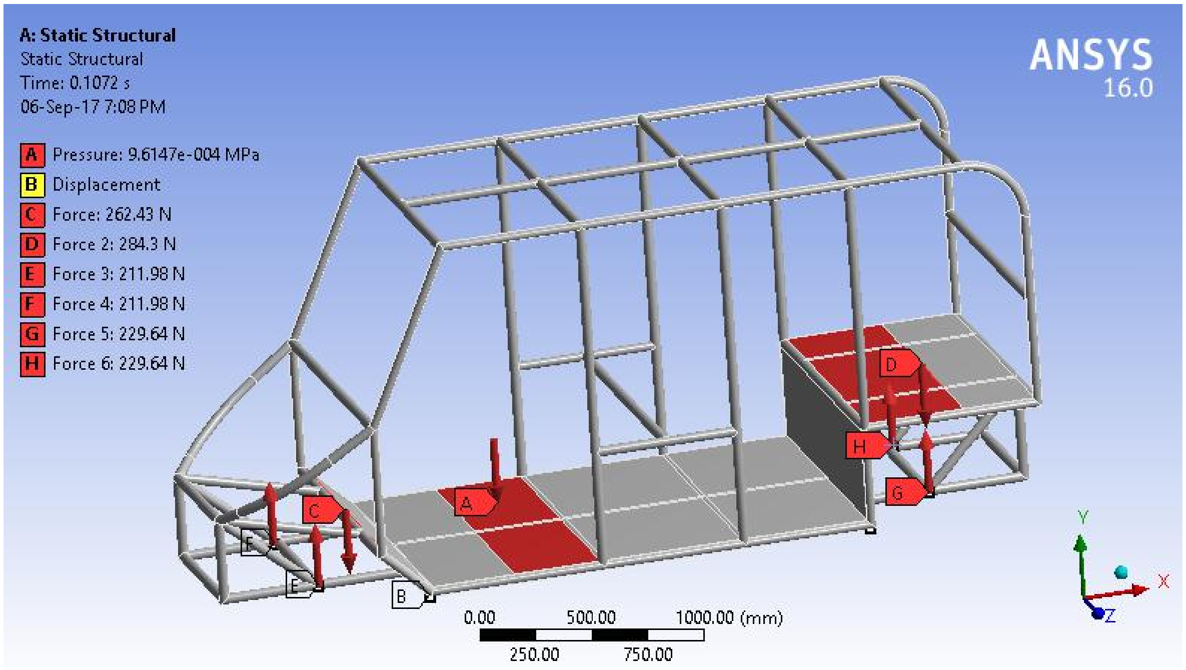

Figure 3.11: Loading and Initial Boundary Conditions for Static Analysis.

Similarly as it has been used in the analysis of the existing chassis, Tetrahedron mesh has been used for the analysis. Fine mesh was used on the whole body of the vehicle and further refinement has been made on the areas suspected to have more stress. Before becoming sure on the quality of the mesh, mesh convergence analysis was made and finally the mesh with 371994 nodes and 191710 elements were used.

The mesh is shown in figure 3.12 below.

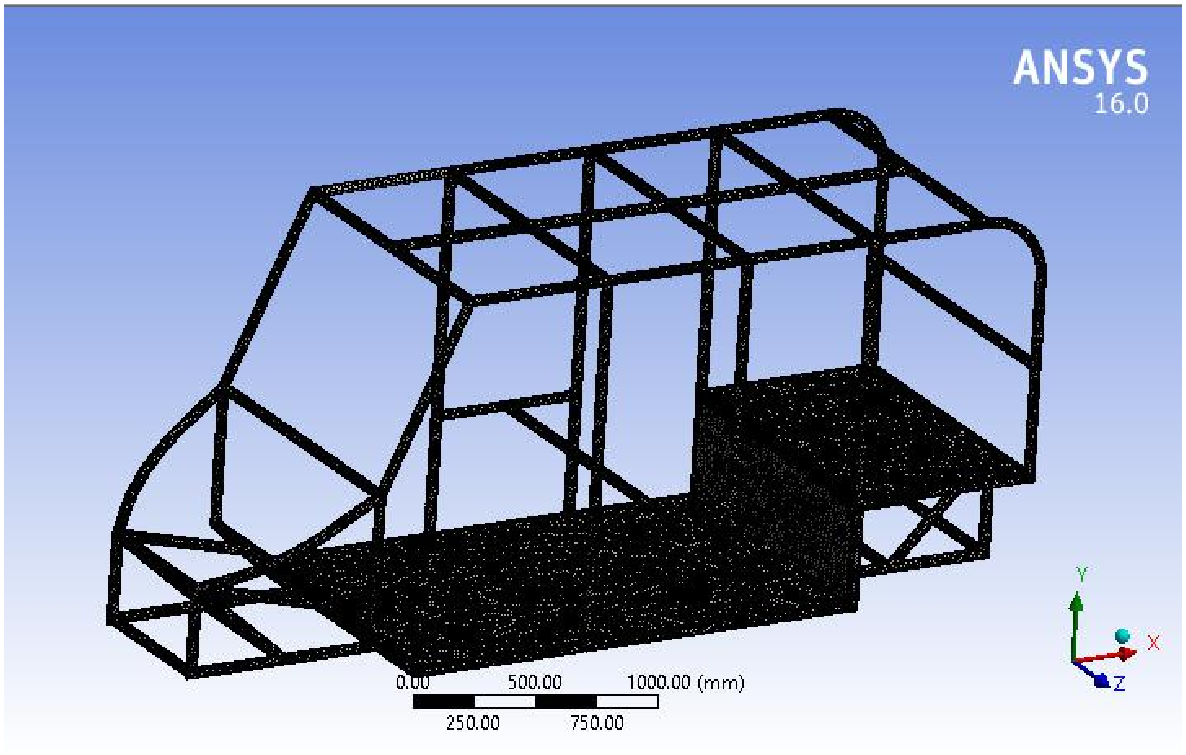

Figure 3.12: Mesh Used for the New Chassis Analysis.

3.8.2 Full Front Impact Analysis

Similarly as the procedures used in the analysis of the existing vehicle, the procedures specified in the Federal Motor Vehicle Safety Standard (FMVSS) has been repeated for frontal impact analysis [16].

The estimated total weight of the new vehicle is 839.9Kg and hence, the impact force during the frontal impact at the maximum specified speed by the FMVSS[16] is $0.25 * 839.9 * 13.33^2\text{N} = 37226.26\text{N}$. this force was applied as a point load on four points on the frontal area of the vehicle. Therefore, each point will be loaded by $37226.26/4\text{N} = 9306.6\text{N}$. The other loads remain unaltered as it was applied in static analysis.

Finally, the Loading and boundary condition is shown in figure 3.13 below.

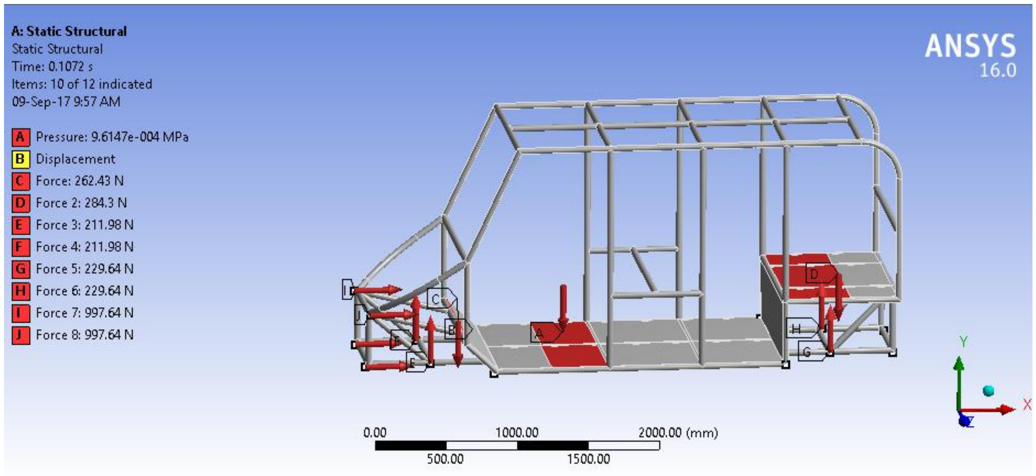

Figure 3.13: Loading and Initial Boundary Conditions for Frontal Impact Analysis

3.8.3 Side Impact Analysis

In this case, the impact force was applied as a point load on four points which are liable to the impact.

Then the magnitude of the load at each point will be $37226.26\text{N}/4 = 9306.565\text{N}$(Using equation 2.1).

This load was applied on four points of the side rails. The edges, opposite to the impacted side were constrained in X, Y and Z direction. The other loads which were applied in static analysis remain unaltered.

Generally, the loading and boundary condition is shown in figure 3.14 below.

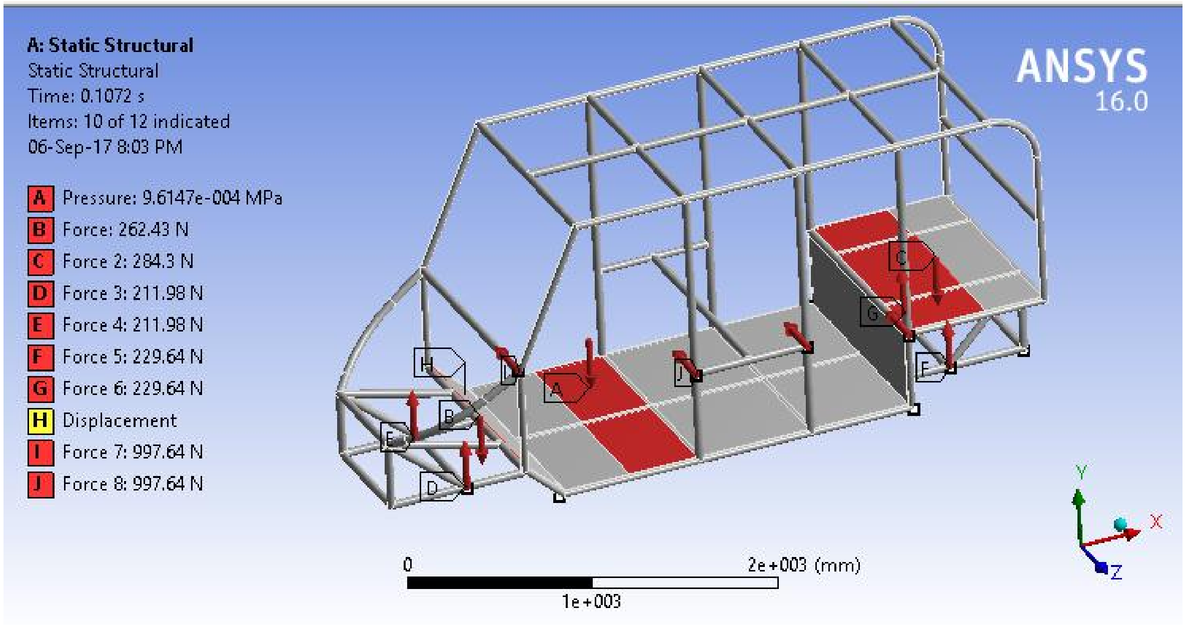

Figure 3.14: Loading and Boundary Conditions for Side Impact Analysis.

3.8.4 Rear Impact Analysis

The impact load was applied on eight points as point load in the case of rear impact. The magnitude of each point load is 9306.565N as it is shown in section 3.7.3. The lower edges of the vehicle are constrained in X, Y and Z direction except the two rear edges. The other loading conditions used in static analysis remained unaltered.

Generally, the loading and boundary condition is shown in figure 3.15 below.

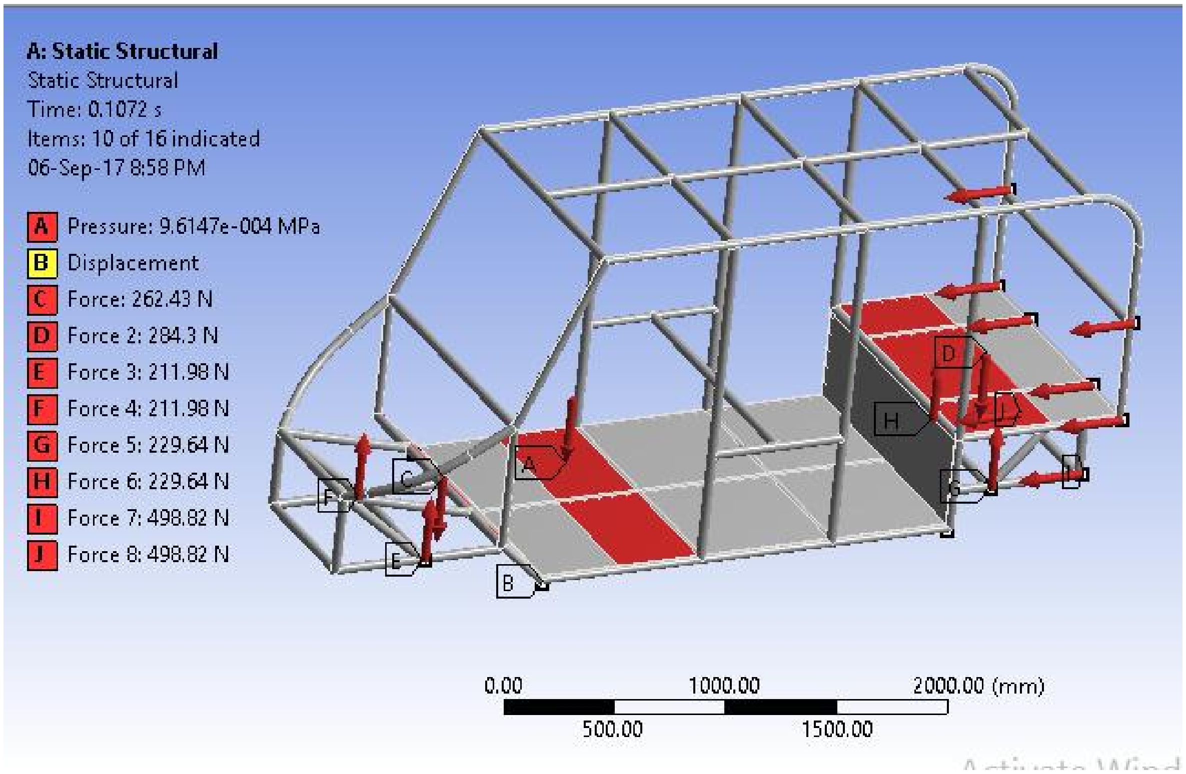

Figure 3.15: Loading and Boundary Conditions for Rear Impact Analysis.

3.8.5 Front Rollover Analysis.

To make the front rollover analysis, the procedures specified by the Federal Motor Vehicle Safety Standard were repeated. The weight of the vehicle excluding the weight of passengers and driver is 519.9Kg. Hence the force which will be applied on the respective roof beams will be $3 * 519.9 * 9.8N = 15285.06N$. This load was applied as point load on three points on the front roof cross beam. The magnitude of the load at each point will be $15285.06N/3 = 5095.02N$. The other boundary conditions and loads in static analysis remain unaltered.

Genarally, the loading and boundary condition is shown in figure 3.16 below.

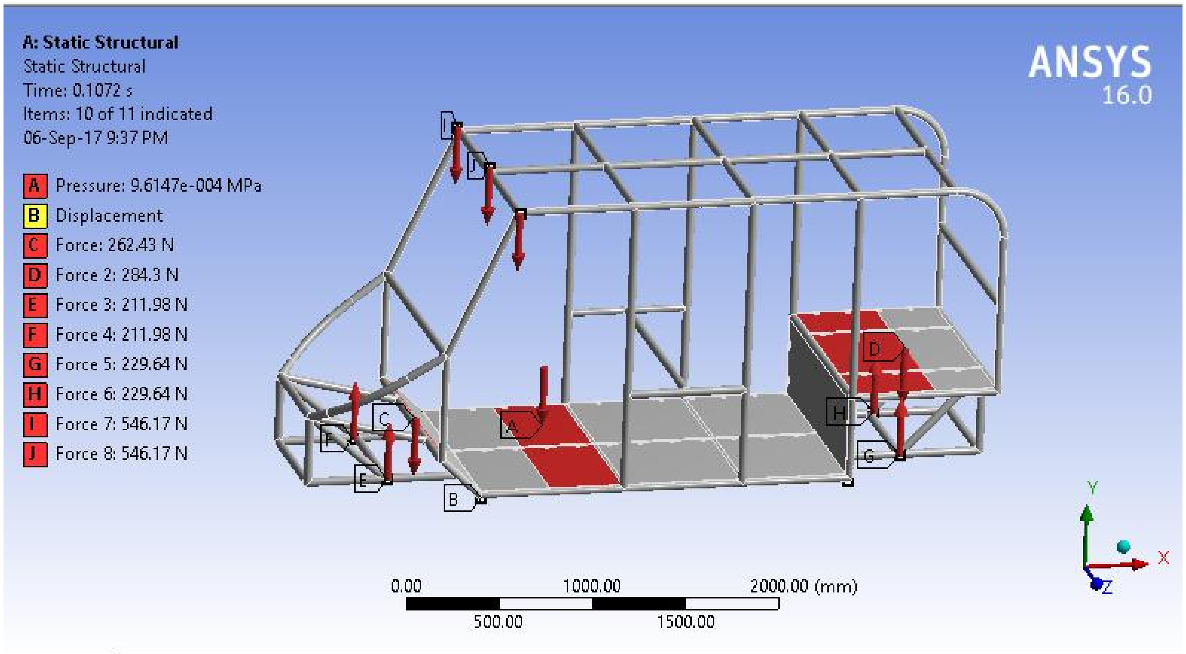

Figure 3.16: Loading and Boundary conditions for Front Rollover Analysis.

3.8.6 Side Rollover Analysis.

In the case of side rollover analysis, the load 15285.06N which was determined in section 6.7.5 was applied as a point load on five points of the roof side rail. Then the magnitude of the load at each point will be $15285.06\text{N}/5 = 3057.012\text{N}$.

The other boundary conditions used in static analysis remain unaltered.

Generally, the loading and boundary condition used is shown in figure 3.17below.

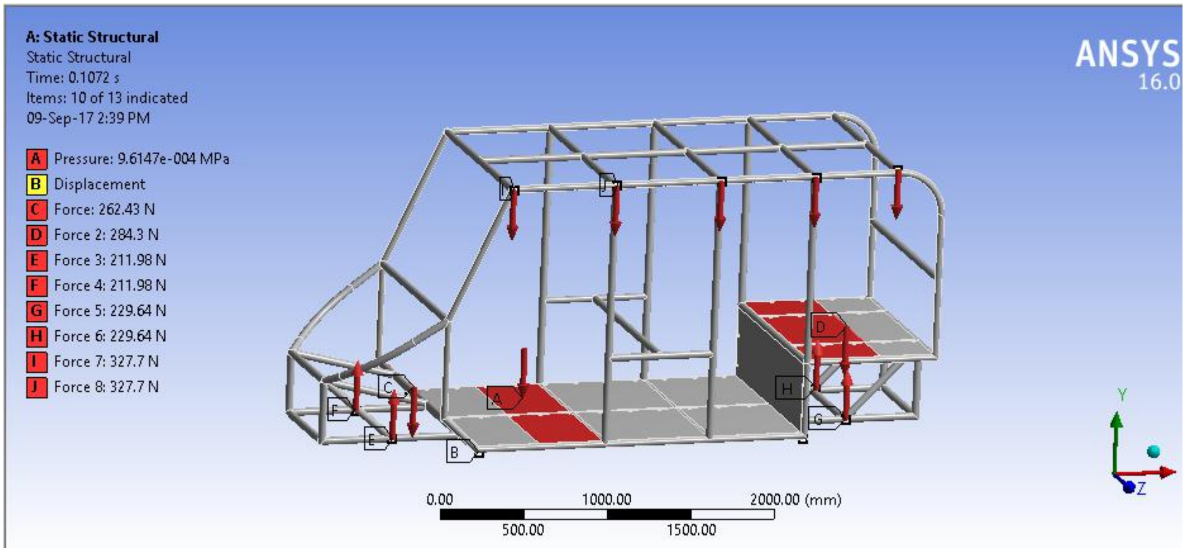

Figure 3.17: Loading and Boundary Condition for Side Rollover Analysis.

3.8.7 Modal Analysis.

The first 12 modes were extracted and simulated to see the natural frequencies and mode shapes of the chassis. the analysis was peformed by constraining the lower edges of thechassis and witout applying any load.

CHAPTER FOUR

RESULT AND DISCUSSION

4.1 Results and Discussion on the Existing Chassis

4.1.1 Static Analysis Results

The simulation results for static analysis are shown in figure 4.1.

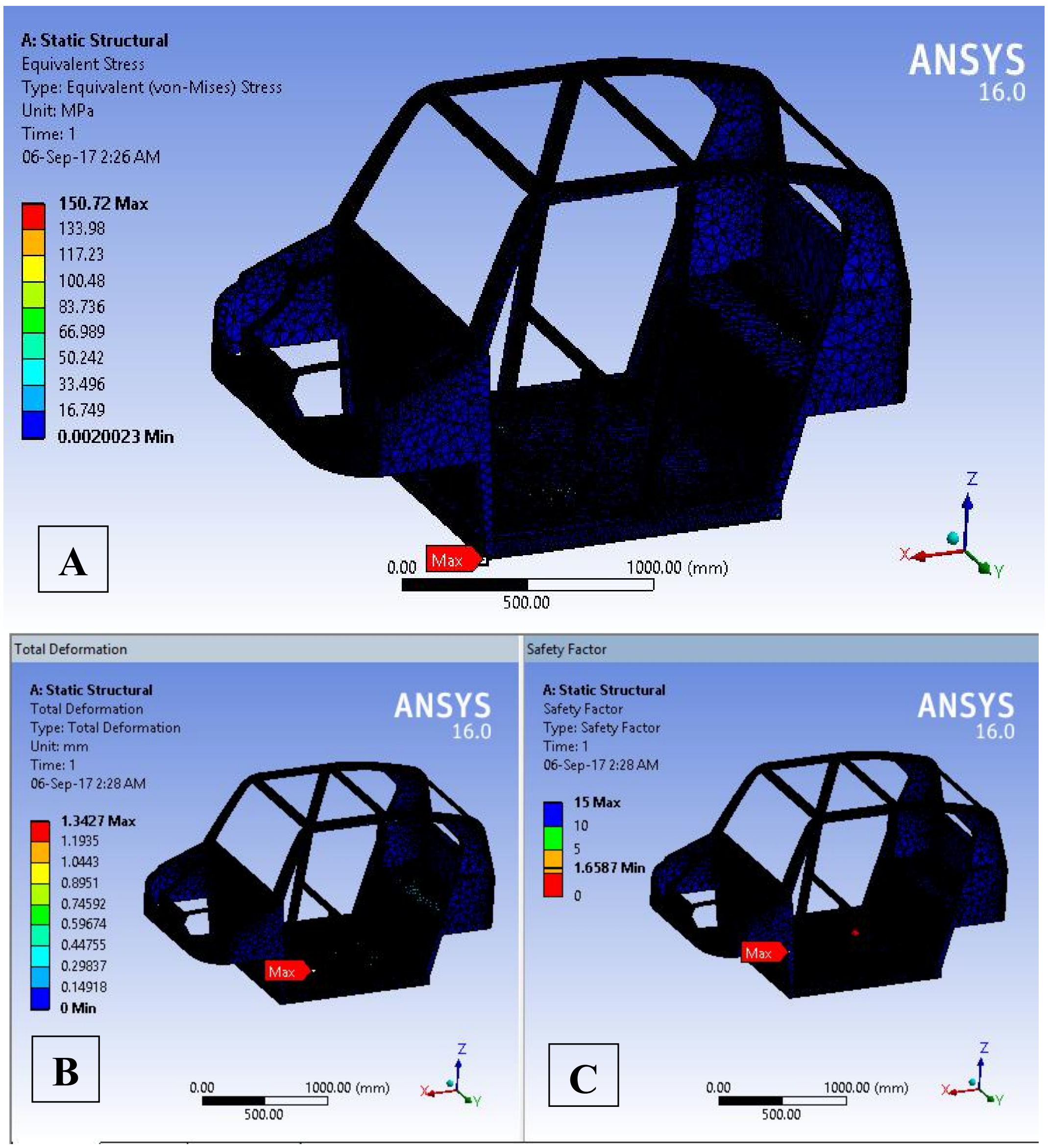

Figure 4.1: Simulation Results of the Static Analysis

The yield strength of the material used for the chassis is 345 Mpa. From the simulation results (A) it can be observed that the maximum equivalent stress detected on the chassis due to the applied steady static loads was 150.72 Mpa which occurred at the point where the side fender intersects with the floor around the door closing points. The detected maximum equivalent stress is smaller than the yield strength of the material. It can also be seen that the maximum deflection detected was 1.34mm (B) which is not huge and it occurred on the floor. The safety factor is also 1.66(C) which is above unity (1) indicating that the chassis is safe under the applied steady static loads. Therefore, the performance of the existing chassis is good under static load analysis.

4.1.2 Frontal Impact Analysis Results

The simulation results of the frontal impact analysis are shown in figure 4.2 - 4.13 below.

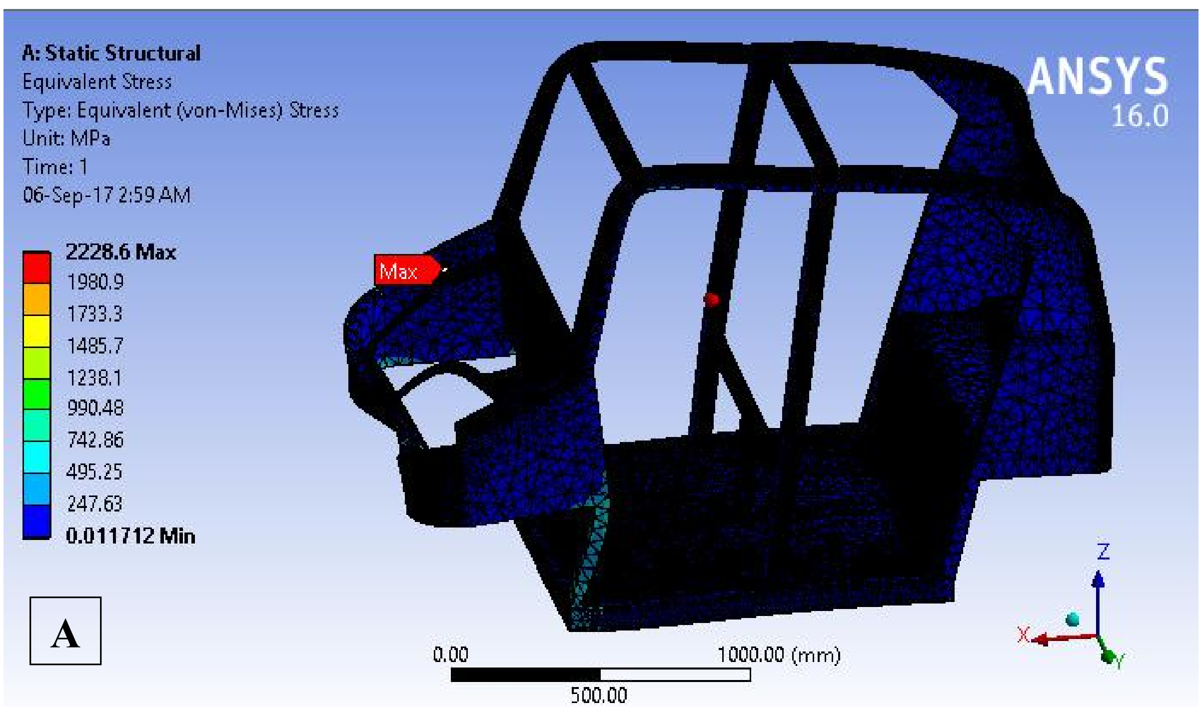

Figure 4.2: Equivalent stress under Frontal Impact Analysis

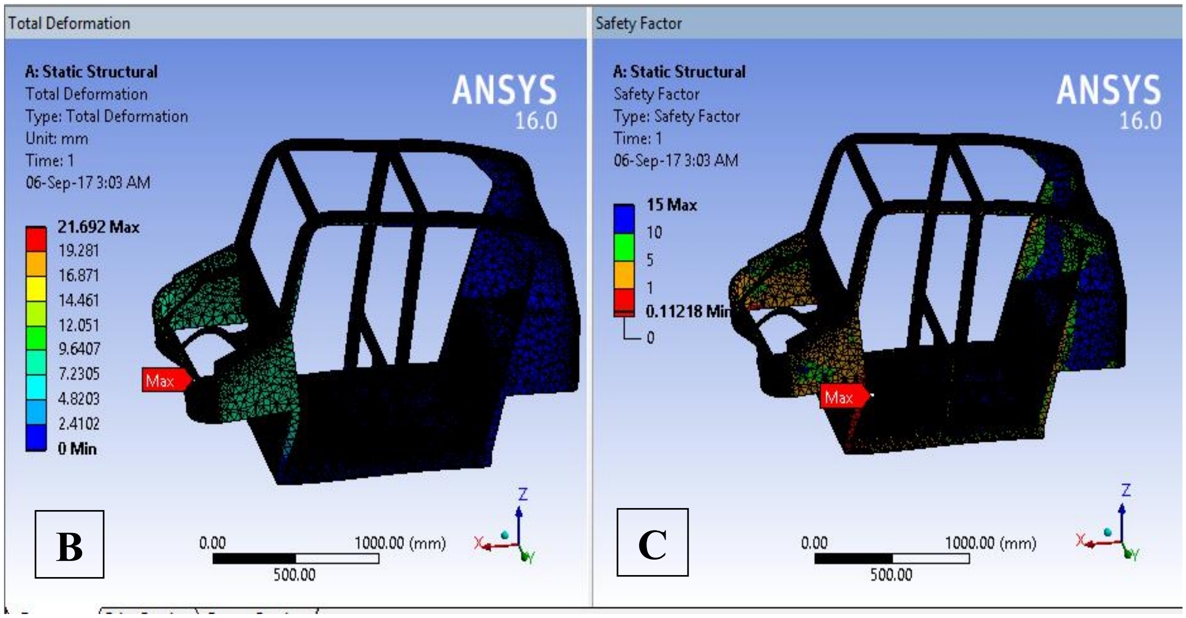

Figure 4.3: Simulation Results of the Frontal Impact Analysis

According to the maximum tolerable deformation level specified in the FMVSS [16] in the case of frontal impact, no part of the vehicle outside the occupant compartment, except windshield molding and other components designed to be normally in contact with the windshield, shall penetrate the protected zone template to a depth of more than 6.4 mm.

As it can be seen from the simulation results (A), the maximum equivalent stress detected on the vehicle under the head on collision is 2228.6 Mpa, which occurred on the bumper. This stress is much higher than the material strength (material yield strength is 345Mpa). This means that the stress of the bumper has surpassed material limit (yield strength) and the bumper is not capable of resisting all the loads applied on it. However, it can be seen on the deformation of the vehicle from figure 4.3 (B) under this condition that there is no structure which penetrated in the windshield or the instrument panel or any direction into the passengers' compartment. This shows that the extent of injury on the passengers is not huge and the passengers are safe if they appropriately used the vehicle safety facilities. However, since high damage occurs to the bumper and components around the frontal area of the vehicle, this components need replacement after the occurrence of the impact.

4.1.3 Side Impact Analysis Results

The simulation results of the side impact are shown in figure 4.4.

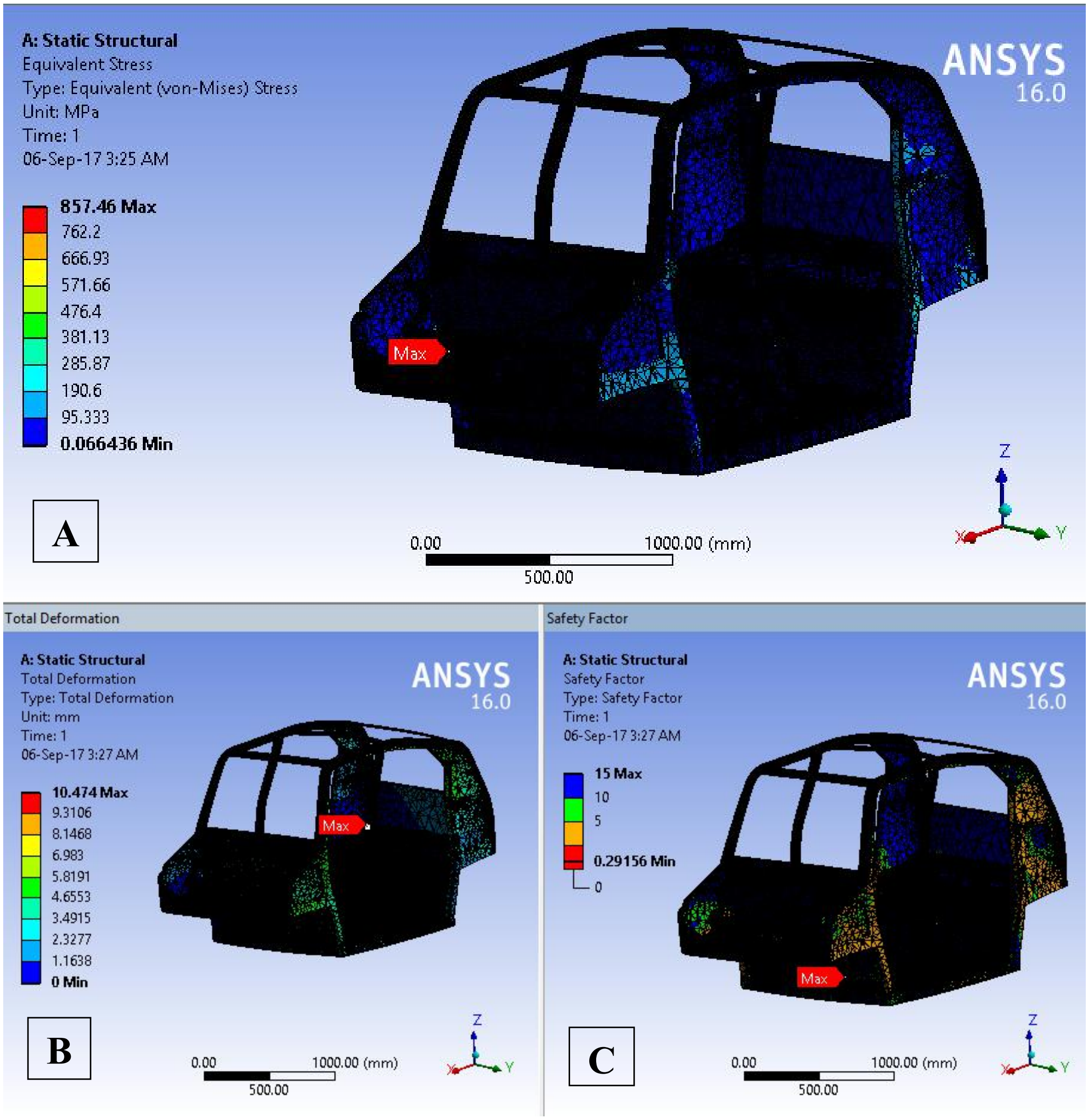

Figure 4.4: Simulation Results of Side Impact Analysis

According to the FMVSS under the side impact [17]:

- Any side door that is struck shall not separate totally from the vehicle.
- Any door that is not struck must meet the following requirements:

- The door shall not disengage from the latched position.
- The latch shall not separate from the striker, and the hinge components shall not separate from each other or from their attachment to the vehicle
- Neither the latch nor the hinge systems of the door shall pull out of their anchorages

As it can be seen from figure 4.4(A), the maximum equivalent stress detected under this accident is 857.46 Mpa which is far larger than the yield strength of the material. The side protective rail was deformed inwards towards the driver and passenger's compartment 10.47 mm inward which is very large indicating that the struck door disengages from the latched position. Hence, the driver and passengers are liable to injury under this condition. Furthermore, the safety factor is 0.3 which indicates that the chassis is not safe under side impact.

4.1.4 Rear Impact Analysis Results

The simulation results of the rear impact analysis are shown in figure 4.5.

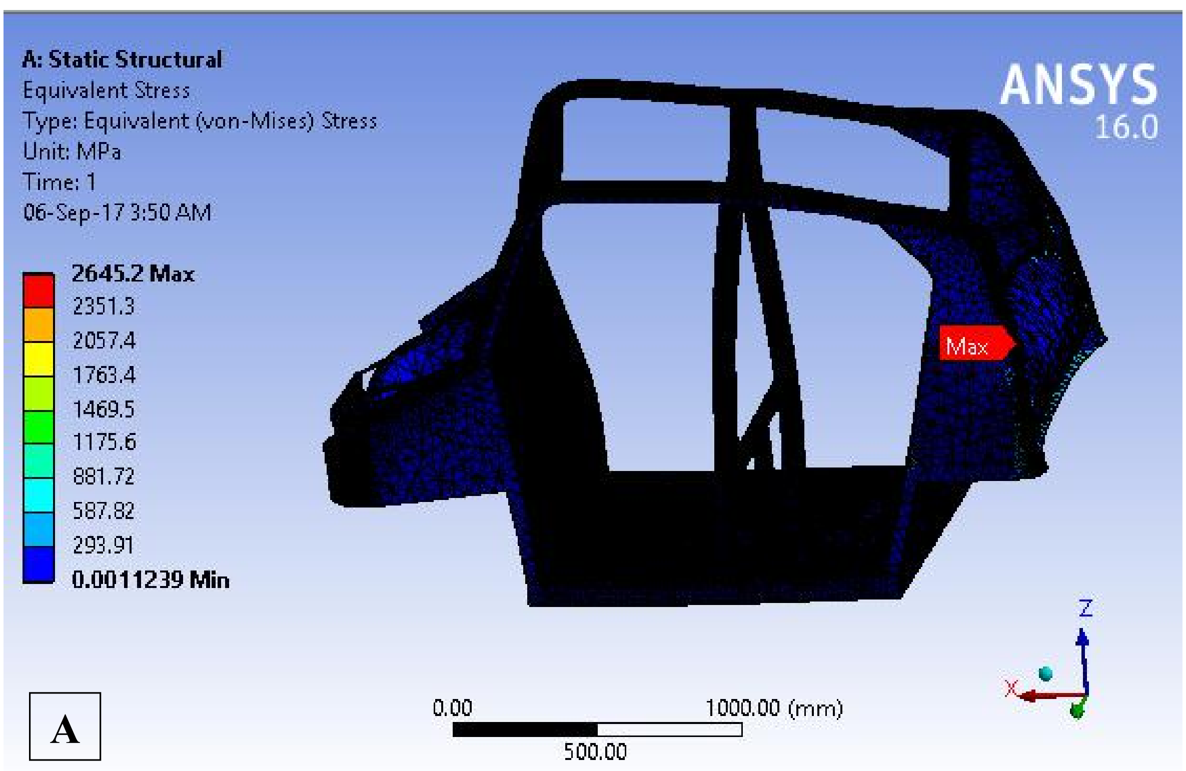

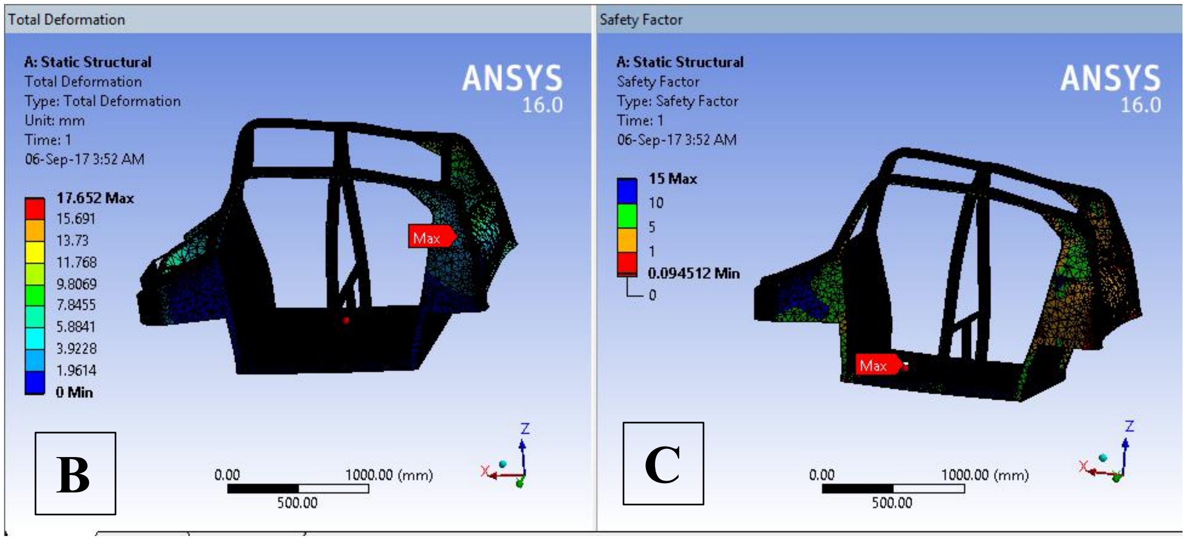

Figure 4.5: Simulation Results of the Rear Impact Analysis

As it can be seen from the simulation results, the maximum detected equivalent stress was 2645.2 Mpa which is much higher than the yield strength of the material. The inward intrusion on the crushed part is 17.65 mm in to the passenger's compartment. In addition to this, the safety factor was 0.09 which is much lower than unity (1), which is very critical. This shows that the vehicle is not safe under the rear impact.

4.1.5 Front Rollover Analysis Results

The simulation results are shown in figure 4.6.

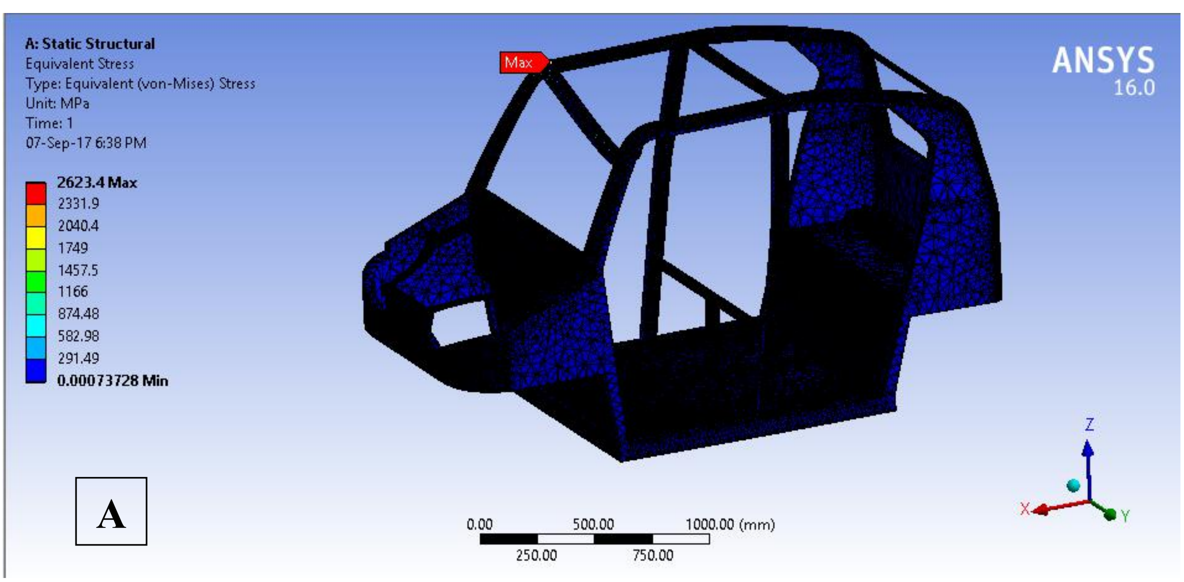

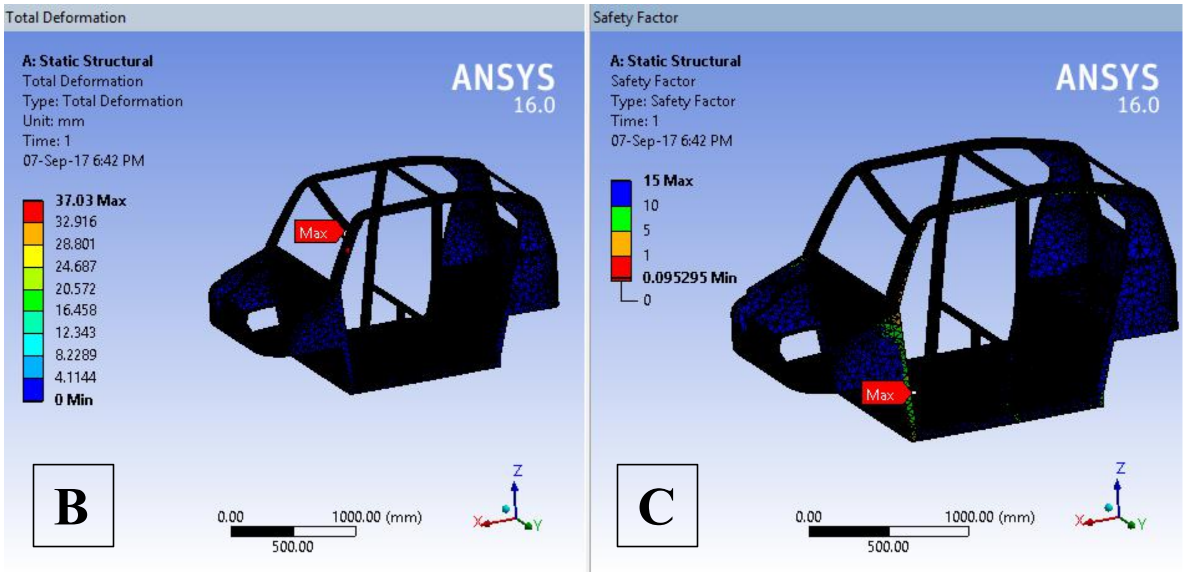

Figure 4.6: Simulation Results of the Front Rollover Analysis

As it can be seen from the simulation results, the maximum equivalent stress detected under the analysis was 2623.4 Mpa which is much higher than the yield strength of the material. A deflection of 37.03 mm was detected on the front roof cross beam. The detected deflection is much high. This shows that there is a high need of design modification of the vehicle on this area and the vehicle is not safe under front rollover.

4.1.6 Side Rollover Analysis Results

The simulation results are shown in figure 4.7.

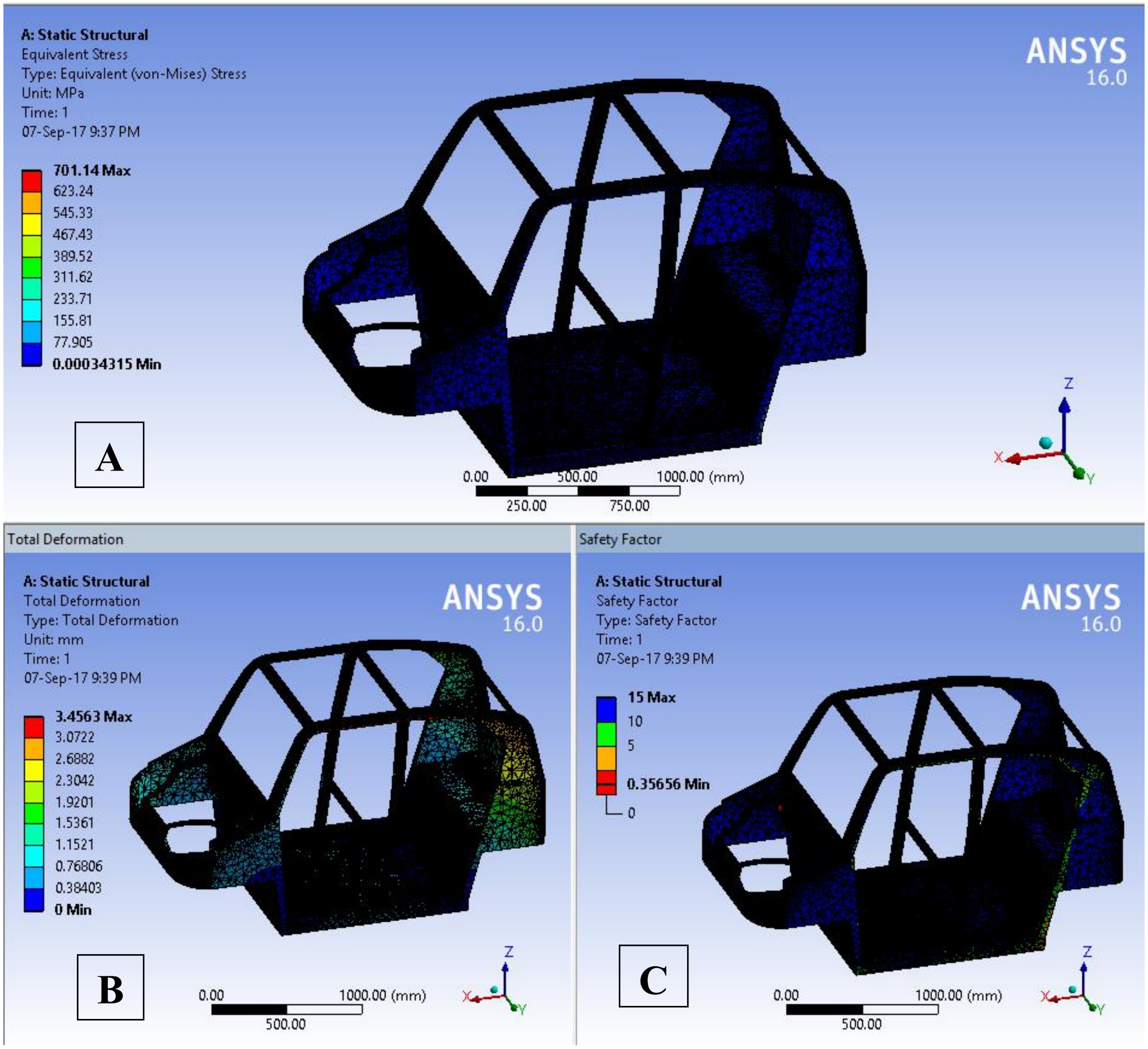

Figure 4.7: Simulation Results of Side Rollover Analysis.

The simulation results show that the detected maximum equivalent stress was 701.14 Mpa which is far greater than the yield strength of the material. This means that the level of deformation of the roof side rail has exceeded its elastic limit. Also it can be seen from the deformation size that the maximum detected deformation was 3.456mm which is not very large. Under the side rollover accident, the vehicle is safe.

4.1.7 Modal Analysis Results

The first 12 modes of vibration were extracted for the analysis. The natural frequency observed from the simulation result is tabulated in table 4.1 below.

Table 4.1: Frequency and Maximum Deformation of the Existing Bajaj qute for the first 12 Modes

Mode	Frequency [Hz]	Deformation [mm]
1.	34.174	5.8016
2.	43.514	33.14
3.	48.237	9.9704
4.	57.467	23.943
5.	58.982	37.392
6.	59.295	8.3063
7.	60.857	29.199
8.	61.996	24.64
9.	63.497	39.833
10.	64.262	80.043
11.	66.619	58.244
12.	73.049	9.914

The graph of the first 12 natural frequencies of the existing chassis is shown in figure 4.8 below.

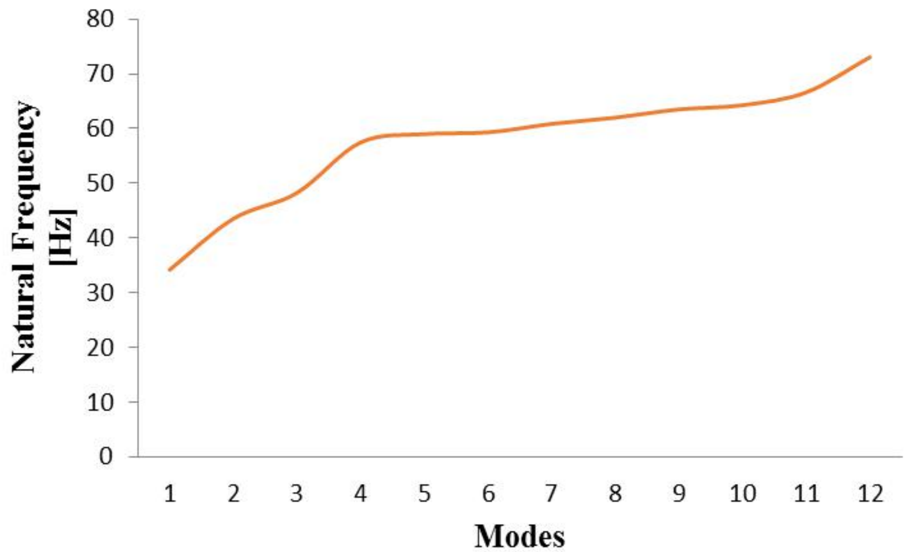

Figure 4.8: Natural Frequency vs Modes of Vibration

If any one of the natural frequencies matches with excitation frequency, the frame doesn't satisfy the dynamic characteristics and resonance occurs. Resonance is the condition of the chassis at which failure occurs [43].

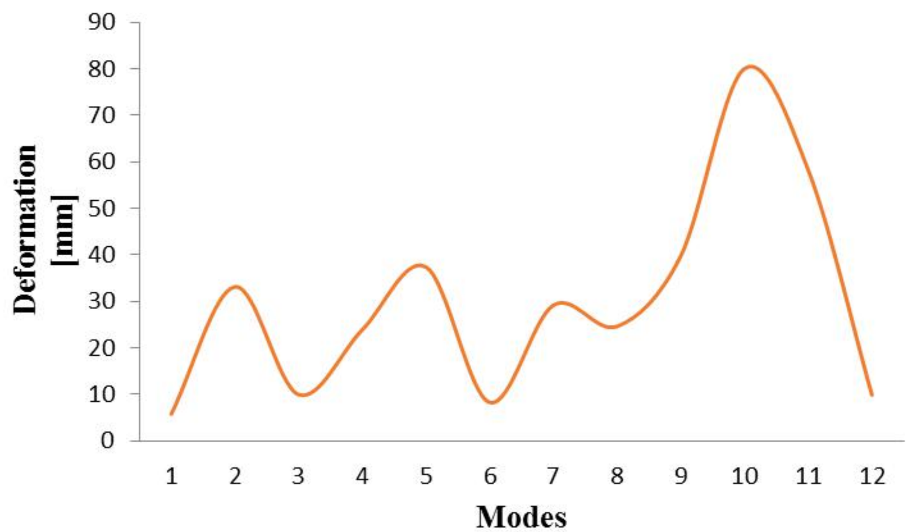

Figure 4.9: Maximum Deformation vs Modes of vibration

The value of deformation detected under the modal analysis is not exact deformation, because there is no load applied to the object under the analysis. But, it gives good information to identify the weak component in the structure [43]. From figure 4.9, maximum deformation occurred at the 10^{th} mode of vibration and attention has to be given to this component. Four of the mode shapes which showed maximum local peak deformations (mode 2,5,7 and 10) are shown in figure 4.10 below.

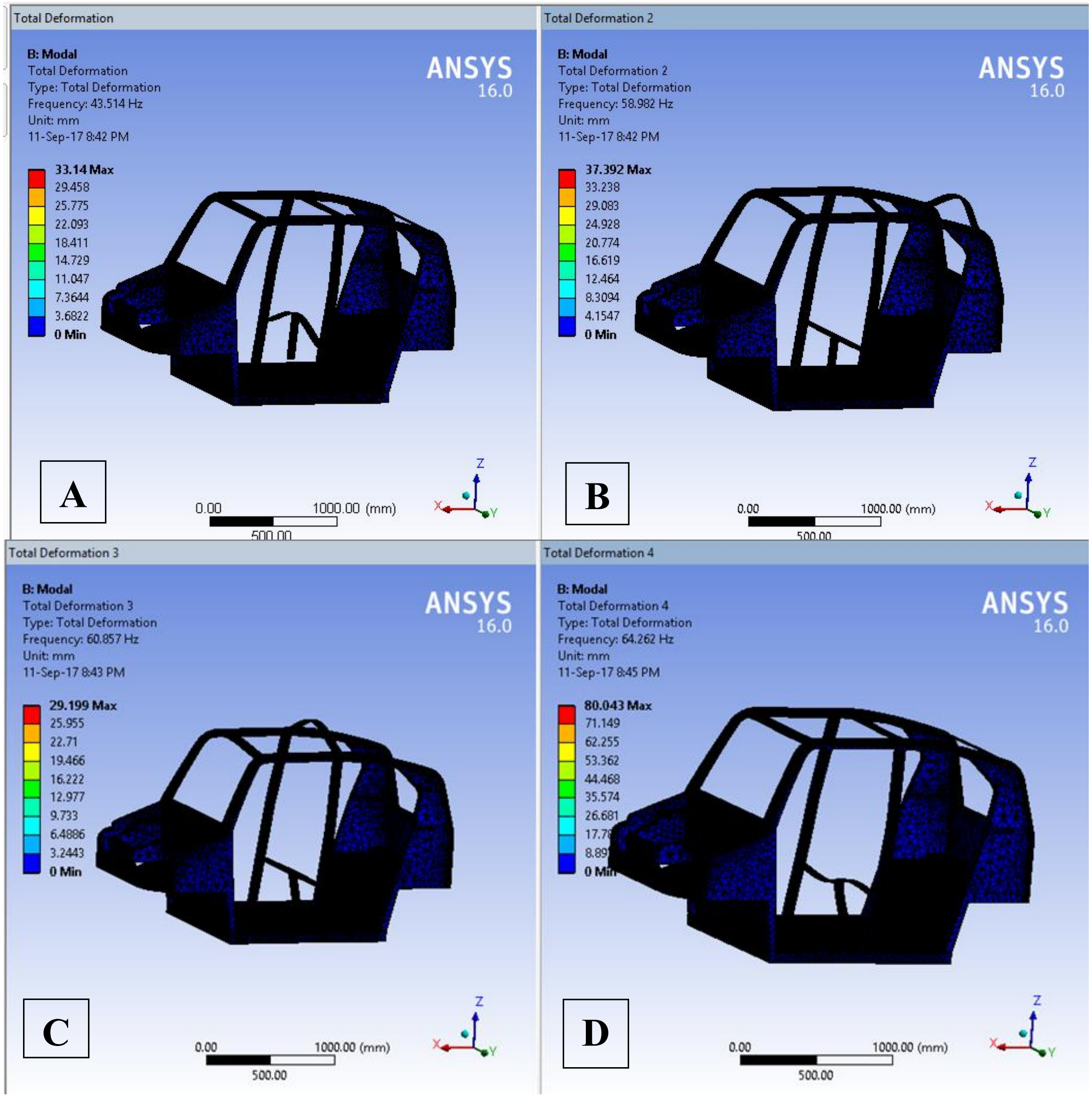

Figure 4.10: Mode shapes at the 2^{nd}, 5^{th},7^{th} and 10^{th} Natural Frequencies respectively.

The modal analysis shows that, there are weak components in the structure off the existing chassis. the front roof cross beam, the centeral roof cross beam, the rear roof cross beam and beam which connects the two B pillars should be more stiffened.

4.2 Results and Discussion on the New Chassis

4.2.1 Static Analysis Results

The simulation results are shown in figure 4.11 below.

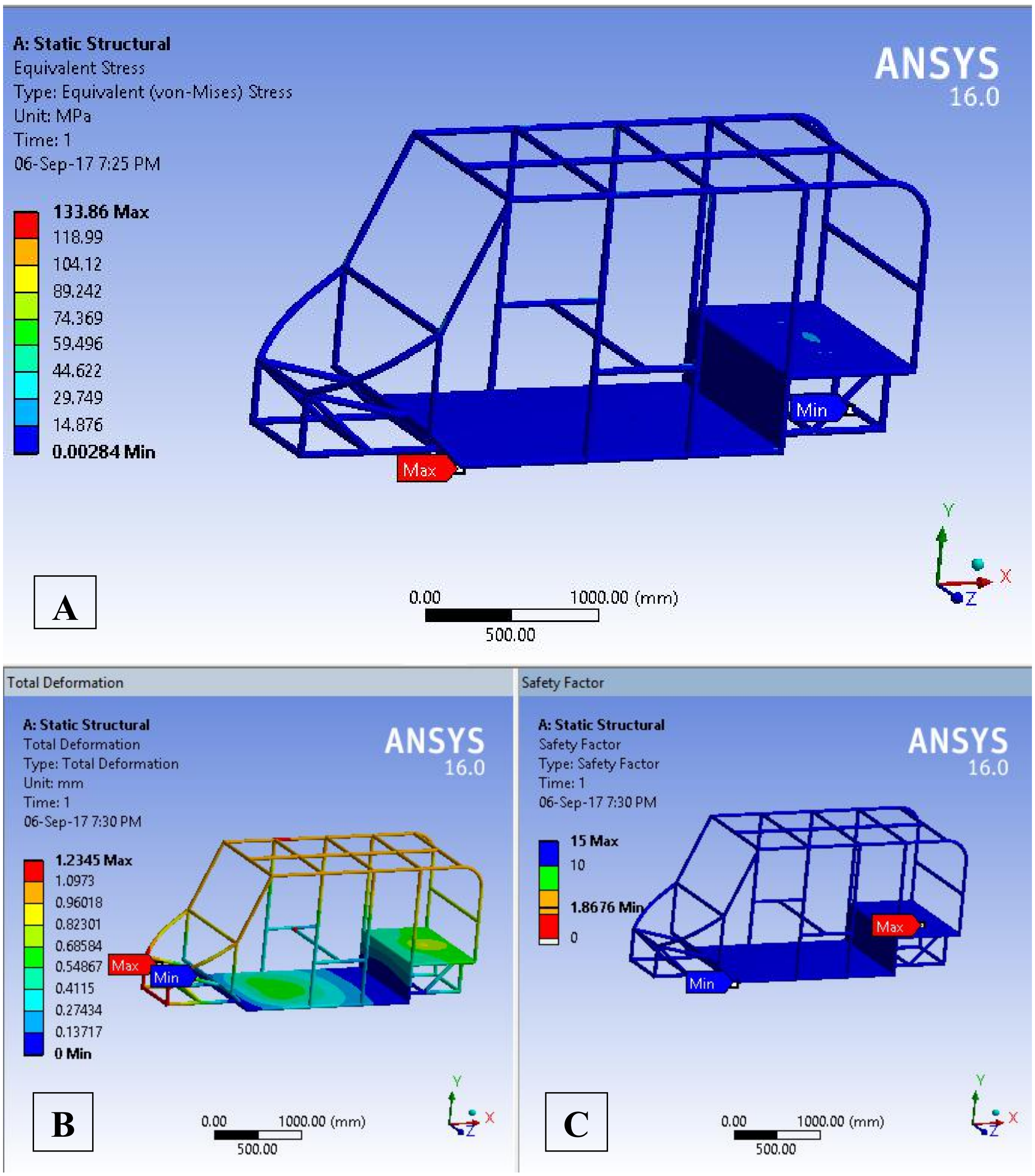

Figure 4.11: simulation Results of Static Analysis.

The maximum detected equivalent stress in static load analysis is 133.86 Mpa. According to the maximum equivalent stress failure theory for ductile materials, a particular combination of principal stresses causes failure if the maximum equivalent stress in a structure equals or exceeds a specific stress limit of the material (yield strength)[10]. The yield strength of the material used for the chassis is 345Mpa. From the simulation results (A) it can be observed that the maximum equivalent stress detected on the chassis due to the applied steady static loads was 133.86 Mpa which occurred on the floor in-front of the front seat row. The detected maximum equivalent stress is smaller than the yield strength of the material. It can also be seen that the maximum deflection detected was 1.23 mm (B) which is not huge and it occurred on the floor. The safety factor is also 1.86(C) which is above unity (1) indicating that the chassis is safe under the applied steady static loads.

4.1.2 Frontal Impact Analysis Results.

The simulation results of the frontal impact analysis are shown in figure 4.12 below.

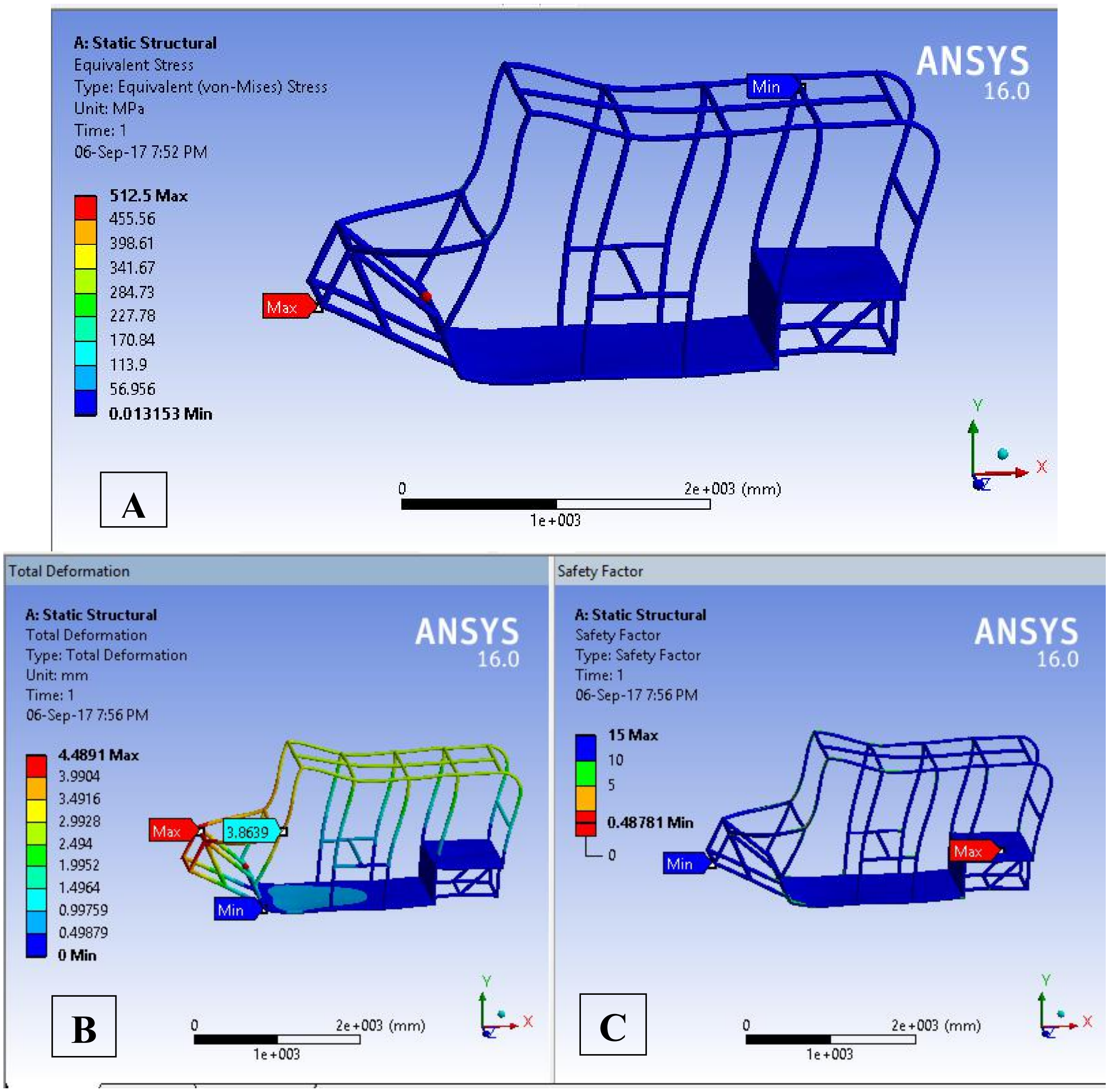

Figure 4.12: simulation Results of Front Impact Analysis.

The maximum detected inward intrusion of the structure into the passengers area is 3.86 mm (probe value). The maximum equivalent von misses stress was 512.5Mpa. This stress is higher than the material strength (material yield strength is 345Mpa). This means that the deformation of the impacted part of the chassis has exceeded its material limit. However it can be seen on the deformation of the vehicle under this condition that there is no structure which penetrated in the windshield or the instrument panel or any direction into the passengers' compartment. This shows that the extent of injury on the passengers is not huge and the passengers are safe if they appropriately used the vehicle safety facilities. However, since high damage occurs on the components around the frontal area of the vehicle, this components need replacement after the occurrence of the impact.

4.1.3 Side Impact Analysis Results

The simulation results of the side impact analysis are shown in figure 4.13 - 4.14 below.

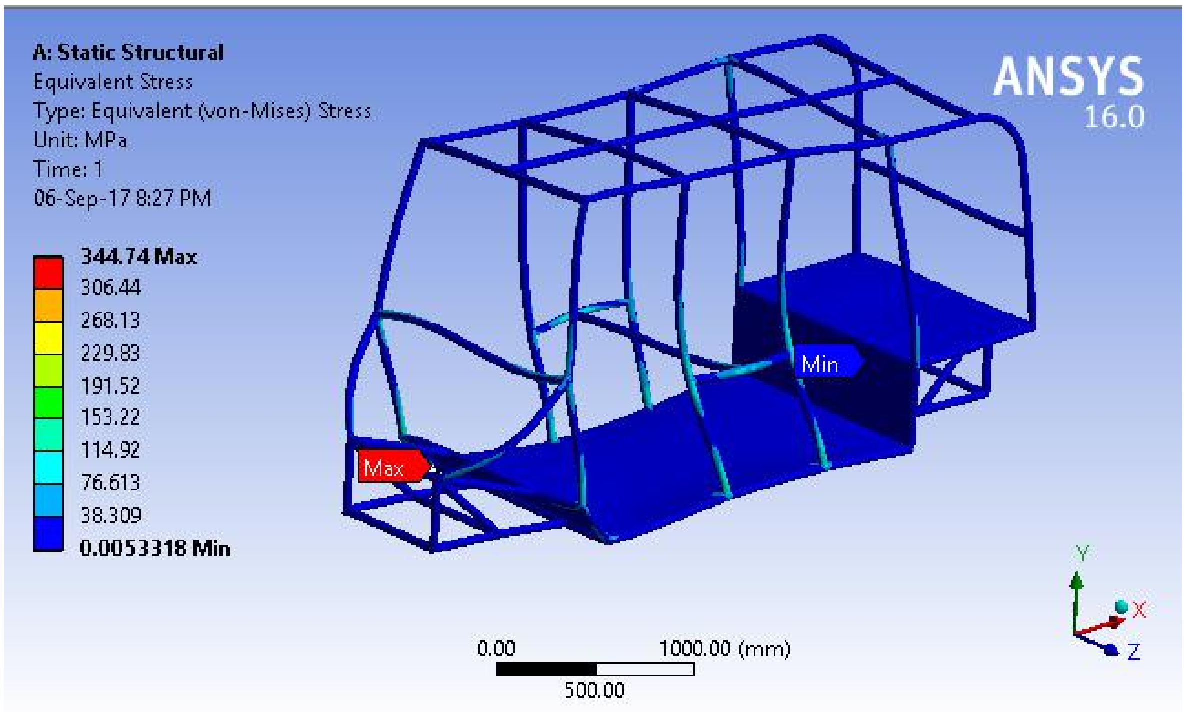

Figure 4.13: Equivalent Stress Results Under the Frontal Impact Analysis

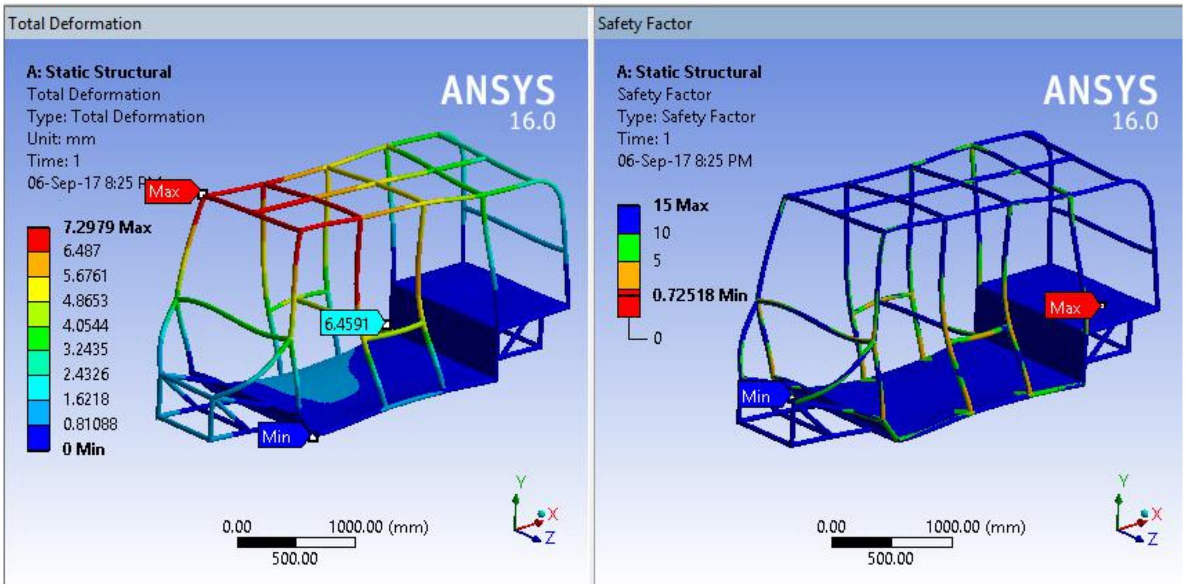

Figure 4.14: Simulation Results of Side Impact Analysis.

The detected intrusion of the structure into the passengers compartment is 6.46mm (from the probe value). This deformation is much improved from the deformation of the existing vehicle under side impact (10.47mm). The safety factor of the vehicle under this accident is 0.72 which is much better than that of the existing one. Even though the vehicle is not fully safe under side impact, the level of injury will be much lower than that of the existing one.

4.1.4 Rear Impact Analysis Results

Simulation results of the analysis is shown in figure 4.15 below.

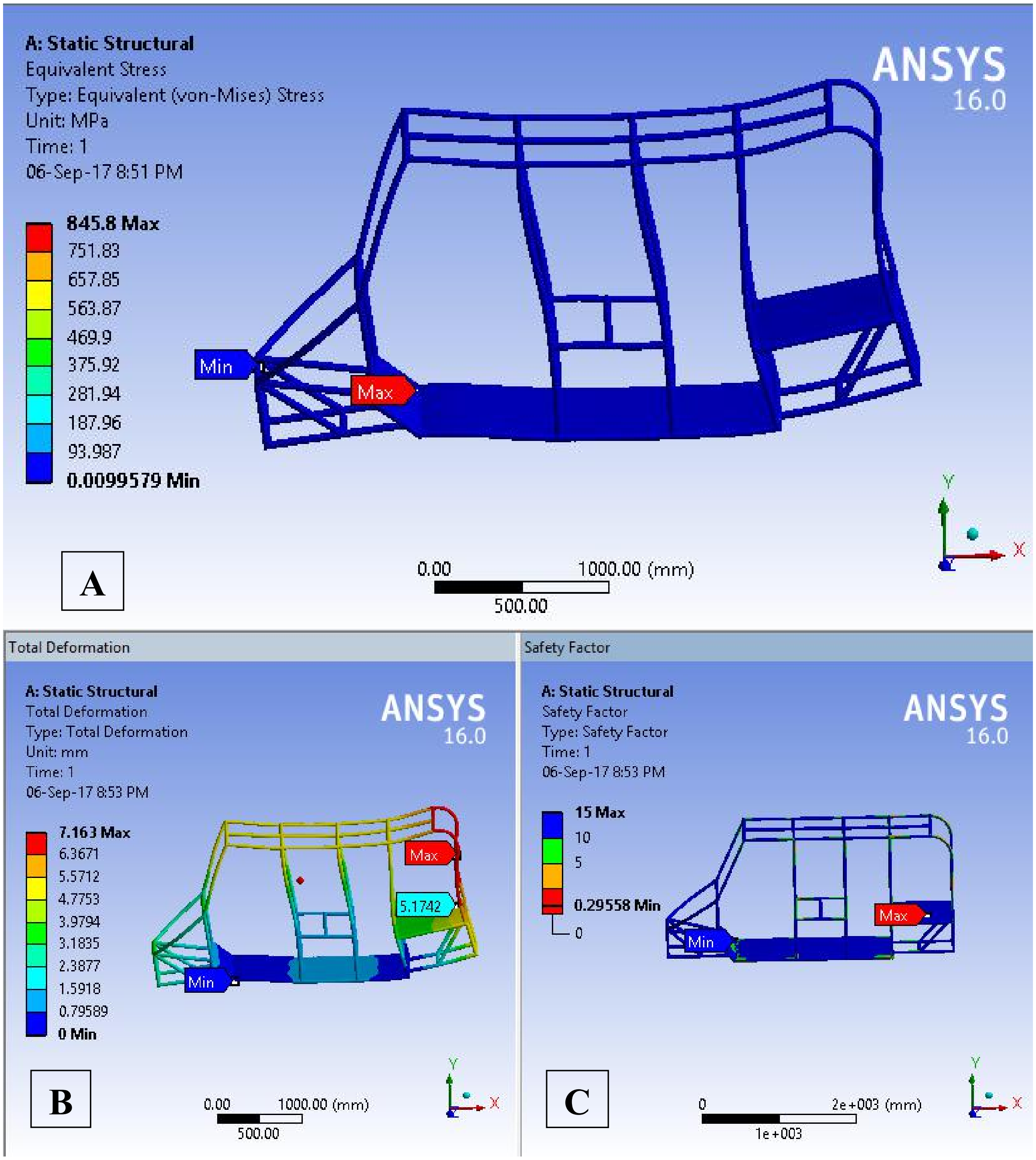

Figure 4.15: Simulation Results of Rear Impact Analysis.

As it can be seen from the simulation results, the maximum detected equivalent stress was 845.8 Mpa which is higher than the yield strength of the material. The inward intrusion of the crushed part is 5.177mm (probe value) in to the passenger's compartment. The safety factor was 0.29 which is much lower than unity (1), but much better than the baseline value (0.09). This shows that the safety of the vehicle is much improved under the occurrence of rear impact.

4.1.5 Front Rollover Analysis Results

The simulation results are shown in figure 4.16 below.

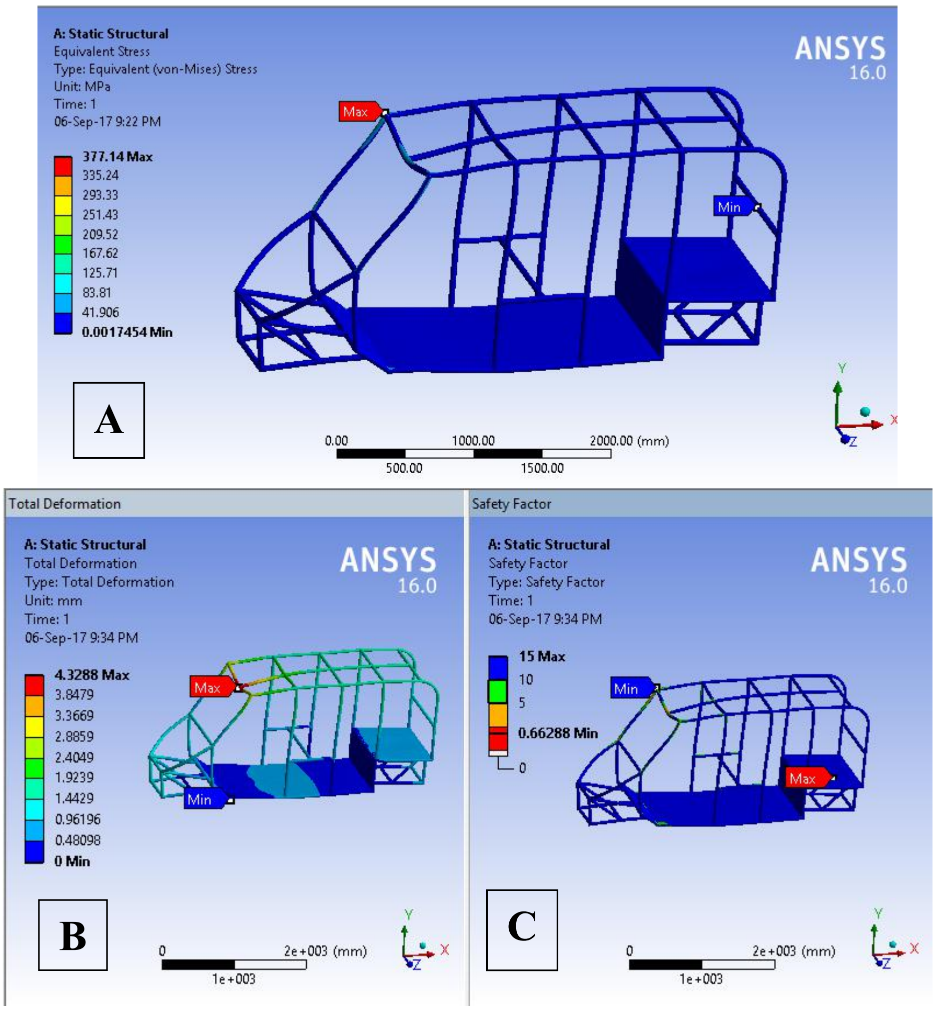

Figure 4.16: Simulation Results of Front Rollover Analysis.

As it can be seen from the simulation results, the maximum equivalent stress detected under this analysis was 377.14 Mpa which is higher than the yield strength of the material. A deflection of 4.33 mm was detected on the front roof cross beam. The detected deflection is much lower than the deformation of the existing vehicle (37.03 mm). This shows that there is a high performance improvement with new design under front rollover accident.

4.1.6 Side Rollover Analysis Results.

Simulation results of the side rollover analysis are shown in figure 4.17 below.

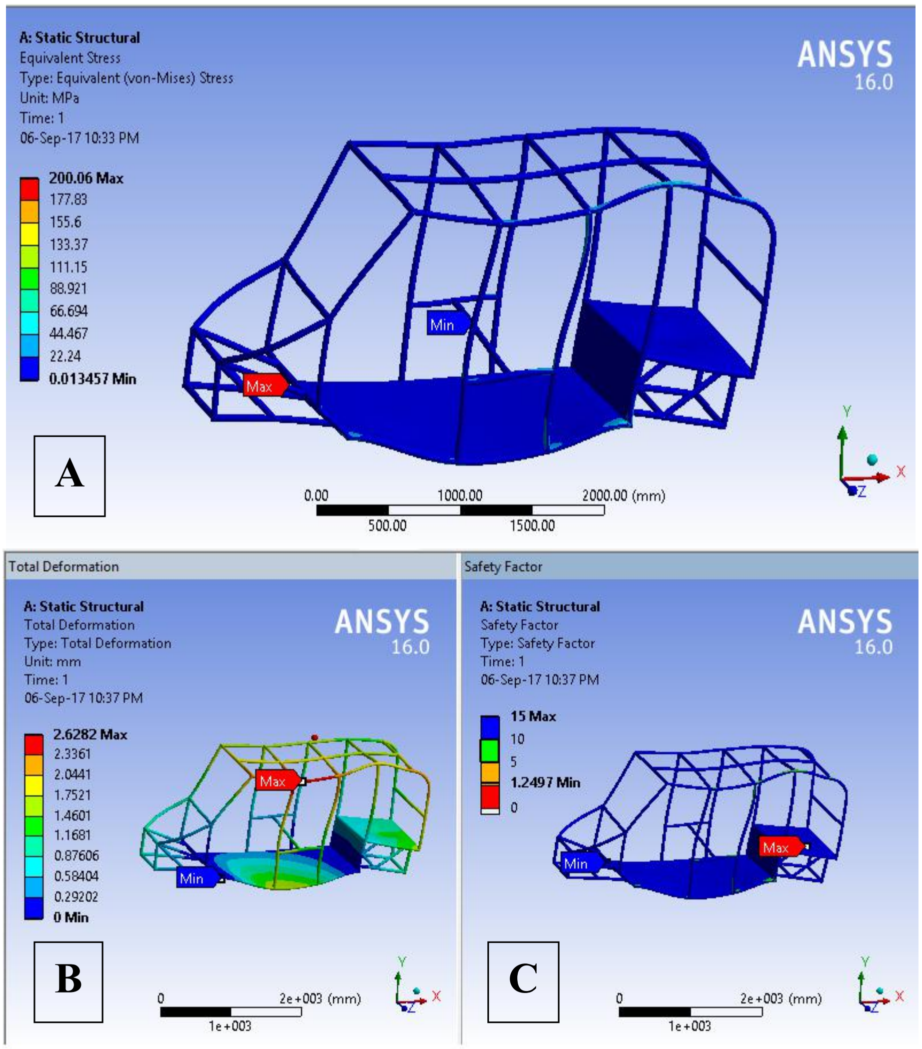

Figure 4.17: Simulation Results of Side Rollover Analysis.

The simulation results show that the detected maximum equivalent stress was 200.06 Mpa which is smaller than the yield strength of the material. This means that the level of deformation of the roof side rail is within its elastic limit. Also it can be seen from the deformation size that the maximum detected deformation was 2.62mm which is very small. Hence, the passengers are safe under the side rollover.

4.1.7 Modal Analysis Results

Table 4.2: Natural Frequency and Maximum Deformation of the New Chassis under the First 12 Modes.

Mode	Frequency [Hz]	Deformation[mm]
1.	12.696	2.4245
2.	14.8	2.0205
3.	20.625	3.3186
4.	24.21	1.9323
5.	28.65	1.9128
6.	34.374	2.4641
7.	37.656	2.6157
8.	45.069	3.3374
9.	46.527	2.3199
10.	49.798	3.3439
11.	50.784	3.719
12.	52.034	2.9943

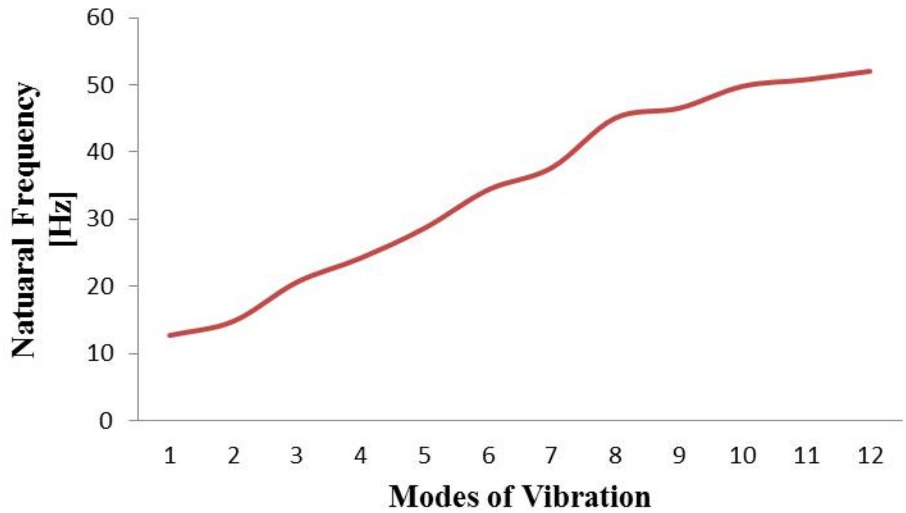

Figure 4.18: Natural Frequency vs Modes of Vibration

None of the excitation frequencies should overlap with the natural frequencies. If the excitation frequencies equal one of the natural frequencies, resonance occurs and the structure fails [43].

The deformations at each modes of vibration are shown in figure 4.17 below.

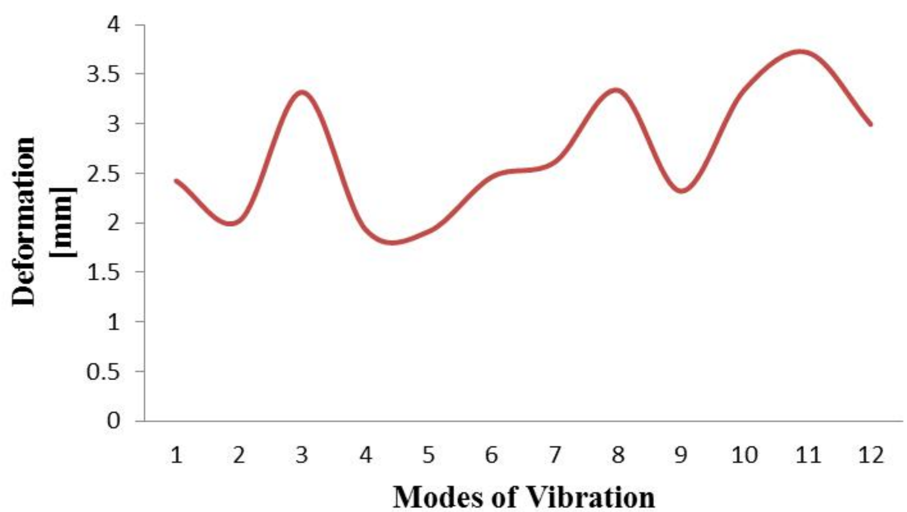

Figure 4.19: Maximum Deformation vs. Modes of Vibration.

The deformations evaluated under the modal analysis are not exact deformation, because there is no load which is applied on the model during the analysis. But the local peak deformations are used to identify the weak components in the structure. From figure 6.21, local peak deformations occurred at the 3rd, 6th, 8th and 11th modes of vibration. The mode shapes at these natural frequencies are shown in figure 4.20 below.

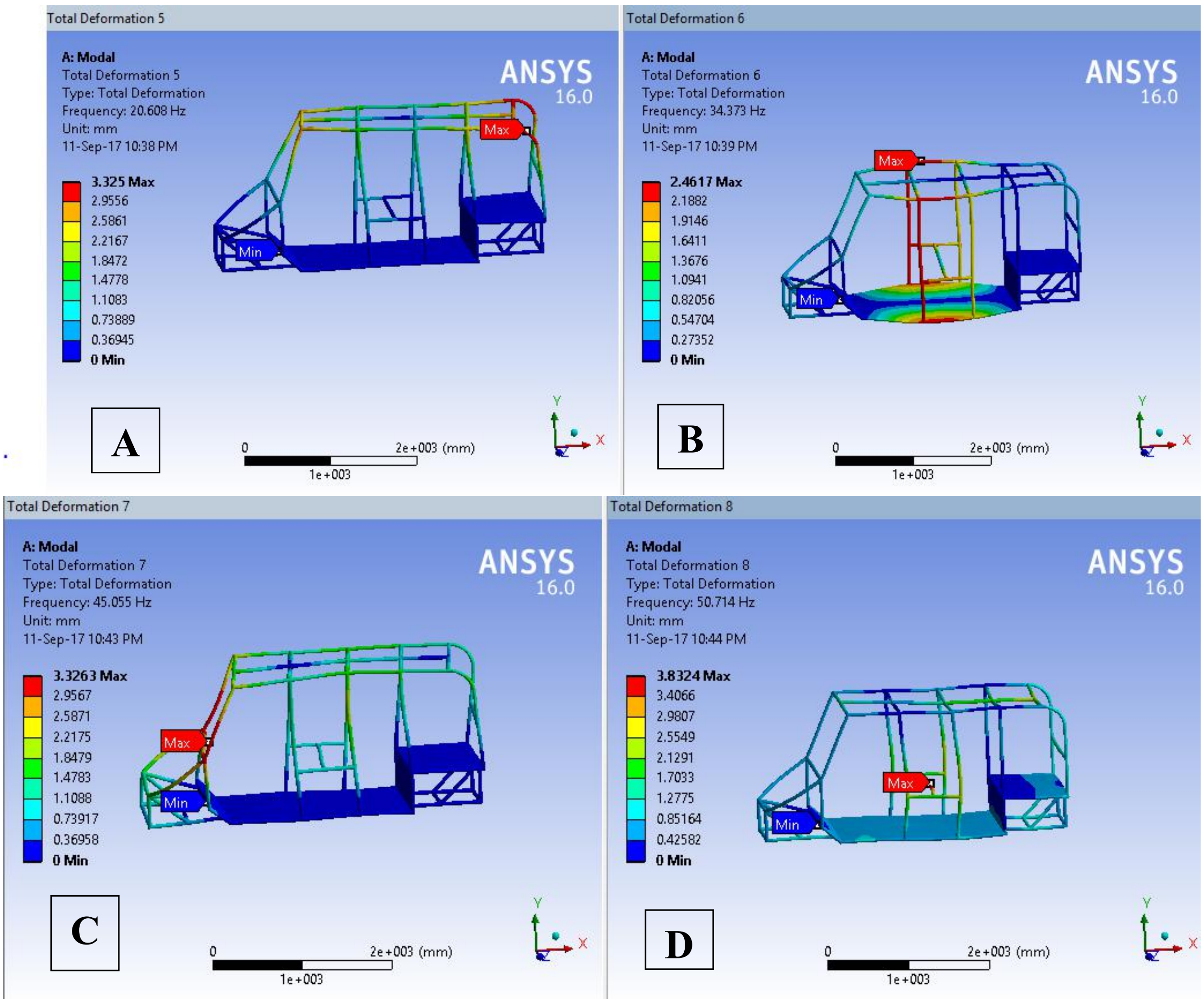

Figure 4.20: Mode Shapes of the 3rd, 6th, 8th and 11th modes of vibration respectively.

The modal analysis shows that there is no extremely weak component in the structure of the new chassis. Therefore, the structure of the new chassis is much better than the structure of the existing chassis in minimizing extremely weak components.

4.3 COMPARISON OF THE TWO MODELS

The simulation results of the two models are summarized in table 4.3 below.

Table 4.3: Summary of Simulation Results of the Existing and New Chassis

STATIC ANALYSIS		
	Existing Model	**New Model**
Maximum Equivalent stress[Mpa]	150.72	133.86
Maximum Deflection[mm]	1.32	1.23
Safety Factor	1.66	1.86
FULL FRONTAL IMPACT		
Maximum Equivalent stress[Mpa]	2226.8	512.5
Maximum Deflection[mm]	21.69	4.49
Safety Factor	0.112	0.48
SIDE IMPACT		
Maximum Equivalent stress[Mpa]	857.46	344.74
Maximum Deflection[mm]	10.47	7.29
Safety Factor	0.29	0.73
REAR IMPACT		
Maximum Equivalent stress[Mpa]	2645.2	845.8
Maximum Deflection[mm]	17.65	7.16
Safety Factor	0.09	0.29

FRONT ROLL-OVER		
Maximum Equivalent stress[Mpa]	2623.4	377.14
Maximum Deflection[mm]	37.03	4.33
Safety Factor	0.095	0.66
SIDE ROLL-OVER		
Maximum Equivalent stress[Mpa]	701.14	200.06
Maximum Deflection[mm]	3.46	2.63
Safety Factor	0.36	1.25

Under all of the above analysis, better performance has been achieved with the new chassis. The maximum equivalent stress under static analysis was improved from 150.72Mpa to 133.86Mpa, the maximum deflection was improved from 1.32mm to 1.23mm and the safety factor was improved from 0.112 mm to 0.48 mm.

Under frontal impact analysis, the maximum equivalent stress was improved from 2226.8Mpa to 512.5Mpa. Furthermore, from the deformation figure of the analysis, the level of intrusion of the external components into the passengers compartment has been greatly minimized.

Under the side impact analysis, the maximum equivalent stress was improved from 857.46Mpa to 344.74Mpa, the maximum deformation was improved from 10.47mm to 7.29mm, and also from the figures of the simulation results, the inward intrusion into the passengers compartment has been much minimized with the new model.

From the rear impact analysis, the maximum equivalent stress was improved from 2645.2Mpa to 845.8Mpa, and also the intrusion of the external components into the passengers compartment has been much improved.

From the front roll over analysis, the magnitude of intrusion of the deformed part into the passengers compartment is much reduced with the new model.

Under side rollover analysis, the safety of the vehicle has been much improved.

The deformation graphs of the two models are shown in figure 4.21 below.

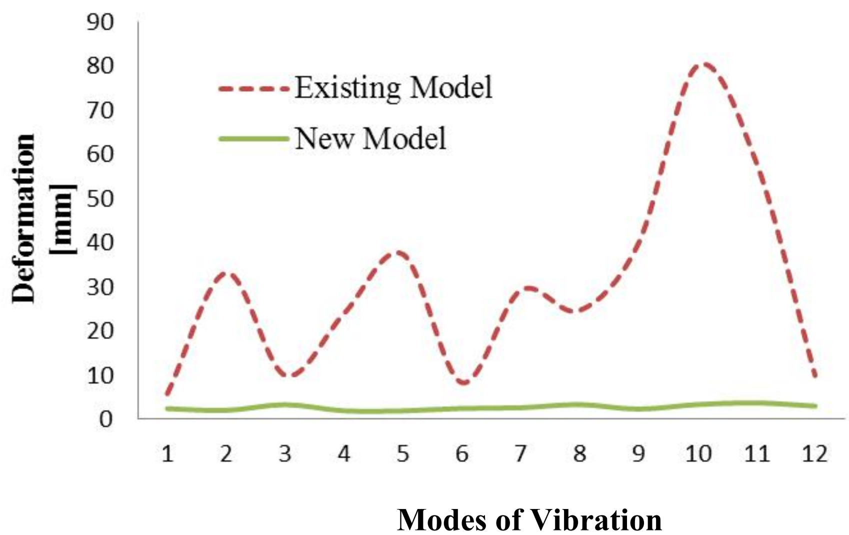

Figure 4.21: Maximum Deformation vs Modes of Vibration

From figure 4.21, it can be observed that the deformation of the existing chassis is highly fluctuating from one mode to the other mode. This shows that there are weak components which need further strengthening. But, the deformation of the new chassis is more or less constant, which indicates that the components of the chassis are stiff enough under the first 12 modes of vibration.

CHPTER FIVE

SUMMARY, CONCLUSION, RECOMMENDATION AND FUTURE WORK

5.1 Summary

The performance of the existing Bajaj Qute chassis was evaluated under static loading, frontal impact, side impact, rear impact, front roll-over, and side roll-over accidents. The performance of the existing chassis was poor under the side impact, rear impact and front rollover. The modal analysis showed that there are weak components in the structure of the existing vehicle. Finally, a new chassis was designed minimizing the shortcomings of the existing chassis. From the simuation results, the following conclusions are made.

5.2 Conclusion

1. The existing chassis is strong enough under the static analysis.
2. Under the front impact analysis, even though the extent of deformation of the chassis is very high, there is no part which showed high intrusion into the passengers compartment and therefore, the passengers are safe when the vehicle travels with a velocity lower than 48.3Km/h and collides with stationary objects.
3. Under the side impact, the level of intrusion of components into the passengers compartment is very high and the passengers are not safe when the vehicle is hit on the side with another vehicle of equal weight with the existing vehicle and travelling at a speed of 48.3Km/h and above 48.3Km/h.
4. Under the rear impact accident, the level of intrusion of the impacted components is very large and the passegers are not safe when the vehicle is hit on its rear side with a vehicle of equal mass and traveling at a velocity of 48.3Km/h or above.
5. Under the front roll-over, the level of deformation of the roof is very high and the passengers are not safe.
6. Under the side roll-over, the level of deformation of the roof is small and the passengers are safe.

7. From the modal analysis, the deformation of the existing chassis was highly fluctuating under the first 12 modes of vibration and this indicates that there are weak components in the chassis.
8. By changing the chassis to space-frame chassis and optimizing the outer diameter and thickness of the cross-section much performance improvement has been obtained under the accidents of side impact, rear impact and front rollover accidents.
9. There are no weak components in the new chassis. The fluctuation of the graph of the maximum deformation vs modes of vibration is not very high, which indicates that there is no weak component which needs further strengthening in the structure.

5.3 Recommendation.

Depending on the analysis results, the following recommendations are given.

1. The company shall improve the safety level of the existing chassis under the accidents of side impact, rear impact and front roll over by increasing the stiffness of the chassis on these areas. Specially, the intrusion of the structure into the passengers compartment in the case of front rollover is very high and improvement has to be made on the roof front cross beam.
2. The weak components which showed high deflection in the modal analysis shall be more stiffened.
3. It is good to change the chassis of the existing Bajaj Qute to space-frame chassis.

5.4 Future Work

1. Explicit dynamic analysis of the vehicle has to be performed with a complete body together with body panels added to get more accurate results.
2. Torsional Stiffness (bump case) and Stability analysis should be performed.
3. Power train components should be designed and fitted.

.

References

1) Stefano Baldizzone.(2012), Performance and Fuel Economy Analysis of a Mild Hybrid Vehicle Equipped with Belt Starter Generator, Master's Thesis Paper, University of Windsor, Ontario, Canada,.
2) Antoni Szumanowski. (2013), Hybrid electric power train engineering and technology : modeling, control, and simulation, Warsaw University of Technology, Poland.
3) Mehrdad Ehsani, Yimin Gao, Sebastien E. Gay and Ali Emadi.(2005), Modern Electric, Hybrid Electric, and Fuel Cell Vehicles, Fundamentals, Theory, and Design, Reference book, CRC Press.
4) Sheldon S. Williamson. (2013), Energy Management Strategies for Electric and Plug-in Hybrid Electric Vehicles, Reference book, Concordia University, Montreal, QC, Canada.
5) Wei Liu. (2013), Introduction to Hybrid Vehicle System Modeling and Control, New Jersey.
6) Liew Zhen Hui. (2012), Design, Analysis and Experimental Verification of Tubular Spaceframe Chassis for FSAE Application, Master's Thesis, National University of Singapore.
7) Madhu Ps and Venugopal T r. (2014), Static Analysis, Design Modification and Modal Analysis of Structural Chassis Frame, Journal of Engineering Research and Applications, 2014.
8) Suraj Aru, Pravin Jadhav, Vinay Jadhav, AkooL Kumar and Pratim Angane.(2014), Design, Analysis and Optimization of a Multi-Tubular Space Frame, International Journal of Mechanical and Production Engineering Research and Development (IJMPERD), Pune, Maharashtra, India.
9) Ahmad Zainal Taufik, Nur Rashid, Mazlan, Mohd Faruq and Muhammad Zahir.(2014), Electric car chassis design and analysis by using CATIA V5 R19,Journal of Mechanical and Civil Engineering (IOSR-JMCE), Universiti Teknikal Malaysia Melaka, Malaysia.
10) Damtie Enawgew. (2013), Strength analysis of three wheeled vehicle's chassis and body frame assembled in Ethiopia, Master's Thesis, Addis Ababa Institute of Technology, Addis Ababa.

11) Rohit Walia. (2017), Structural Analysis of Car Under Static and Dynamic Condition by Using ANSYS Software, International Journal of Research in Mechanical Engineering.
12) Harinath and Sartaj Patel. (2016), Design, Analysis and Optimization of Race Car Chassis, International Journal of Innovative Research in Science, Engineering and Technology.
13) Hybrid Electric Vehicle Technology Assessment: Methodology, Analytical Issues, and Interim Results, Center for Transportation Research, Argonne National Laboratory, technical paper, 2001.
14) The European Parliament and the Council of the European Union, Regulation (EU) No 168/2013 of the European Parliament and of the Council of 15 January 2013 on the approval and market surveillance of two- or three-wheel vehicles and quadricycles. Technical paper, 2013.
15) Uniform provisions concerning the approval of vehicles with regard to specific requirements for the electric power train, Addendum 99: Regulation No. 100, technical paper,2013.
16) U.S. Department of Transportation, National Highway Traffic Safety Administration Laboratory Test Procedure for New Car Assessment Program Frontal Impact Testing, Office of Vehicle Safety Crashworthiness Standards, Technical Paper,2012.
17) U.S. Department of Transportation, National Highway Traffic Safety Administration Laboratory Test Procedure for New Car Assessment Program Side Impact Rigid PoleTesting, Office of Vehicle Safety Crashworthiness Standards, Technical Paper, 2012.
18) U.S. Department of Transportation, National Highway Traffic Safety Administration Laboratory Test Procedure for New Car Assessment Program Rear Impact Testing, Office of Vehicle Safety Crashworthiness Standards, Technical Paper, 2012.
19) U.S. Department of Transportation, National Highway Traffic Safety Administration Laboratory Test Procedure for New Car Assessment Program Roll-over Testing, Office of Vehicle Safety Crashworthiness Standards, Technical Paper, 2012.
20) Bajaj Qute Training Guide on Maintenance Procedures to be followed at Authorized Service Centers and Dealership.

21) Venkatesh S P, Mayur D Pawar and Maruthi B H.(2014), Design, Optimisation and Impact Analysis of a Chassis System of Race Car, International Journal of Enhanced Research in Science Technology & Engineering,
22) Iqbal Hussain. (2005), Electric and Hybrid Vehicles Design Fundamentals, Book published in the Taylor & Francis e-Library.,
23) Sheldon S. Williamson. (2013), Energy Management Strategies for Electric and Plug-in Hybrid Electric Vehicles, book, New York.
24) The National Academy of Science, Transitions to Alternative Vehicles and Fuels, Technical Paper, Washington DC, 2013.
25) John Warner. (2015), The Handbook of Lithium-Ion Battery Pack Design Chemistry, Components, Types and Terminology.
26) Jörnsen Reimpell, Helmut Stoll and Jürgen W. Betzler.(2001), The Automotive Chassis: Engineering Principles, 2nd edition, Book Translated from the German by AGET Limited, Reed Elsevier and Professional Publishing Ltd.
27) Giancarlo Genta and Lorenzo Morello.(2009), The Automotive Chassis Components Design, Volume 1.
28) Anoop Bharadwaj Yellambalse Prem Kumar.(2016), Design and Construction of Chassis for Uniti L7e vehicle, Master's thesis. Halmstad University.
29) Eric E. Adams.(2095), Hybrid-Electric Vehicle Design and Applications, Master's thesis, Rochester Institute of Technology.
30) Jacob I. Salter, Design, Analysis and Manufacture of REV Formula SAE Vehicle Chassis,Msc thesis, The University of Western Australia,2011.
31) Nagarjuna Reddy.Y and Vijaya Kumar.S.(2011), Study of Different Parameters on the Chassis Space Frame For the Sports Car by Using FEA, IOSR Journal of Mechanical and Civil Engineering.
32) Allan Bonnick.(2008), Automotive Science and Mathematics,1st edition, Hungary.
33) Jason C. Brown, A. John Robertson and Stan T. Serpento.(2002), Motor Vehicle Structures: Concepts and Fundamentals.
34) Matthew Huang.(2002), Vehicle Crash Mechanics, International Standard Book Number 0-8493-0104-1.

35) Economic Commission for Europe Inland Transport Committee, World Forum for Harmonization of Vehicle Regulations, Consolidated Resolution on the Construction of Vehicles(R.E.3) Technical paper,2014.

36) Regulation No. 100 ,Uniform provisions concerning the approval of vehicles with regard to specific requirements for the electric power train, RESS-11-06,Technical paper,2014

37) M Edwards, M Seidl, J Carroll & A Nathanson.(2014), Provision of information and services to perform an initial assessment of additional functional safety and vehicle construction requirements for L7e-A heavy on-road quads, Research paper.

38) Kevin Anthony Brown. (2007), Finite element modeling of the static and dynamic impact behaviour of thermoplastic composite sandwich structures. PhD thesis, University of Nottingham.

39) Daniel Northcott.(2007), Design, Simulation and Construction of Series Hybrid Electric Vehicles. Master's thesis, University of Manitoba.

40) Eswar Vijayakumar.(2013), Chassis Strength Evaluation and Rollover Analysis of a Single Seat Electric Car, Master's Thesis, Halmers University of Technology, Gothenburg, Sweden.

41) Vikram Nair.(2012), Determination of Factors to Improve Effectiveness of Triangulation Members for a Formula SAE Race Car Frame, Master's thesis, University of Texas, Arlington.

42) R.Rajappan and M.Vivekanandhan.(2013), Static and Modal Analysis of Chassis by Using Fea, International Journal Of Engineering and Science (Ijes).

43) Abhinn Bajaj, Shahnawaz Alam and Akshansh Uniyal.(2016), Static and Modal analysis of Truck Chassis, International Journal of Advanced Technology in Engineering and Science.

Appendix A: The dimensions of the new chassis.

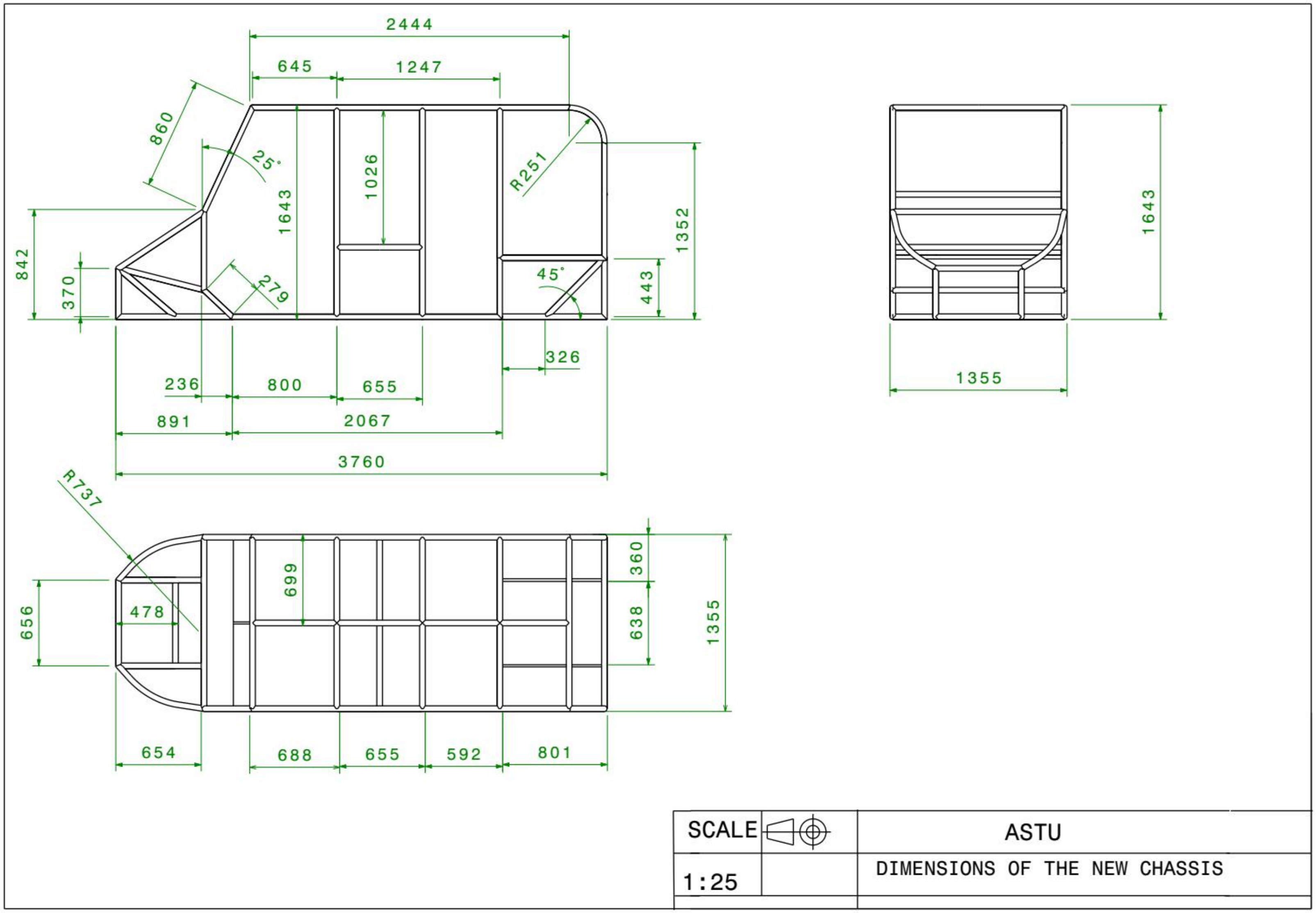

Appendix B: 95^{th} Percentile Man Ergonomic Sitting Position.

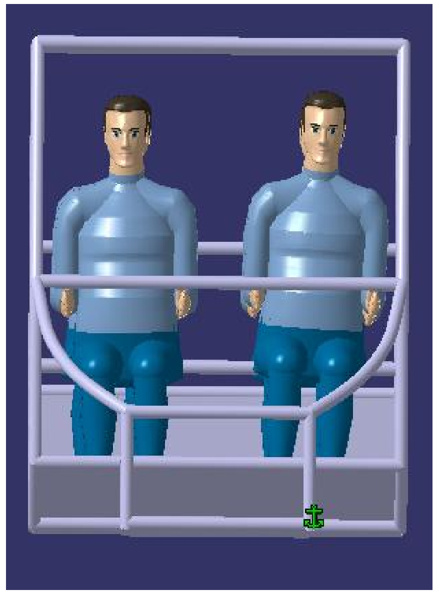

Front view

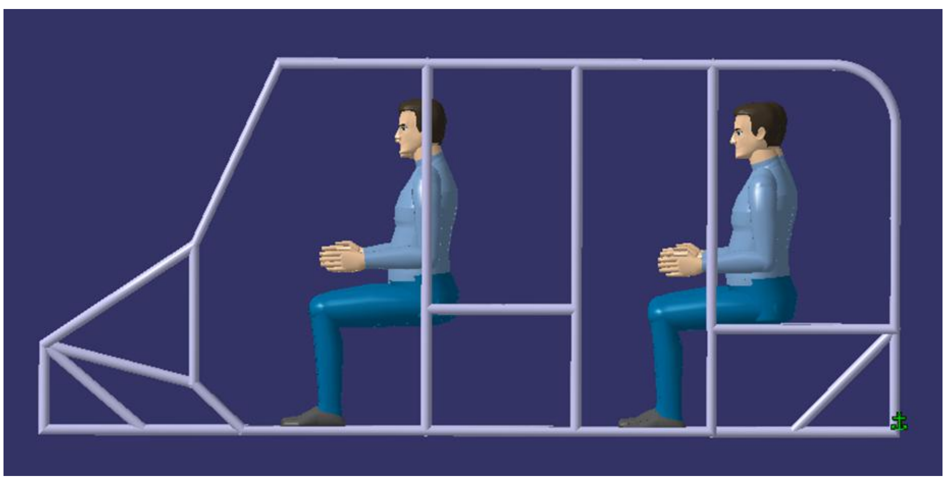

Side View

Top View

Appendix C: Mounting Places of the Drive-line Components.